

Spring 2017

# Development of DNA assembly and error correction protocols for a digital microfluidic device

Yuliya Khilko  
*San Jose State University*

Follow this and additional works at: [https://scholarworks.sjsu.edu/etd\\_theses](https://scholarworks.sjsu.edu/etd_theses)

---

## Recommended Citation

Khilko, Yuliya, "Development of DNA assembly and error correction protocols for a digital microfluidic device" (2017). *Master's Theses*. 4805.

DOI: <https://doi.org/10.31979/etd.uys4-w4m9>

[https://scholarworks.sjsu.edu/etd\\_theses/4805](https://scholarworks.sjsu.edu/etd_theses/4805)

This Thesis is brought to you for free and open access by the Master's Theses and Graduate Research at SJSU ScholarWorks. It has been accepted for inclusion in Master's Theses by an authorized administrator of SJSU ScholarWorks. For more information, please contact [scholarworks@sjsu.edu](mailto:scholarworks@sjsu.edu).

DEVELOPMENT OF DNA ASSEMBLY AND ERROR CORRECTION PROTOCOLS  
FOR A DIGITAL MICROFLUIDIC DEVICE

A Thesis

Presented to

The Faculty of the Department of Biomedical, Chemical and Materials Engineering

San José State University

In Partial Fulfillment

of the Requirements for the Degree

Master of Science

by

Yuliya Khilko

May 2017

© 2017

Yuliya Khilko

**ALL RIGHTS RESERVED**

The Designated Thesis Committee Approves the Thesis Titled

DEVELOPMENT OF DNA ASSEMBLY AND ERROR CORRECTION PROTOCOLS  
FOR A DIGITAL MICROFLUIDIC DEVICE

by

Yuliya Khilko

APPROVED FOR THE DEPARTMENT OF BIOMEDICAL,  
CHEMICAL, AND MATERIALS ENGINEERING

SAN JOSÉ STATE UNIVERSITY

May 2017

Melanie McNeil, Ph.D.

Department of Biomedical, Chemical, and  
Materials Engineering

Liat Rosenfeld, Ph.D.

Department of Biomedical, Chemical, and  
Materials Engineering

Peter Griffin, Ph.D.

Stanford Genome Technology Center

## ABSTRACT

### DEVELOPMENT OF DNA ASSEMBLY AND ERROR CORRECTION PROTOCOLS FOR A DIGITAL MICROFLUIDIC DEVICE

by Yuliya Khilko

Customized production of synthetic DNA from oligonucleotides is in high demand. However, current technologies are costly and labor-intensive. A microfluidic technology can significantly decrease cost and labor. The purpose of this study was to develop a gene assembly protocol that was utilized on the Mondrian™ SP digital microfluidic device. The fragment of the human influenza virus hemagglutinin (HA) gene (339 bp) was assembled from 12 oligonucleotides by the Gibson assembly method and error corrected with CorrectASE™ enzyme twice. The samples were analyzed by Sanger sequencing to verify the final accuracy of the assembly. A complete automation of droplet generation and movement on digital microfluidic droplet technology was achieved in the study. The reactions were scaled down to 0.6-1.2 µL. Gibson assembly, PCR, and enzymatic error correction reactions were optimized and combined in a single protocol. The microfluidic assembly demonstrated approximately 3 errors/kb error frequency. Polymerase chain reaction supplemented with additional MgCl<sub>2</sub>, Phusion, and PEG 8000 provided amplification of the assembly and error correction products. The lowest error frequency of 0.3 errors/kb was achieved after one CorrectASE™ treatment. However, microfluidic error correction was not reliable due to CorrectASE™ interactions with the microfluidic surface, which need to be the subject of future work.

## ACKNOWLEDGMENTS

I am very grateful to Dr. Peter Griffin for giving me the opportunity to conduct my research at the Stanford Genome Technology Center. Dr. Griffin created the environment where I could learn and develop new skills.

I would like to thank our collaborators at J. Craig Venter Institute for funding this study and providing me with all necessary supplies for the experiments. I owe my deepest gratitude to Dr. Philip Weyman for his help and professional expertise in molecular biology. Also, I wish to thank Illumina for donating the equipment and microfluidic cartridges.

I would like to show my gratitude to my advisor, Dr. Melanie McNeil. Her valuable advice has helped me tremendously to complete this manuscript.

I would like to thank my family and friends for their support. My special thanks go to my husband Sergey. Without his emotional and financial support this thesis would not be possible.

Finally, I am grateful to all people at the Stanford Genome Technology center for their help and professional advice.

## TABLE OF CONTENTS

LIST OF FIGURES .....	viii
LIST OF TABLES .....	x
CHAPTER ONE INTRODUCTION .....	1
1.1 Deoxyribonucleic Acid .....	2
1.2 Polymerase Chain Reaction .....	3
1.3 Gene Assembly .....	4
1.4 Error Correction .....	6
1.5 Programmable Digital Microfluidics .....	6
1.6 Significance of Research .....	8
CHAPTER TWO LITERATURE REVIEW .....	11
2.1 Gene Assembly Methods .....	11
2.1.1 Polymerase-based DNA Assembly .....	12
2.1.2 Exonuclease-based Assembly Methods .....	15
2.2 Microfluidic PCR .....	19
2.3 Reduction of Errors in Synthetic Genes .....	25
2.4 Literature Review Summary .....	29
CHAPTER THREE RESEARCH OBJECTIVES .....	30
3.1 Research Objectives .....	30
3.2 Justification .....	30
CHAPTER FOUR MATERIALS AND METHODS .....	31
4.1 Equipment .....	31
4.1.1 Mondrian™ SP Microfluidic Device .....	31
4.1.2 Bacterial Electroporation Transformation Equipment .....	34
4.1.3 DNA Analysis Equipment .....	35
4.2 Experimental Procedures for Microfluidic Polymerase Chain Reaction .....	37
4.2.1 Optimization of PCR Reagents .....	37
4.2.2. Reduction of Phusion Polymerase Adsorption During Microfluidic PCR .....	40
4.2.3 Automation Program for Microfluidic PCR .....	43
4.3 Experimental Procedures for Microfluidic Gibson Assembly .....	45
4.3.1 Optimization of Gibson Assembly Reaction Time and Determination of Suitable Reagent Concentrations .....	45
4.3.2. Optimization of Dilution Prior to Amplification and Determination of PCR Conditions .....	47

4.3.3 Automation Program for Microfluidic DNA Assembly .....	49
4.4 Procedures for Development of the Automation Protocol for Gibson Assembly with Two CorrectASE™ Treatments.....	50
4.4.1 Determination of Temperature Settings for Error Correction Experiments	50
4.4.2 Automation Program for Microfluidic DNA Assembly with Error Correction .....	53
4.4.3 Experimental Protocols for Microfluidic DNA Assembly with Error Correction .....	55
4.4.4 Experimental Matrices for Validation of DNA assembly and Error Correction Protocols on the DMF .....	56
4.5 Data Analysis .....	58
4.5.1 Preparation of Samples for Sanger Sequencing.....	58
4.5.2 Sequencing Data Analysis .....	60
 CHAPTER FIVE RESULTS .....	 62
5.1 Results of Microfluidic PCR Experiments.....	62
5.2 Reduction of Adsorption of Phusion Polymerase on the Microfluidic Surface.	64
5.3 Results of Microfluidic DNA Assembly .....	67
5.4 Temperature Settings for Error Correction Experiments .....	72
5.5 Sanger Sequencing Results of Assembly Samples .....	76
5.6 Sanger Sequencing Results for Gibson Assembly with Error Correction for Protocol 1 .....	78
5.7 Sanger Sequencing Results for Gibson Assembly with Error Correction for Protocol 2 .....	82
 CHAPTER SIX DISCUSSION .....	 90
6.1 Microfluidic PCR with Phusion Polymerase .....	90
6.2 Microfluidic Gibson Assembly .....	93
6.3 Microfluidic Error Correction with CorrectASE™ .....	95
 CHAPTER SEVEN CONCLUSIONS .....	 98
 CHAPTER EIGHT FUTURE STUDIES .....	 101
 REFERENCES .....	 102
Appendix A: Materials.....	107
Appendix B: Master Mixes for Microfluidic Assembly and Error Correction Experiments.....	110
Appendix C: List of Materials Used to Prepare Samples for Sanger Sequencing....	112
Appendix D: Procedures for Cloning of DNA Samples to pUC19 Vector .....	114
Appendix E: Procedures for Colony PCR .....	116
Appendix F: Microfluidic Assembly Sanger Sequencing Results.....	117



## LIST OF FIGURES

Figure 1. Structure of DNA. ....	2
Figure 2. A description of one cycle of polymerase chain reaction.....	3
Figure 3. Gene assembly method.....	5
Figure 4. A contact angle reduction under applied electrical field. ....	7
Figure 5. A cross-section of an EWOD cartridge. ....	8
Figure 6. Polymerase cycling assembly (PCA) process flow (reprinted with permission from Elsevier) [12].....	13
Figure 7. Gibson assembly.....	16
Figure 8. Isothermal hierarchical DNA construction coupled with Gibson assembly (reprinted with permission from BioMed Central Ltd.) [17].....	18
Figure 9. Polymerase adsorption experiments (reprinted with permission from Elsevier) [29]. ....	21
Figure 10. Relative PCR efficiency on PDM-glass chip coated with 10% polymer solutions . ....	22
Figure 11. Results of confocal microscopy of Pluronic additive on protein adsorption..	23
Figure 12. Results of Pluronic type effects on maximum actuation time (Reprinted with permission from ([32]))......	24
Figure 13. Schematic of error correction procedure (reprinted with permission from Oxford University Press) [37].....	27
Figure 14. Effect of incubation times and iterations on error correction results (reprinted with permission from Oxford University Press) [37]. ....	28
Figure 15. An image of the Mondrian™ SP device used in this study.....	32
Figure 16. An image of Mondrian™ SP microfluidic cartridge. ....	33
Figure 17. Generation of 1X, 2X, and 4X droplets on the DMF. ....	34

Figure 18. Bio-Rad Gene Pulser II Porator electroporation system. ....	35
Figure 19. An image of the NanoDrop ND-1000 instrument. ....	36
Figure 20. Error correction process with CorrectASE™ enzyme. ....	52
Figure 21. Automation program for microfluidic DNA assembly with two rounds of error correction.....	54
Figure 22. Polymerase chain reaction with iso the buffer and Phusion additives. ....	63
Figure 23. Polymerase chain reaction with two components of the iso buffer.....	64
Figure 24. Microfluidic PCR with 0.02% w/v Pluronic F68 and variable Phusion concentration.....	65
Figure 25. Microfluidic PCR with 10% w/v PEG 8000 pre-coat. ....	67
Figure 26. Microfluidic assembly at different times.....	68
Figure 27. Microfluidic assembly of 250 nM oligos for 60 min.. ....	69
Figure 28. Dilution of the 50 nM oligo assembly product prior to PCR. ....	70
Figure 29. Dilution of assembly product by 8-fold and 16-fold.....	71
Figure 30. Variation of temperatures on the DMF cartridge .....	73
Figure 31. Average variation of temperatures during EC denature/anneal treatments. ..	74
Figure 32. Average temperature variation during CorrectASE™ incubation. ....	75
Figure 33. Average error frequency for sequences assembled from 250 nM and 50 nM oligos.....	76
Figure 34. Error frequency of assembly samples followed by two rounds of error correction obtained using automation protocol 1.....	79
Figure 35. Error frequency of untreated and treated with CorrectASE™ samples on a benchtop and on the DMF following protocol 2.....	83
Figure 36. Error frequency of assembly samples followed by two rounds of error correction obtained using the automation protocol 2.....	86

## LIST OF TABLES

Table 1. Microfluidic assembly methods.....	12
Table 2. Basic microfluidic PCR protocol.....	38
Table 3. Experimental design to determine microfluidic PCR conditions. ....	38
Table 4. Experimental design for polymerase adsorption. ....	42
Table 5. Microfluidic DNA assembly experiments. ....	46
Table 6. Experinetal design to study optimization of the microfluidic DNA assembly process. ....	48
Table 7. Steps of DNA assembly and error correction process. ....	55
Table 8. Experimental matrix for microfluidic protocol 1.....	57
Table 9. Experimental matrix for microfluidic protocol 2.....	57
Table 10. Error analysis of assembly constructs based on Sanger sequencing. ....	77
Table 11. Error analysis of assembly and error correction experiments using protocol 1. ....	81
Table 12. Error analysis of benchtop and microfluidic assembly and error correction samples obtained using protocol 2.....	84
Table 13. Error analysis assembly and error correction experiments using protocol 2..	87
Table 14. A list of oligonucleotide sequences. ....	108
Table 15. Oligo master mixes. ....	110
Table 16. Gibson assembly master mix. ....	110
Table 17. PCR master mixes.....	110
Table 18. Dilution master mix. ....	111
Table 19. Denature/anneal master mix. ....	111
Table 20. CorrectASE™ master mix. ....	111

Table 21. Master mix for amplification of pUC19 plasmid DNA.....	114
Table 22. Example of Gibson assembly DNA fragments into pUC19 vector. ....	114
Table 23. Master mix 2X CBA for cloning. ....	115
Table 24. Colony PCR Master Mix. ....	116
Table 25. Sequencing results of 50 nM oligos assembly samples. ....	117
Table 26. Sequencing results of 250 nM oligos assembly samples. ....	118

## CHAPTER ONE

### INTRODUCTION

Over the last decade, major research advances in genome sequencing (i.e. “DNA reading”) are slowly being matched by advances in synthetic biology (i.e. “DNA writing”). Naturally occurring genomes have been modified with synthetic DNA for changing existing or engineering new biological pathways. Advancements in synthetic genomics went beyond the scope of gene editing. Researchers at the J. Craig Venter Institute (JCVI) were able to create a minimal synthetic cell. In that work, the chromosome of *Mycoplasma mycoides* syn3.0 was synthesized from oligonucleotides and consisted of 531 kilobase pairs (kbp). The minimal cell had 323 genes out of 473 that were identified to be essential for cell growth and survival [1]. This research opens opportunities to understand the functions of genes found in the human genome and to develop new gene editing techniques. Additionally, synthetic genes are employed in the production of bio-derived chemicals and clean energy. For example, metabolic pathways in cyanobacteria were modified, so they could produce 1,3-propanediol, which is the important intermediate of polyethylene terephthalate and nylon synthesis [2]. There is a demand for synthetic DNA that will only increase in the future. However, the ability to synthesize long DNA molecules in a short period of time without significant expense remains one of the main challenges in synthetic biology.

The next sections provide a short introduction to several concepts that important for understanding the background behind DNA assembly.

## 1.1 Deoxyribonucleic Acid

Deoxyribonucleic acid (DNA) is a biological polymer with a double helix structure. The molecule is composed of a number of repeated nucleotides, the building blocks of DNA. Deoxyribose, phosphate and a nitrogenous base (purine or pyrimidine) are the three main components of nucleotides. The purines, found in DNA molecules, are adenine (A) and guanine (G), and pyrimidines are thymine (T) and cytosine (C). A helical structure of DNA is caused by the ability to form complementary base pairs. Adenine forms hydrogen bonds with thymine. Guanine pairs with cytosine [3]. A basic DNA structure is shown in Figure 1.

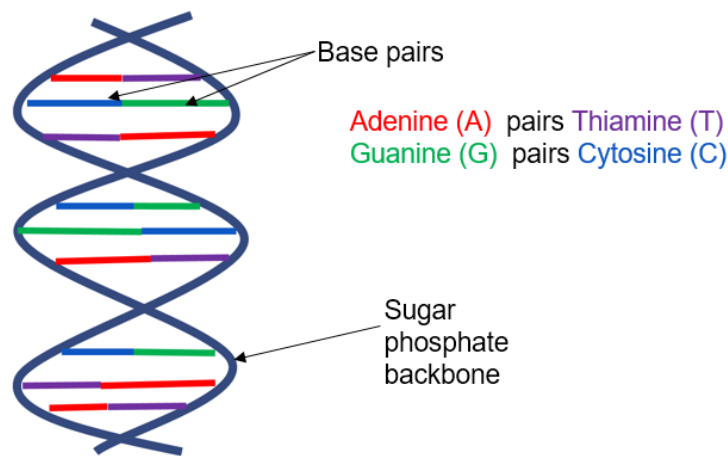


Figure 1. Structure of DNA.

## 1.2 Polymerase Chain Reaction

The polymerase chain reaction (PCR) is one of the most used amplification techniques in molecular biology and is an essential step for DNA assembly. The reaction is used to make multiple copies of a target DNA fragment. The process is based on the use of a DNA polymerase, a temperature resistant enzyme, which can build a complementary strand. A polymerase, a DNA template, oligonucleotide primers, buffer solutions, and deoxynucleotide triphosphates (dNTPs) are the necessary reagents. The reaction pathway is shown in Figure 2. First, a template (dsDNA) is separated at high temperature. Then, the mixture is cooled down, which allows primers to bind. Finally, the DNA polymerase extends strands by adding dNTPs. At the end of the first cycle, two identical nucleic acids are produced. In order to achieve sufficient amplification, the process is repeated for 25-40 times [3].

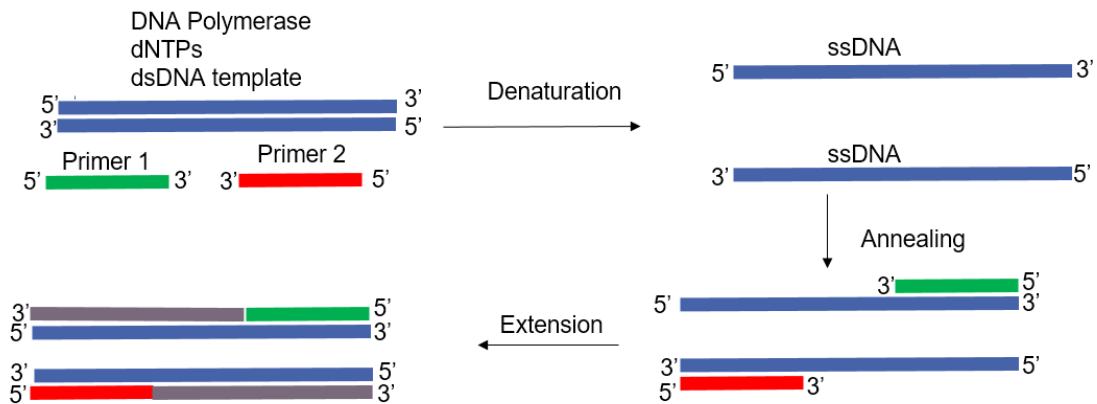


Figure 2. A description of one cycle of polymerase chain reaction.

### 1.3 Gene Assembly

Gene assembly is a method of constructing long molecules from DNA oligonucleotides (oligos). The oligonucleotides are single-stranded (ssDNA) fragments, which are usually 50-100 bases long. The oligonucleotides are designed to overlap by 20-30 bases. Figure 3 demonstrates step by step gene assembly. The ends of oligos are joined together in a series of enzymatic reactions to make larger fragments of DNA. These fragments of DNA can be assembled into genomes up to hundreds of kilobases (kb) in a hierarchical order. Smaller molecules (several hundred base pairs) assembled from oligonucleotides can themselves be assembled into larger fragments (up to ~10 kb). Each step is followed by PCR amplification. After ~10 kb, PCR becomes difficult, so the assembly of larger fragments must use a restriction enzyme. Digested and purified constructs are mixed together and either joined using the Gibson assembly or by the assembly in yeast [4]. The obtained nucleic acids are ligated into a vector. The vectors are transformed into *E. coli*. In order to obtain error-free products, the DNA from a single colony must be sequence verified [5, 6].



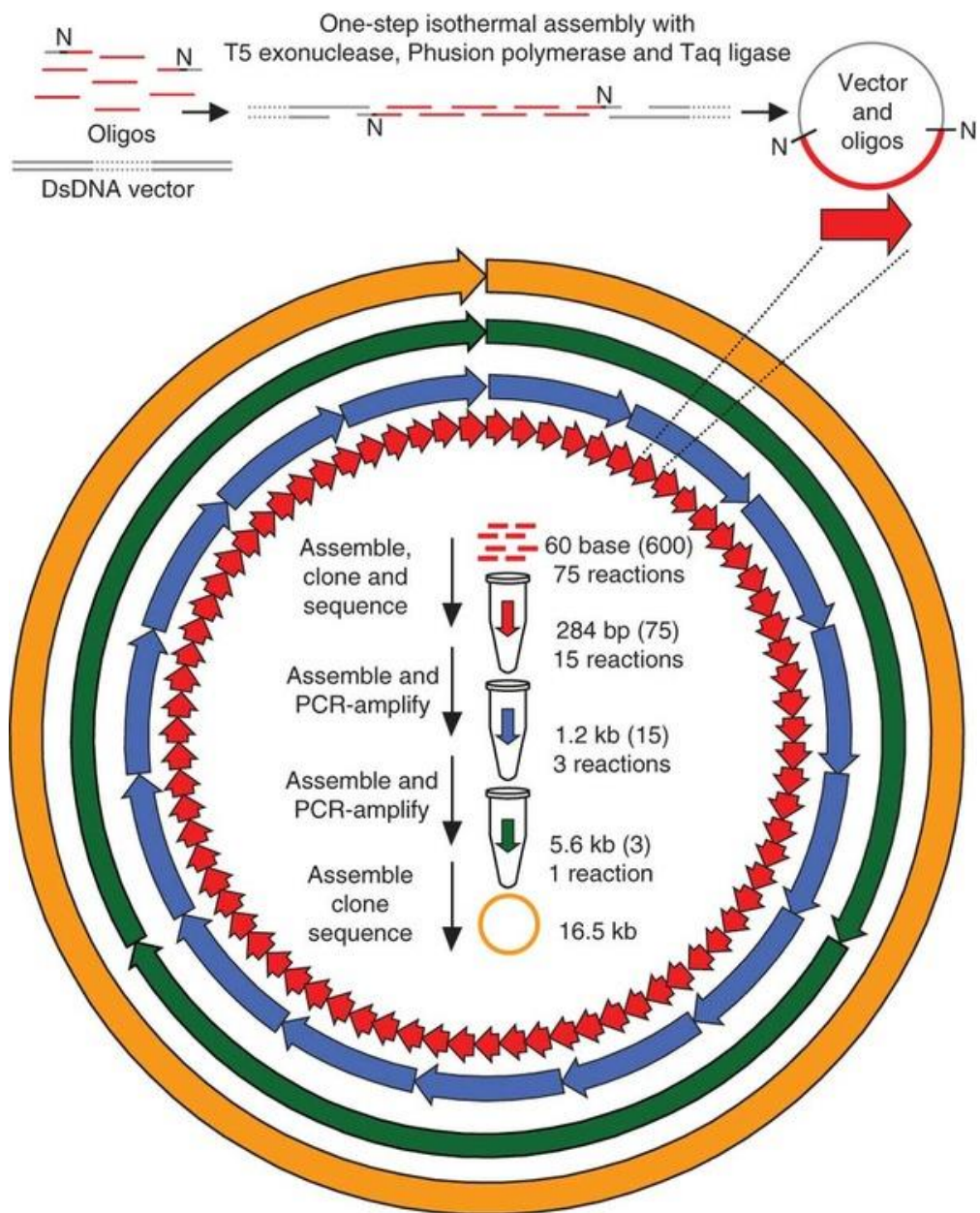


Figure 3. Gene assembly method. (Reprinted by permission from Macmillan Publishers Ltd.: [Nature Methods] ([6]), copyright (2010).

#### 1.4 Error Correction

Genes assembled from oligonucleotides typically contain errors. The majority of the errors come from oligonucleotide synthesis. During DNA assembly, oligonucleotides are used as templates for a complementary strand synthesis, and the existing errors are copied. As a result, there are deletions, substitutions, and insertions in the sequence. Current error correction methods are based on removal of mismatches. In order to recognize mismatches, DNA strands have to be separated and reannealed. When the strands come together, it is unlikely that the DNA strand will come back together with a complementary strand containing the mismatch and non-base paired “bulges” are formed in the mismatch areas. Mismatch-binding proteins and mismatch-cleavage enzymes are two types of error correction agents. The mismatch-binding protein MutS recognizes and binds to heteroduplexes. Next, error free sequences are separated by the mobility shift assay. Unfortunately, this method is only suitable for sequences having a small amount of errors. On the other hand, error removal with mismatch-cleavage enzymes is a one-step process. The enzymes can recognize bulges and cut out errors [7].

#### 1.5 Programmable Digital Microfluidics

Digital microfluidics (DMF) is a technology based on the electrowetting phenomenon. The phenomenon describes a change of surface tension at a solid/liquid/gas interface by application of the electric field [8]. The change of surface tension under applied voltage is described by Equation 1, which was introduced by Lippmann.

$$\gamma = \gamma_0 - \frac{1}{2}CV^2 \quad \text{Equation 1}$$

where  $\gamma_0$  is the initial surface tension (N/m),  $C$  is the capacitance per unit area of dielectric ( $J/V^2m^2$ ),  $\gamma$  is the surface tension after applied electrical field (N/m), and  $V$  is the voltage (V). The voltage applied on the electrodes lowers the surface tension, which leads to a reduction of the contact angle and increases the wettability of the surface. The reduction of the contact angle is shown in Figure 4. Consequently, the liquid spreads over the surface where the voltage was applied. Thus, a hydrophobic surface becomes hydrophilic. By the application of a voltage on a dielectric surface, the liquids can be transported over the surface of a microfluidic cartridge [8, 9].

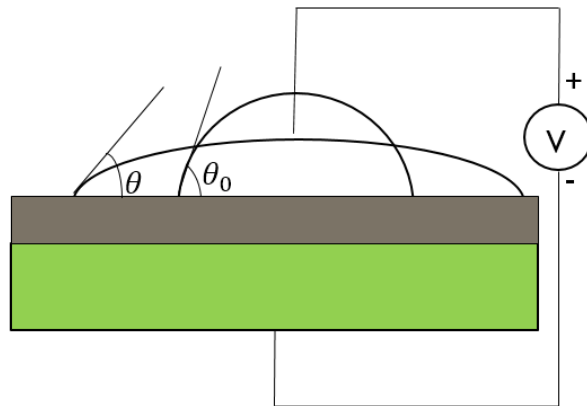


Figure 4. A contact angle reduction under applied electrical field.

Figure 5 demonstrates a microfluidic cartridge operated by electrowetting on dielectric (EWOD). A droplet is sandwiched between two hydrophobic plates and the remaining volume is filled with immiscible liquid, for example, a silicone oil. The oil adds an additional layer of insulation, coats droplets to prevent evaporation, and facilitates transport. The bottom plate is the array of electrodes, which can locally control

the surface tension. By turning on and off the voltage on certain electrodes, the droplets can be directed anywhere on a chip. They can also be split, fused, and held in certain regions. The cartridge is inserted in to a machine that is operated by a software program [10, 11].

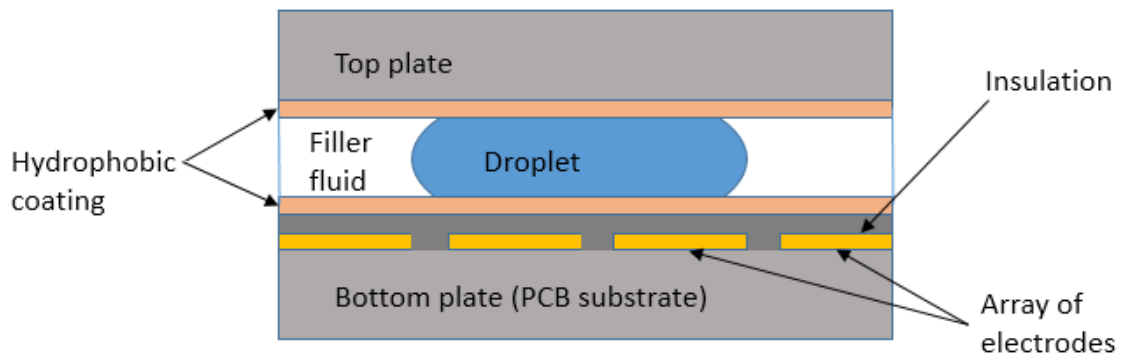


Figure 5. A cross-section of an EWOD cartridge.

## 1.6 Significance of Research

Gene synthesis is a costly and labor intensive process. The cost of synthetic DNA is directly related to the cost of oligonucleotides. The cheapest oligos that can be purchased from commercial suppliers are usually unpurified and contain errors. Thus, the genes, assembled from the unpurified oligos, have to be sequence verified to find a correct assembly. Typically, tedious molecular biology operations are performed to assemble DNA in recombinant plasmids and to clone them in bacterial cells. The plasmids are isolated from bacterial cultures and Sanger sequenced. It can take from three days up to a week to process the samples. The time and expense required to obtain high quality DNA are the major drawbacks preventing gene synthesis technology from becoming more

mainstream. Implementation of an enzymatic error correction step could greatly improve the quality of assemblies, which will reduce the number of clones that have to be sequence verified. Integration of a digital microfluidics into DNA assembly coupled with error correction can potentially increase the throughput of gene synthesis.

Digital microfluidic devices are applicable for gene assembly because DNA is typically handled in microliter amounts. The microfluidic devices are capable of generating droplets in the microliter to picoliter range. The microliter droplets act like reaction and transportation vessels. The ability to program liquid handling operations such as split, merge, mix, and transport allows a researcher to simplify the gene assembly process. Time-consuming steps like pipetting, transferring reagents, tube labeling, incubation at certain temperature, and thermocycling can be performed by programmable droplet generation and routing. The sequential reactions can be carried on a single microfluidic cartridge without any human intervention. Automation programs can be designed to conduct multiple experiments in parallel. Since the devices are fully automated, the sources of human errors and labor costs can be greatly reduced. In addition, DNA assembly protocols can be distributed between laboratories, so the scientists can use the equipment to generate novel ideas.

Because DNA assembly and error correction reactions require the use of expensive enzymes, scaling down to smaller reaction volumes reduces reagent expenses. Due to the large surface-to-volume ratio, microdroplet reactors have high heat and mass transfer rates. This makes it possible to increase kinetics and speed up reactions. Integration of effective error correction procedures has the potential to perform DNA assembly on a

single microfluidic cartridge without the need for expensive and lengthy sequence verification.

The purpose of this research is to develop a DNA assembly protocol for a programmable digital microfluidic device. The process consists of three major parts. First, oligos are assembled into a double-stranded DNA fragment. The oligo assembly is then amplified by PCR. The next step is to remove the errors, which came from the original oligonucleotides. The repaired fragments are Sanger sequenced to verify the efficiency the error removal process. The data is analyzed to determine the most efficient DNA assembly and error correction protocols. The ultimate goal is to be able to design a reliable and cost- effective DNA assembly protocol that will be widely applicable in biological research.

## CHAPTER TWO

### LITERATURE REVIEW

In order to develop a rapid and cost-effective process, DNA assembly, amplification, and error correction procedures have to be adapted to the microfluidic platform. This literature review will examine each step of the gene construction process and illustrate methods that have been successfully integrated with microfluidics. Additionally, prevention of protein adsorption on microfluidic surfaces will be discussed.

#### 2.1 Gene Assembly Methods

A number of DNA assembly protocols have been developed to date. A summary of gene construction methods performed on microfluidic devices is shown in Table 1. For the scope of this study, only assembly methods from oligonucleotides will be discussed. It can be observed that the most popular gene construction methods for microfluidic applications are polymerase-based and endonuclease-based assembly. Both approaches utilize oligonucleotides as DNA building blocks. Oligonucleotides are typically 10 to 100 bases in length. One of the requirements is that oligos need to have complementary sequences on both ends, so pieces could overlap to form a longer DNA strand [12].

Table 1. Microfluidic assembly methods.

Authors	Type of microfluidics	Assembly method	Assembly size	Error rates
Kong <i>et al.</i> [13]	Droplet	Polymerase-based (PCA)	500 –1000 bp	1.78 errors/kb
Huang <i>et al.</i> [14]	Microchannel	Polymerase-based (PCA)	760 bp	4.1 errors/kb
Quan <i>et al.</i> [15]	Microarray	Polymerase-based (PCA)	500 – 1000 bp	1.9 errors/kb
Tian <i>et al.</i> [16]	Microarray	Polymerase-based (PAM)	14500 bp	2.2 errors/kb
Linshiz <i>et al.</i> [17]	Chanel	Exonuclease-based (Gibson) and polymerase-based (IHDC)	754 bp	N/A
Shih <i>et al.</i> [18]	Combined digital and droplet microfluidics	Exonuclease-based assembly of dsDNA (Gibson)	2100 bp	N/A
Tangen <i>et al.</i> [19]	Droplets	Polymerase-based (PCA) and Exonuclease-based (Gibson)	525 bp	N/A
Yehezkel <i>et al.</i> [20]	Digital microfluidics	Polymerase-based (POP)	800 bp	2.22 errors/kb

### 2.1.1 Polymerase-based DNA Assembly

Polymerase cycling assembly (PCA) is one of the most popular polymerase-based DNA assembly techniques. Polymerase cycling assembly procedures are similar to PCR. Instead of using forward and reverse primers, oligonucleotides overlap and serve as templates for a complimentary strand. The oligos are designed to be either a part of the top or the bottom DNA strand. As seen in Figure 6, in the first PCA cycle, oligos overlap, and the polymerase extends the complementary strand only in a 5' to 3' direction. In the next cycle, the double-stranded DNA pieces are separated and overlapped with the oligonucleotides or other single-stranded fragments. The process of



denaturation, annealing, and extension is repeated until the desired sequence has been built [21].

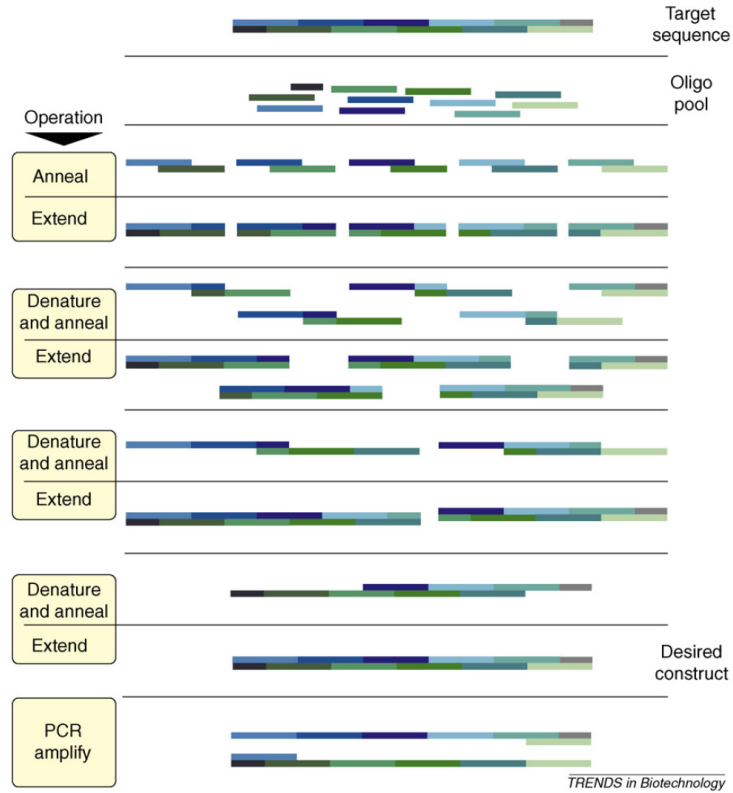


Figure 6. Polymerase cycling assembly (PCA) process flow [12] (reprinted with permission from Elsevier).

Huang *et al.* used PCA to synthesize a 760 bp segment of GFPuv gene from a pool of oligonucleotides on a microfluidic device. The group was able to join 39 chemically synthesized oligonucleotides, which were 20-40 bases-long, each overlapping another oligo by 20 bases. The researchers demonstrated that a two-step assembly process based on PCA followed by PCR was more effective than a one-step assembly. It has been shown that a two-step assembly produced a larger amount of the full-length product. The yield of assembly on a microfluidic device was 50% lower than on a conventional

thermocycler. The reaction yield was dependent on the dead-volume formed between the valves and a PCR chamber. The oligos that were trapped in the dead volume were not assembled. Sequencing results showed that the average error rate was 4.1 errors per thousand bases. It has been determined that the majority of errors came from oligonucleotides [14].

Quan and colleagues demonstrated that the oligonucleotide synthesis, amplification, and assembly could be achieved on a single microfluidic device. Oligonucleotides were synthesized on a microarray surface using an inkjet DNA synthesizer. Prior to assembly, the oligonucleotides were amplified and released from the microarray surface. The oligos were assembled by the same PCA method described above into 0.5-1 kb double-stranded DNA fragments [15]. The error rate of assemblies has been found to be 1.9 errors/kb, which is lower than the results obtained by Huang's group [14, 15].

Chip synthesized oligos were used by Tian and colleagues to assemble 21 protein coding genes of the *E. coli* 30s ribosomal subunit. The group developed a hybridization method to remove oligos containing mutations. Next, in a single step selected oligonucleotides were joined by a variation of the PCR-based assembly reaction, which they called a polymerase assembly multiplexing (PAM) reaction. The intermediates were joined sequentially by PAM into protein coding genes with the approximate length of 14.6 kb. [16].

Yehezkel *at al.* developed a polymerase-based assembly method called programmable order polymerization (POP). The method was successfully automated on the Mondrian™ SP microfluidic device. The assembly consisted of four phases. In each

phase, one dsDNA piece was extended by two overlap extension oligos in 4 denature/anneal cycles. A dilution step was employed between each assembly step to remove primers from the previous step. The group reported 1/450 bp (2.22 errors/kb) error rate for their assembly method. The errors were identified as substitutions [20].

Polymerase based methods are very robust and easy to perform, but have several disadvantages. The assembly of long sequences will increase reaction time. Since the quality of oligos decreases with the length, it is important to use shorter oligos for accurate gene assembly. This means that for long sequences, the number of building blocks has to be higher, and the assembly reaction will require more denaturing, annealing, and extension cycles. With each amplification cycle, errors, which came from oligos, will be amplified. The use of an expensive high-fidelity polymerase is necessary to minimize amplification errors.

#### 2.1.2 Exonuclease-based Assembly Methods

Among exonuclease mediated assembly methods, Gibson assembly is considered to be one of the most suitable for microfluidic applications. It is a one-step isothermal assembly method developed at the J. Craig Venter Institute. Double-stranded DNA pieces are joined into longer fragments by three enzymes, T5 exonuclease, DNA polymerase, and Taq DNA ligase. The reagents are incubated at 50 °C for an hour. As shown in Figure 7, two oligonucleotides overlap at the 3' end, and T5 exonuclease reveals these overlaps by digesting some DNA from each 5' end. Next, the complementary strands anneal and the gaps are filled in by the action of Phusion

polymerase. Taq ligase creates covalent bonds between annealed complementary strands by removing sequence discontinuities [22].

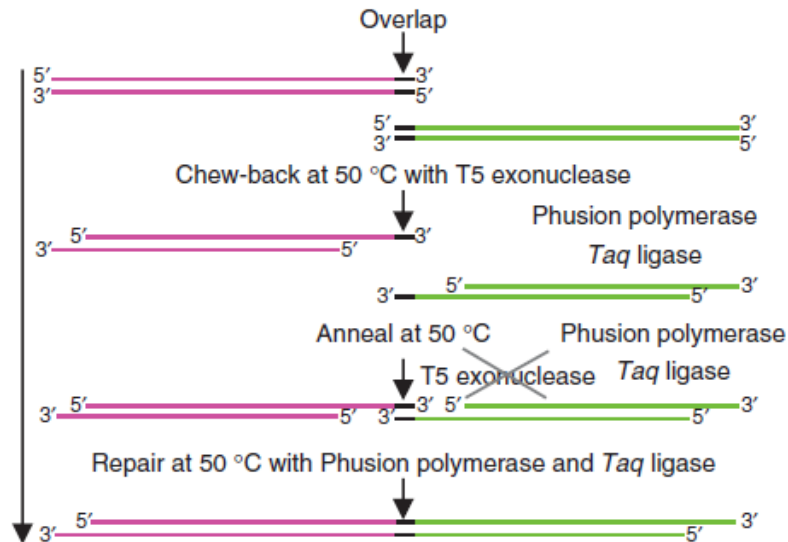


Figure 7. Gibson assembly. (Reprinted by permission from Macmillan Publishers Ltd.: [Nature Methods] ([22]), copyright (2009).

Gibson Assembly can be utilized to build short DNA fragments or full functional genomes. The mouse mitochondrial genome (16.5 kb) was synthesized by assembling 600 oligos in four stages. After each stage, PCR amplification was used to increase the concentration of assembly intermediates. In order to obtain an error-free genome, intermediate sequences were cloned and sequenced. It has been shown that assemblies had one error per every 325 bp, which resulted in only one of four error-free clones. Only error-free clones were used for the next assembly stage [6].

Akama-Garren *et al.* developed modular gene assembly platform (GMAP) based on the Gibson method. Five oligonucleotides were designed to code for 30 common promoters and 140 genes with 30 bp overlaps. The researchers were able to reduce the

assembly time to 20 min instead of the original one hour proposed by Gibson *et al.* [22]. The assemblies were successfully inserted into viral backbones. This method allows a researcher to assemble oligos into complex functional genes in less than one day [23].

It has been shown that Gibson assembly can be successfully integrated into a microfluidic gene synthesis process. Shih *et al.* designed a microfluidics device that combined droplet-based and microchannel microfluidics. The microfluidic chip had three compartments designed for the assembly of plasmids from dsDNA fragments, electroporation, and incubation. The configuration of the microchip enabled 16 simultaneous assembly reactions [18].

Linshiz *et al.* developed an automated microfluidic platform that combined polymerase-based and Gibson gene construction methods. As shown in Figure 8, eight oligos were combined by an isothermal hierarchical DNA construction method (IHDC) into one 754 bp fragment. This method annealed overlapping single-stranded DNA pieces and elongated them using a polymerase. Next, Gibson Assembly was used to clone the insert into pETBlue-1 plasmid. Gibson assembly combined with IHDC took two hours. Similarly to Shih's group, transformation of *E. coli* with the pETBlue-1 plasmid was performed on the microfluidic device [17].

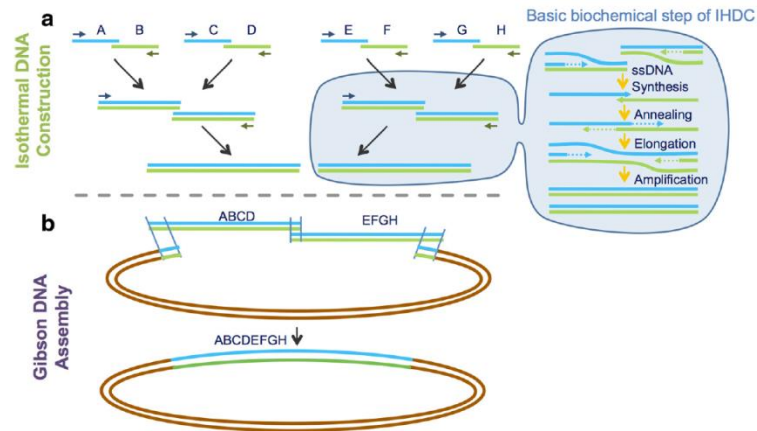


Figure 8. Isothermal hierarchical DNA construction coupled with Gibson assembly (reprinted with permission from BioMed Central Ltd.) [17].

Gibson assembly has several advantages over PCR-based assembly methods. It has been shown that Gibson reaction time could take from 20 min to one hour [22, 23]. On the other hand, an average 30 cycle PCR takes at least 45 min. Gibson assembly is carried out isothermally, whereas PCR requires thermocycling between two or three temperatures. Microchips have to be designed for continuous thermocycling. Thus, polymerase-based assembly methods are more challenging for integration on microfluidic devices. The isothermal process eliminates cross-contamination between samples since the reagents are not moved around on a microfluidic surface. Additionally, Gibson assembly does not increase sequence errors because each oligo serves as a template for a complementary strand only once. In polymerase assembly, the growing DNA sequence serves as a template multiple times until the fragment is built.

## 2.2 Microfluidic PCR

Gene assembly products are typically produced in low concentrations. The next step in gene synthesis is amplification of DNA, so it can be used in subsequent biological manipulations. Polymerase chain reaction is often utilized for DNA amplification. Several studies have been done for PCR optimization on microfluidic devices. Wang *et al.* performed PCR utilizing a droplet microfluidic device with automated heating and temperature control. The researchers investigated the influence of polymerase and magnesium concentration on the reaction yield. It has been found that microfluidic PCR requires a 7-fold increase of polymerase in order to achieve sufficient amplification yield. On the other hand, the optimum magnesium ion concentration of 3.5 mM was the same for both reaction settings, but the chip-based reaction was more sensitive to magnesium fluctuations. It has been suggested that polymerase and magnesium were precipitating out of droplets, so they had to be used in excess [24, 25].

Microfluidic PCR is more time efficient than conventional bench-top PCR. Microfluidic PCR achieved a threshold value of 10 cycles earlier than the same reaction performed using bench-top conditions [25]. Huang *et al.* demonstrated that reaction time on a flow through microfluidic platform was reduced by 64% relative to benchtop [26].

Microfluidic surfaces are prone to biofouling. Cartridges or microfluidic channels are usually coated with either Teflon or Poly(dimethylsiloxane). Both coatings are hydrophobic and susceptible to adsorption of biomolecules. Yoon and Garrell demonstrated that adsorption was caused by a combination of hydrophobic and electrostatic interactions arising from an applied electrical field [27]. The enzymes

trapped on the surface have reduced activities and have to be used in excessive amounts in order to achieve the desired reaction yield. In addition, biofouling can lead to malfunction of a cartridge if it interferes with droplet movement. If the surface has a buildup of contaminants, it would affect electrowetting. The droplets will not be able to move through this area, which leads to experimental failures. In order to obtain robust microfluidic PCR, the adsorption must be minimized.

Adsorption of DNA polymerase on microfluidic surfaces has been found to be one of the main factors reducing PCR yield. Prakash *et al.* studied adsorption of Taq polymerase on Teflon coated surfaces [28]. It has been shown that adsorption of polymerase reduced contact angle of a micro droplet. The reduced contact angle was stable and did not change overtime. The same trend was shown while measuring the concentration of polymerase. The concentration of polymerase reduced from 0.29 to 0.22 mg/mL as soon as the droplet contacted the Teflon surface and did not change in 300 s. It has been determined that the saturation concentration of polymerase on the Teflon coated surface was 0.07 mg/mL [28].

Several ways to minimize fouling were investigated. Erill and colleagues studied the adsorption of Taq enzyme on silicon chips [29]. Surface effects were reduced by the addition of bovine albumin serum (BSA) as well as by increasing the Taq polymerase concentration. Figure 9 shows that the addition of 0.05  $\mu\text{g}/\mu\text{L}$  of BSA greatly increased PCR yield. It has been suggested that polymerase and BSA compete for adsorption sites, but BSA has a higher affinity. The addition of BSA up to 2.5  $\mu\text{g}/\mu\text{L}$  eliminated polymerase adsorption [29].



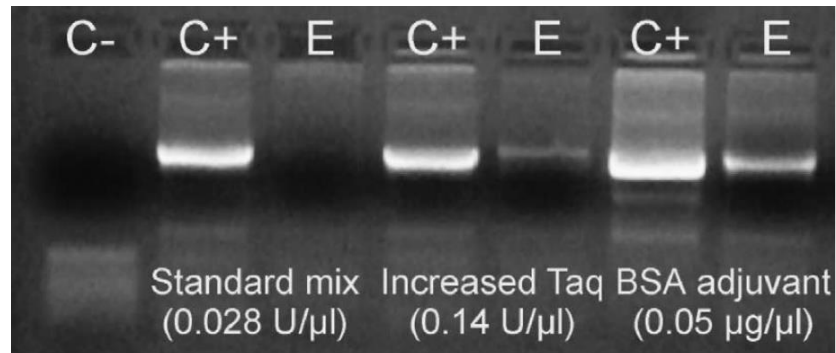


Figure 9. Polymerase adsorption experiments (reprinted with permission from Elsevier) [29].

Xia and colleagues studied prevention of protein adsorption by comparing dynamic and static passivation with polyethylene glycol (PEG) and poly(vinylpyrrolidone) (PVP) on PDMS-glass PCR chips [30]. The solutions containing 10% of polymer were used to pre-coat the surface prior to PCR reaction. In addition, the polymer solutions 0.4% w/v were added into PCR mixes. Figure 10 demonstrates that passivation with 10% PVP 10,000 and PVP 55,000 increased relative PCR efficiency. It has been suggested that polymers with higher molecular weight were trapped in the PDMS matrix. Polymerase could not adsorb on the surface that led to the reduction of surface effects and an increase in PCR efficiency [30].

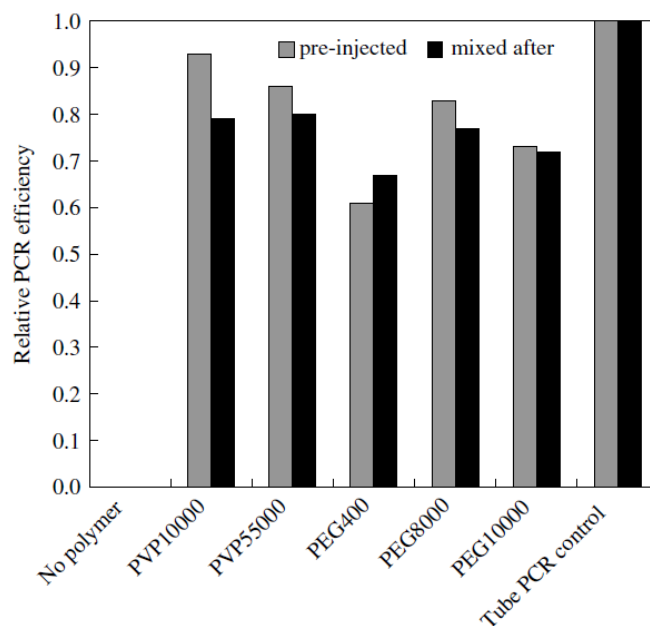


Figure 10. Relative PCR efficiency on PDM-glass chip coated with 10% polymer solutions and polymer solutions added into reaction Mix 0.4% w/v (reprinted with permission from John Wiley and Sons) [30].

One of the possible solutions to biofouling on Teflon-AF surfaces could be the use of Pluronic molecules, which are triblock polymers formed from poly(ethylene oxide) (PEO) and poly(propylene oxide) (PPO) chains. Luk *et al.* demonstrated that the addition of Pluronic F127 (0.08% w/v) into a protein solution significantly reduced adsorption. Figure 11 shows the results of confocal microscopy of FITC-BSA, FITC-Casein, and Alexa Fluor-488Fb with and without a F127 adjuvant (0.08% w/v). Also, it has been determined that the addition of Pluronic F127 showed 1000-fold increase of maximum concentration of a protein permitting droplet to move on the surface without sticky effects [31]. Prevention of protein adsorption on the DMF surfaces is possible due the

formation of ordered Pluronic layers on the oil/water interface. A stabilized interface can eliminate the hydrophobic interactions between proteins and the surface.

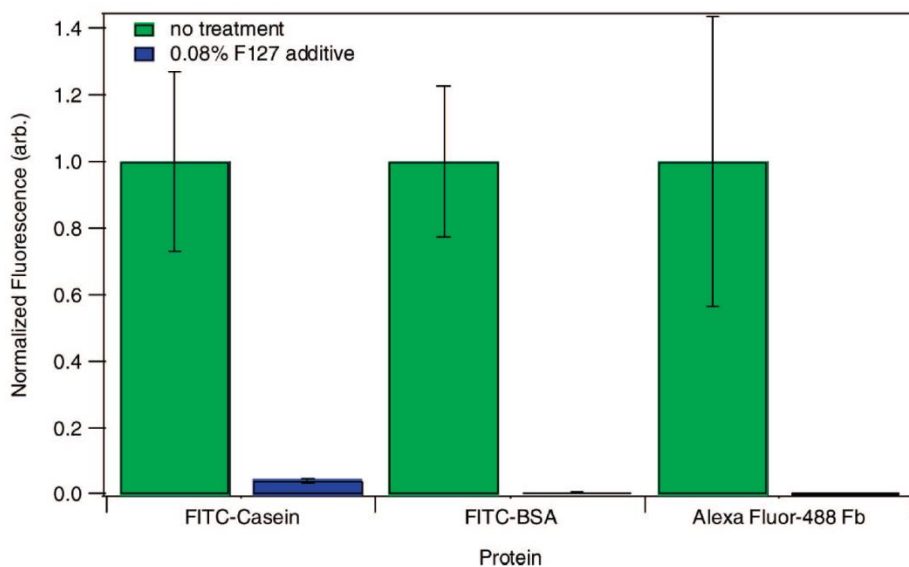


Figure 11. Results of confocal microscopy of Pluronic additive on protein adsorption. (Reprinted with permission from [31]. Copyright (2008) American Chemical Society.

Au *et al.* examined the effects of eight different Pluronic polymers on DMF longevity. The droplets containing 10% fetal bovine serum and 0.02% w/v of Pluronic were moved on the surface until movement failure. Figure 12 shows that Pluronics with PPO chains greater than 30 molecular units (F64, F68, L92, and P105) facilitated droplet movement and prolonged actuation time [32].

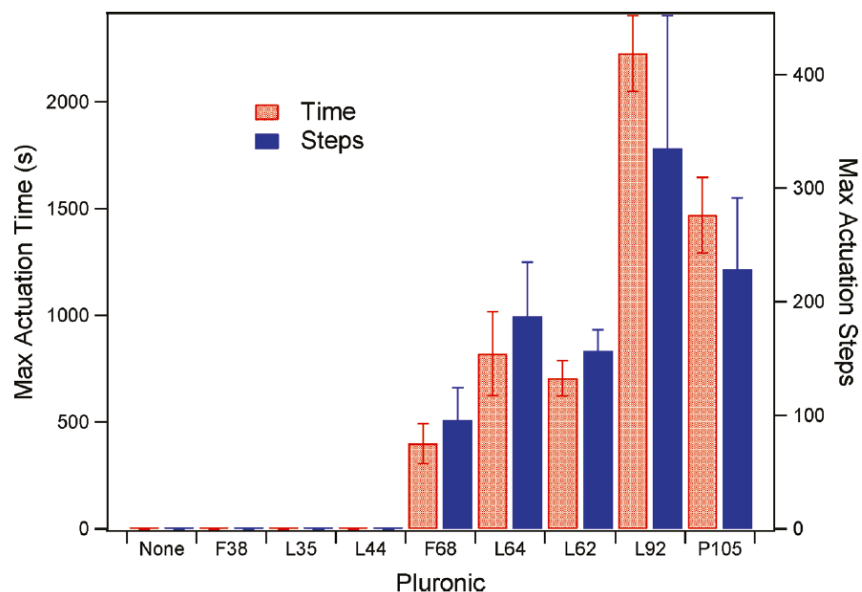


Figure 12. Results of Pluronic type effects on maximum actuation time (Reprinted with permission from ([32]). Copyright (2011) American Chemical Society.

A reduction of actuation voltage on EWOD cartridges prevents nonspecific adsorption of proteins on microfluidic surfaces. At high voltage when the droplets are transported from one energized electrode to another, the oil film between the microfluidic surface and the aqueous droplet breaks down [33]. Under these circumstances, the exposed Teflon surface could easily be contaminated by hydrophobic proteins such as DNA polymerase. Another factor is that the amount of surfactant has to be adjusted for reactions that are carried out at elevated temperatures. The critical micellar concentration of nonionic surfactants such as Tween 20 decreases with temperature [34]. Thus, less surfactant is needed for reduction of a surface tension at high temperatures. According to Yehezkel *et al.*, the amount of Tween 20 for the Mondrian™ SP microfluidic cartridge

should be 0.01-0.05%, and the operation voltage during thermocycling should be 90 V [20].

### 2.3 Reduction of Errors in Synthetic Genes

Genes that are assembled from oligonucleotides typically contain errors that can significantly alter the quality or expression of target proteins. It has been reported in the literature that the majority of the errors in genes originated from the oligonucleotide synthesis. Some errors are introduced during PCR, but the rate is sufficiently low [14, 16]. During DNA assembly, oligonucleotides are used as templates for complementary strand synthesis. If the oligos contained errors, the complementary strand will have them as well. Furthermore, the assembly is usually followed by an amplification step, in which the errors will be propagated with each cycle. As the result, genes synthesized from oligonucleotides will almost always have errors. Screening for mutations and sequencing are necessary steps for obtaining high quality error-free genes, but these steps are expensive and time-consuming. There are error correction methods that can improve the quality of synthetic genes. If assemblies have less mistakes, the number of screened colonies will be lower, with a consequent reduction in time and cost. Current error correction methods are based on DNA mismatch removal by mismatch cleaving enzymes. Several researchers investigated enzymatic error correction of synthetic genes.

Fuhrman and colleagues tested the effectiveness of three enzymes: T7 endonuclease I, T4 endonuclease VII, and *E.coli* endonuclease V on removing mutations from synthetic genes [35]. It has been shown that T4 endonuclease VII and *E.coli* endonuclease V were effective in reduction of insertions and deletions, but T4 endonuclease required 24 hours

to achieve the same level of correctness as *E.coli* endonuclease V produced in 4 hours [35].

Kosuri and colleagues used a commercially available enzyme mix, ErrASE. The mix contains resolvases that target and cleave mismatches as well as additional enzymes that remove cleaved fragments from the sequence. Six different enzyme concentrations were tested. All experiments resulted in successful error removal, but the highest concentration was chosen. After error correction, the assemblies were cloned and screened for errors. The group found that the error rate after the treatment with ErrAse was 1/7,170 bp (0.13 errors/kb). By comparison, the average error rate was 1/250 bp (4 errors/kb) before the ErrASE treatment [36].

Quan *et al.* used a commercial Surveyor nuclease enzyme to correct errors. The Surveyor nuclease is a mismatch-cleaving enzyme that is specifically used for a gene mutation identification. The group performed denaturation and renaturation of assemblies followed by an enzymatic treatment. Furthermore, DNA was amplified by PCR. The researchers observed a 10-fold error reduction in samples that were treated by the nuclease [15].

Surveyor nuclease was used by Saaem *et al.* to repair chip synthesized genes. As shown in Figure 13, DNA fragments were denatured and allowed to reanneal to form heteroduplexes. Mismatches in heteroduplexes were cleaved during incubation with Surveyor exonuclease. During PCR, single-stranded overhangs were chewed back by the proofreading activity of Phusion polymerase, and corrected sequences were amplified [37]. The researchers tested 20 min and 60 min incubation times as well as two rounds of

error correction against one round. Figure 14 demonstrates that the strategy of implementing multiple iterations of error correction was more effective than increasing the incubation time. The sequencing results showed that two rounds of error correction with 60 min incubation time reduced errors from 0.26 to 0.11 errors/kb, which was 58% error reduction compared to a single round of error correction [37].

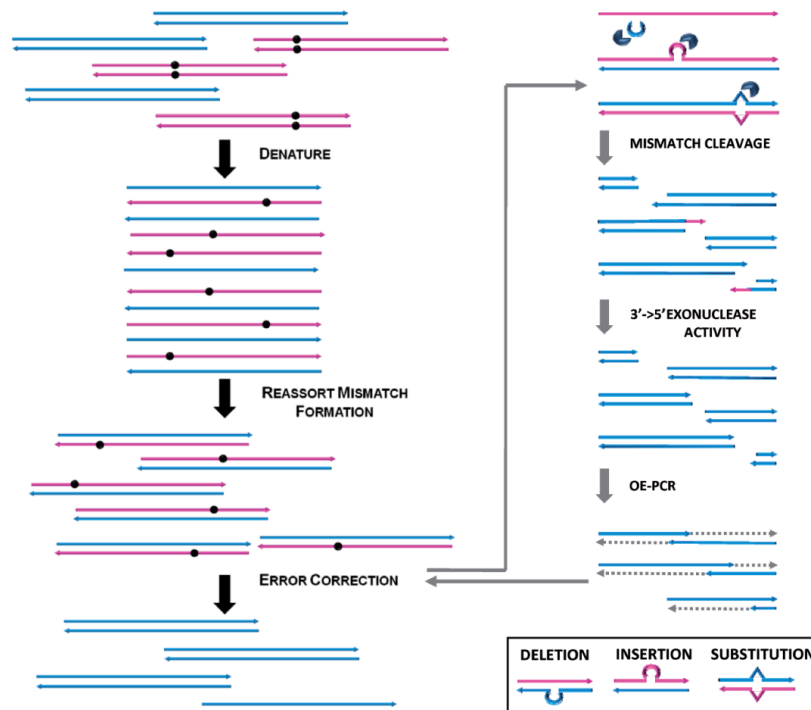


Figure 13. Schematic of error correction procedure (reprinted with permission from Oxford University Press) [37].

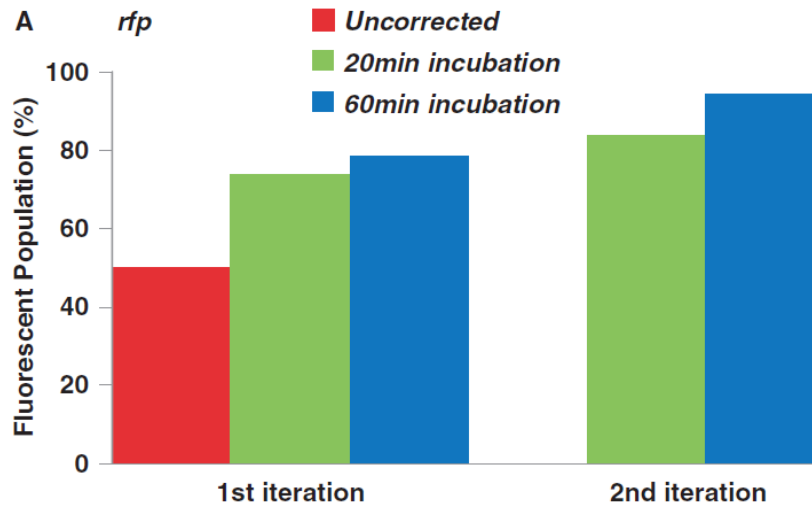


Figure 14. Effect of incubation times and iterations on error correction results (reprinted with permission from Oxford University Press) [37].

According to the Gibson group, error reduction in synthetic genes was even more efficient when Surveyor nuclease treatment was followed by Exonuclease III treatment (Dan Gibson, personal communication). The error frequency was reduced from 0.6 errors/kb to 0.16 errors/kb. The method of error reduction by simultaneous action of Surveyor and Exonuclease III was disclosed [38].

Sequeira *et al.* demonstrated an effective error reduction in synthetic genes based on T7 endonuclease I. It was determined that the enzyme improved fidelity of genes by 8-fold with an error frequency reduction from 3.45 errors/kb to 0.43 errors/kb. Endonuclease was effective at reduction of deletions and insertions, but it increased the rate of substitutions. In contrast, the error frequency of the samples treated with CorrectASE™ enzyme was 1.22 errors/kb. The CorrectASE™ reduced deletions, but increased substitutions and insertions [39].



## 2.4 Literature Review Summary

Different methods for obtaining error-free synthetic genes were discussed in the literature. It has been shown that various assembly methods can be used for microfluidic gene assembly. Gibson assembly has the potential for miniaturization since it is an isothermal process. Additionally, one pot reactions are the most suitable for microfluidic applications because they save time and prevent cross-contamination and reagent losses.

Polymerase chain reaction is extensively used in DNA synthesis. However, microfluidic PCR is not as effective as conventional PCR due to surface effects. Erill *et al.* determined that the adsorption of polymerase on microfluidic surfaces reduces reaction efficiency [29]. Numerous methods have been developed in order to overcome polymerase adsorption. Among those methods is increase of polymerase concentration, addition of BSA and Pluronics, reduction of actuation voltage as well as pre-passivation with PEG.

Error correction of synthetic DNA utilizing mismatch-cleaving enzymes has been used for the reduction of errors. Saaem *et al.* demonstrated that two rounds of error correction with Surveyor endonuclease reduced error rates by 58% over a single round of error correction, with a final error rate of 0.1errors/kb [37]. Gibson *et al.* demonstrated a two-step error reduction method with Surveyor nuclease and Exonuclease III [38]. Improvement of sequence fidelity was also achieved with T7 endonuclease [39]. Enzymatic error correction has never been reported on microfluidic devices. Thus, more research is needed in order to develop an effective error-free gene assembly protocol.

## CHAPTER THREE

### RESEARCH OBJECTIVES

#### 3.1 Research objectives

The purpose of this research is to develop a robust and accurate DNA assembly protocol that utilizes the Mondrian™ SP digital microfluidic device manufactured by Illumina, Inc. The research consists of three objectives. The first objective is to program a protocol using automated microdroplet generation and routing. The second objective is to determine suitable operation conditions for three reactions: Gibson assembly, polymerase chain reaction, and enzymatic error correction. Finally, these reactions are combined in a single protocol that is utilized for the assembly of 12 oligos with two CorrectASE™ treatments on the microfluidic device. The third objective is to verify the effectiveness of DNA assembly and enzymatic error correction methods by Sanger sequencing.

#### 3.2 Justification

Rapid and cost-effective synthesis of error-free genes remains one of the main challenges in synthetic biology. Digital microfluidic devices offer an opportunity to automate and simplify complicated procedures. Electrowetting-on-dielectric systems allow precise generation of microdroplets in the nanoliter to microliter range. The same volumes cannot be accurately measured by a conventional micropipette. An increase in the throughput of gene assembly is achieved by parallelization of reactions and the reduction of reaction volume. Integration of effective DNA assembly and error correction protocols on the DMF device reduces the time and cost of DNA assembly.

## CHAPTER FOUR

### MATERIALS AND METHODS

The main goal of this study was to develop a robust and reliable DNA assembly and error correction protocol for the Mondrian™ SP DMF device provided by Illumina, Inc. A partial sequence (339 bp) originated from the human influenza virus hemagglutinin (HA) gene was assembled from 12 oligonucleotides and error corrected twice. The whole protocol involved six consecutive enzymatic reactions. Prior to incorporating the six enzymatic steps of the gene synthesis in a complete protocol, each enzymatic step was performed separately to find the most favorable reaction conditions. The details on how suitable operation procedures were established are described in subsequent sections. The experiments were carried out on Mondrian™ SP DMF cartridges. All liquid handling operations were programmed using the Application Development Environment software (Illumina, Inc.).

#### 4.1 Equipment

##### 4.1.1 Mondrian™ SP Microfluidic Device

The experiments were performed on the Mondrian™ SP microfluidic system. As shown in Figure 15, the system included a device that was connected to a computer and digital microfluidic cartridges that were inserted into the device. To observe the behavior of the microscopic droplets, the device was connected to a digital camera that produced a magnified image of the DMF cartridge onto a screen. Figure 16 shows a microfluidic Mondrian™ SP cartridge that was used in the experiments. The cartridge consisted of two plates, a glass top and a printed circuit board (PCB) substrate. The area between the

plates was filled with a 2 cSt silicone oil. The configuration of the DMF cartridge allowed eight processes to be performed in parallel. The reagents were loaded through ports on the cartridge, and the samples were withdrawn through other ports. The microfluidic cartridge had three heater bars that contacted the back of the PCB, which was used to set temperatures for the enzymatic reactions. Additionally, the cartridge could be cooled down with Peltier device. The device was operated by the Application Development Environment software. Prior to each experiment, a program was designed to direct droplets' liquid handling operations. The device was operated at a voltage of 90 V or 300 V and a frequency of 30 Hz.

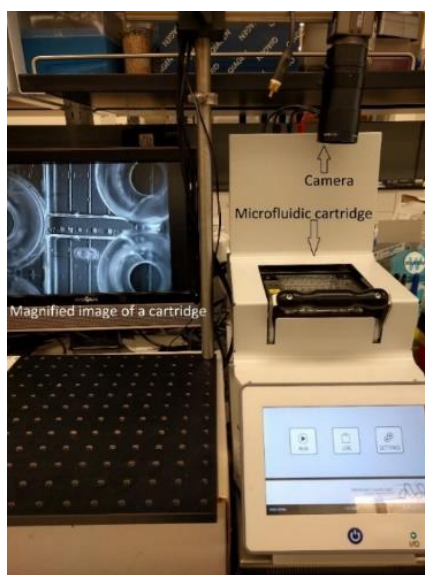


Figure 15. An image of the Mondrian™ SP device used in this study.

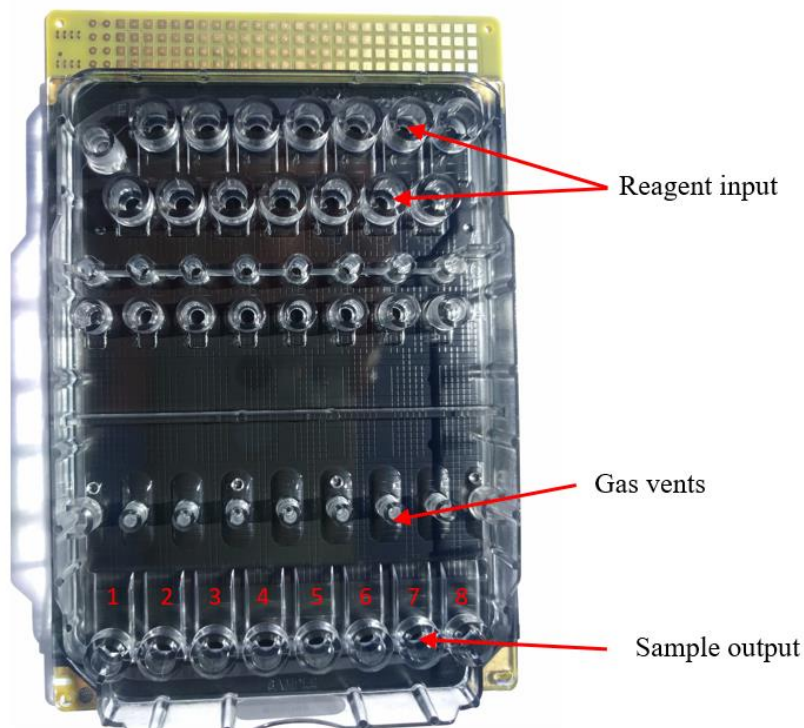


Figure 16. An image of Mondrian™ SP microfluidic cartridge.

The liquid volumes of 0.3, 0.6, and 1.2  $\mu\text{L}$ , referred to as 1X, 2X, and 4X droplets, respectively, were generated and manipulated on the microfluidic cartridge. As seen in Figure 17, to dispense a 1X droplet, three electrodes adjacent to the reagent input port were activated, which caused the liquid to spread over three electrodes. Then, the electrode #2 was switched off. The double 2X droplet was dispensed by turning off the electrode #3. To create a 4X droplet, the electrode between two 2X droplets was turned on.

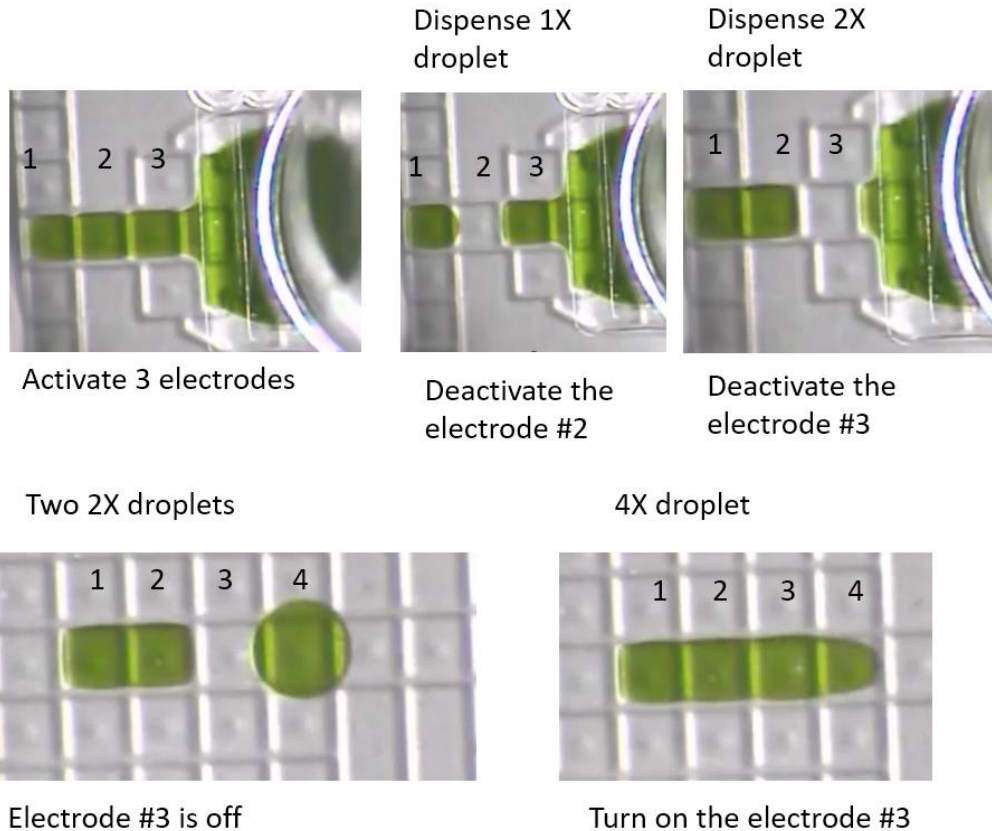


Figure 17. Generation of 1X, 2X, and 4X droplets on the DMF.

#### 4.1.2 Bacterial Electroporation Transformation Equipment

A Bio-Rad Gene Pulser II Porator electroporation system, shown in Figure 18, was used to transform *E. coli* cells with recombinant DNA. The system consisted of electroporator, pulse chamber, cuvette cell holder, and 0.1 cm cuvettes. It was operated at 25  $\mu$ F and 1.8 kV. The electroporation cuvette with *E. coli* cells and synthetic DNA was put in a cuvette holder that was inserted into the pulse chamber. The cells were subjected to a voltage that created pores in cell membranes allowing synthetic DNA to pass to the inside of the cells.

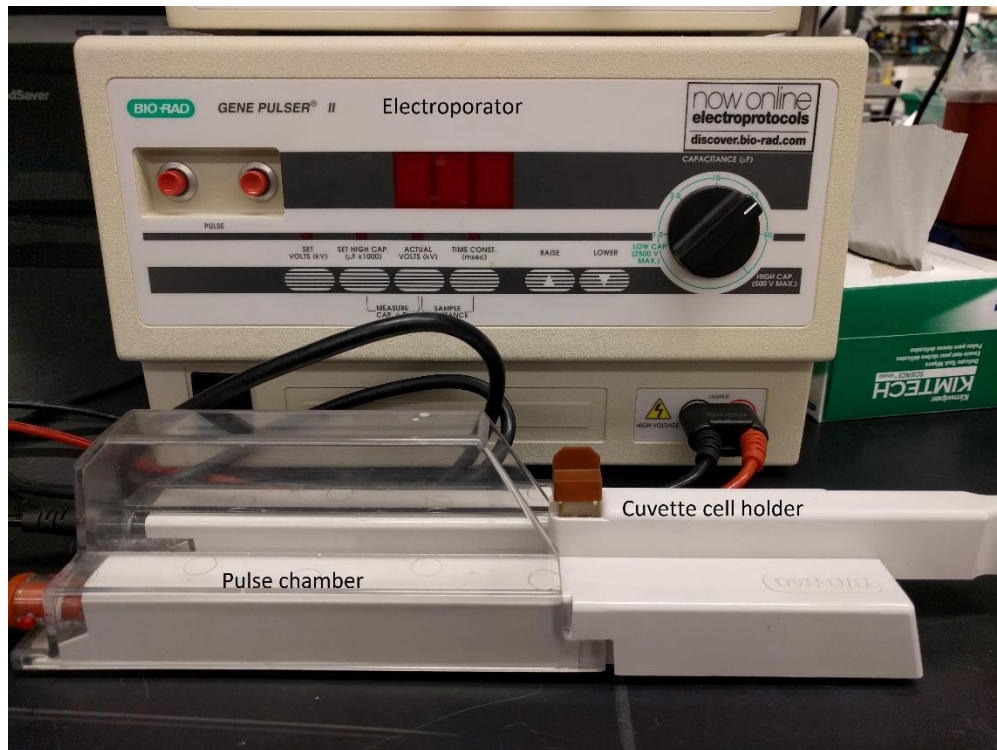


Figure 18. Bio-Rad Gene Pulser II Porator electroporation system.

#### 4.1.3 DNA Analysis Equipment

The presence and size of nucleic acids were analyzed by DNA gel electrophoresis. The samples were loaded on a 2% agarose gel that was inserted in an electrophoresis chamber. The chamber was filled with 1X TAE electrophoresis buffer (Thermo Fisher Scientific) and connected to the power source. When the gel was subjected to an electric current, DNA molecules migrated from a negative electrode to a positive electrode.

The concentration of DNA samples was measured using a NanoDrop ND-1000 spectrophotometer, shown in Figure 19. The NanoDrop instrument is designed to measure DNA absorbance at 230 or 260 nm. To measure concentration, a 1  $\mu$ L sample was pipetted on a lower sample pedestal. Then, the sample was locked between the

lower pedestal and a sample arm, and the absorbance was measured. The concentration of nucleic acids in  $\text{ng}/\mu\text{L}$  was calculated and displayed by the system software installed on a computer connected to the instrument.

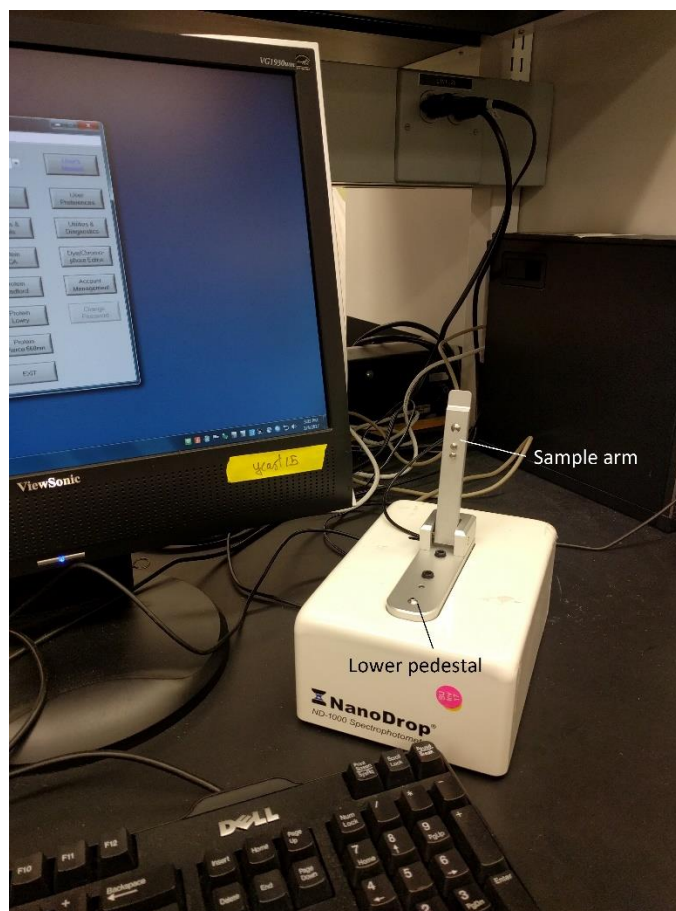


Figure 19. An image of the NanoDrop ND-1000 instrument.



## 4.2 Experimental Procedures for Microfluidic Polymerase Chain Reaction

Amplification of assembled DNA by polymerase chain reaction is the second step of gene assembly. In order to develop a successful DNA assembly protocol, PCR performed on the DMF cartridge must be robust and reliable. Microfluidic PCR is challenging for the reasons discussed in Chapter 2. The first challenge for the process used in this study was to demonstrate that PCR could be performed on the microfluidic device. The second challenge was to prevent biofouling of the DMF cartridge. The subsequent subsections detail the experiments and logic designed to achieve the following objectives.

- Determine PCR reagents that lead to successful and consistent DNA amplification on the microfluidic device.
- Improve the on-cartridge droplet transfer process during PCR – reduce biofouling.
- Automate droplet generation and routing for PCR.

The materials used in the following subsections are shown in Appendix A.

### 4.2.1 Optimization of PCR Reagents

In this section the experiments were performed to determine reagent compositions for successful microfluidic PCR. It was established in preliminary benchtop experiments that 30 cycles of PCR amplification were sufficient to obtain a band that was visualized by DNA electrophoresis. According to Erril *et. al*, microfluidic amplification of DNA was improved by increasing the concentration of polymerase [29]. Thus, the amount of Phusion polymerase was increased by 5-fold in a basic microfluidic protocol. Table 2 shows the DMF protocol that was used as a baseline for microfluidic PCR experiments.

Table 2. Basic microfluidic PCR protocol.

Reagent	Concentration
Phusion detergent-free buffer (Thermo Fisher Scientific)	1X
Forward and reverse PCR primers (IDT DNA)	0.8 $\mu$ M
HA-049 DNA template (Prepared by the J. Craig Venter Institute)	1.75 ng/ $\mu$ L
Tween 20 (Sigma Aldrich)	0.0025%
Phusion polymerase (Thermo Fisher Scientific)	0.1 U/ $\mu$ L
DNase, RNase-free UltraPure™ DI water (Invitrogen)	Up to a final volume

Many experiments were conducted utilizing the basic microfluidic PCR protocol. None of these attempts were successful because no amplification was achieved. By trial and error, it was determined that PCR worked using templates that had previously been assembled using Gibson assembly. It was hypothesized that Gibson isothermal (iso) buffer or additional Phusion was responsible for the improvement of PCR performance. The experimental plan to determine appropriate PCR reagents for this study is shown in Table 3.

Run 1 was performed to mimic reagents of the PCR reaction that was done after Gibson assembly. Since the Gibson reaction contains Gibson iso buffer and Phusion polymerase, the addition of extra Phusion or the iso buffer or a combination of both was tested. For these experiments, the baseline microfluidic protocol was modified. The difference between the reactions was that one contained additional 1X Gibson iso buffer and 0.025 U/ $\mu$ L of Phusion polymerase. The second master mix had only additional 0.025 U/ $\mu$ L of Phusion while the third mix contained only additional 1X Gibson iso buffer. The last sample was a negative control, so there were no additional reagents. The

experiments conducted in Run 1 demonstrated that the iso buffer remaining from the Gibson assembly reaction improved amplification yield.

Table 3. Experimental design to determine microfluidic PCR conditions.

Run No.	Treatment type	Variables (final concentrations in reaction)
1	Mimic the same conditions as PCR after assembly reaction	0.125 U/ $\mu$ L Phusion
		0.125 U/ $\mu$ L Phusion + 1X Gibson iso buffer
		1X Gibson iso buffer
		Control – 0.1 U/ $\mu$ L Phusion
2	PCR with PEG against the iso buffer	1 mM MgCl <sub>2</sub>
		1.25 mM PEG 8000
		0.2 mM NAD
		2 mM DTT
3	PCR with combination of PEG and the other components of Gibson iso buffer	1X Gibson iso buffer
		1.25 mM PEG + 1 mM MgCl <sub>2</sub>
		1.25 mM PEG + 0.2 mM DTT
		1.25 mM PEG + 2 mM NAD

In Run 2, four individual components of Gibson iso buffer were tested to see which component was responsible for the PCR improvement. To prepare reagents for Run 2, four different solutions were mixed. The amount of polymerase, polymerase buffer, dNTPs, Tween 20, and PCR primers was kept the same as in Table 2. The only difference was that each master mix contained either additional 1 mM MgCl<sub>2</sub>, 1.25 mM PEG 8000, 0.2 mM NAD or 2 mM DTT. The results of Run 2 demonstrated that addition of PEG 8000 slightly improved the amplification yield, but it was not as effective as with the iso buffer additive.

Run 3 was conducted to see if the combination of PEG 8000 and one of other three components of the iso buffer were responsible for successful amplification on the DMF cartridge. To prepare reactions for Run 3, a combination of 1.25 mM of PEG 8000 with

either 1 mM MgCl<sub>2</sub>, 0.2 mM NAD or 2 mM DTT were tested against the 1X iso buffer. The rest of the reagents were prepared according to Table 2. The results of Run 3 demonstrated good amplification of DNA when the reaction was supplemented with extra MgCl<sub>2</sub>, Phusion, and PEG 8000.

#### 4.2.2. Reduction of Phusion Polymerase Adsorption During Microfluidic PCR

Microfluidic PCR was very challenging due to surface contamination with Phusion polymerase. The experiments showed that during microfluidic PCR, droplets in the 98 °C zone were not wetting activated electrodes. At these conditions, the oil/water interface became unstable, and the polymerase was adsorbed on the microfluidic surface. When the polymerase stuck to the surface, it reduced the amount of enzyme available for the reaction. Another issue encountered was that the droplets were releasing gas bubbles. The resulting air bubbles were blocking pathways, pushing droplets off the electrodes and out to the gas vents. This made it difficult to transport the droplets in a reproducible manner and to retrieve samples from the cartridge.

Multiple methods discussed in Chapter 2 were used to strengthen the oil/water interface of a liquid droplet. The experimental plan shown in Table 4 was designed with the aim to reduce polymerase adsorption on the microfluidic surface, to improve the droplet fluidics in the hot zone of the cartridge, and to achieve the same level of amplification as on the benchtop.

It has been shown by Erril *et al.*, that the addition of bovine serum albumin (BSA), which formed stronger hydrophobic interactions with the microfluidic surface, prevented adsorption of polymerase on the microfluidic surface and reduced the amount of enzyme

to achieve good amplification [29]. Run 1 was performed to see if the addition of 0.1  $\mu\text{g}/\mu\text{L}$  of BSA would prevent Phusion polymerase adsorption on the microfluidic surface, increase PCR yield, and reduce the amount of enzyme needed for successful amplification. For Run 1, four reactions were performed. The amount of Phusion was varied to observe the effect of BSA on adsorption. In each reaction, the concentration of Phusion was either 0.02, 0.08, 0.14, or 0.2  $\text{U}/\mu\text{L}$ , which was 1X, 4X, 7X, and 10X amount of enzyme relative to a standard benchtop PCR. If PCR worked at 1X Phusion concentration, it would suggest that the adsorption was eliminated. Alternatively, amplification of DNA with 4X and 7X Phusion indicated some reduction of adsorption. Amplification with 10X Phusion would demonstrate no reduction of adsorption. The final concentration of reagents in PCR mixes were 1X HF detergent-free buffer, 0.25 mM of each dNTP, 0.8  $\mu\text{M}$  of forward and reverse primers, 0.14  $\text{ng}/\mu\text{L}$  DNA template, 0.0025% of Tween 20, 1.25 mM PEG 8000, 1 mM  $\text{MgCl}_2$ , and DI water up to a volume of 50  $\mu\text{L}$ .

Since Au *et al.* demonstrated that Pluronic substances improved droplet transfer of concentrated protein solutions and reduced protein adsorption, Pluronic F68 was added to PCR reactions [32]. Runs 2 and 3 were performed to see if Pluronic F68 could strengthen the oil/water interface of a droplet and prevent polymerase adsorption. In Run 2, the concentration of Pluronic F68 was kept constant while the concentration of polymerase varied. The reaction mixes were prepared the same way as in Run 1, but instead of BSA, Pluronic F68 was added in a final concentration of 0.02% w/v. To

optimize the amount of Pluronic F68, in Run 3, the concentration varied from 0.04% to 0.1%.

Table 4. Experimental design for polymerase adsorption.

Run No.	Treatment type	Final concentration of Phusion polymerase in PCR	Variables (final concentrations)	
1	Addition of BSA	0.02 U/ $\mu$ L of Phusion	0.1 $\mu$ g/ $\mu$ L of BSA	
		0.08 U/ $\mu$ L of Phusion		
		0.14 U/ $\mu$ L of Phusion		
		0.2 U/ $\mu$ L of Phusion		
2	Addition of Pluronic F68	0.02 U/ $\mu$ L of Phusion	0.02% w/v of Pluronic F68	
		0.08 U/ $\mu$ L of Phusion		
		0.14 U/ $\mu$ L of Phusion		
		0.2 U/ $\mu$ L of Phusion		
3	Addition of Pluronic F68 at different concentrations	0.02 U/ $\mu$ L of Phusion	0.04% w/v of Pluronic F68	
			0.06% w/v of Pluronic F68	
			0.08% w/v of Pluronic F68	
			0.1% w/v of Pluronic F68	
4	Pre-coat lanes with different types of PEG	0.02 U/ $\mu$ L of Phusion	10% w/v PEG 8000	
			10% w/v PEG 6000	
			10% w/v PEG 4000	
			10% w/v PEG 3350	
5	Pre-coat lanes with PEG 8000	0.02 U/ $\mu$ L of Phusion	10% w/v PEG 8000	
				0.08 U/ $\mu$ L of Phusion
				0.14 U/ $\mu$ L of Phusion
				0.2 U/ $\mu$ L of Phusion
6	Reduction of actuation voltage	0.02 U/ $\mu$ L of Phusion	90 V	

Xia *et al.* demonstrated that biofouling could be greatly reduced if the microfluidic surface was pre-coated with different molecular weight PEG solutions [30]. In Runs 4 and 5, different types of PEG were tested to see if this approach worked for the microfluidic device used in this study. In Run 4, the experimental lanes were coated with 10% w/v solutions of PEG 8000, PEG 6000, PEG 4000, and PEG 3350. The

amplification was carried with the same amount of Phusion polymerase as on benchtop to see if the adsorption of the enzyme was eliminated. In Run 5, the experimental lanes were coated with 10% PEG 8000, and the concentration of Phusion varied.

Yehezkel *et al.*, carried out PCR on the Mondrian™ SP cartridge at a reduced voltage of 90 V [20]. Thus, Run 6 was performed to see if lower actuation voltage improved droplet movement between the denaturation and annealing zones. The reaction mix was prepared with the same final concentration of HF detergent-free buffer, dNTPs, DNA template, PCR primers, Tween 20, MgCl<sub>2</sub>, and PEG 8000 as in Run 1. The concentration of Phusion was 0.02 U/μL, which is a standard amount of enzyme used in a benchtop PCR.

Pluronic solutions of 0.02%, 0.04%, 0.08%, and 0.1% were prepared from a 10% stocks of Pluronic F68 by mixing it with DI water. To prepare 10% w/v PEG 8000, PEG 6000, PEG 4000, and PEG 3350, 1 g of solute was dissolved in 10 mL of DI water. The solutions were mixed in a shaker until the solute was completely dissolved. Forward and reverse primers were prepared from 100 μM stock solutions by diluting 10 μL of each in 80 μL of DI water. A blend of 25 mM dNTPs was prepared from 100 mM deoxynucleotide kit by mixing equal amounts of dATP, dGTP, dCTP, and dTTP. Diluted deoxynucleotides and primers were stored at -20 °C in the freezer.

#### 4.2.3 Automation Program for Microfluidic PCR

To perform microfluidic amplification experiments shown in Tables 2 and 3, an automation program for the DMF was developed. The reactions were carried out in 1.2 μL droplets, which are described in this manuscript as 4X. The droplets were brought to

the PCR area, which consisted of two temperature zones. The denaturation zone was set to 98 °C, and the annealing/extension zone was set to 72 °C.

The thermocycling procedure for experiments in Table 3 and Runs 1-5 in Table 4 is described below. During thermocycling, the droplets were moved at a speed of 3 s/electrode. There was no need to hold the droplets in the denaturation area because the slow transport took about 5-10 s, which was a sufficient time at 98 °C for denaturation. In the 72 °C area, the droplets were oscillated for 10 s to allow enough time for primer annealing and polymerase extension. Oscillation of the droplets in the 72 °C area was achieved by activation and deactivation of the electrodes every 500 ms. When thermocycling was finished, the heater responsible for denaturation zone was shut down, and the droplets were held at 72 °C for 5-10 min to allow final extension. After the final extension, the reaction products were brought to the collection reservoirs and recovered manually.

The thermocycling procedure was modified for Run 6 in Table 3. The droplets were transported to the area where the voltage was reduced to 90 V. Then, the droplets were moved to the 98 °C zone where they were held for 30 s to perform initial denaturation. After, 30 cycles of PCR were performed. During thermocycling, the droplets were transported from 98 °C to 72 °C at 1.5 s/electrode, and from 72 °C to 98 °C at 1 s/electrode. Annealing/extension was done by oscillation of the droplets at 72 °C for 20 s, and denaturation was performed by holding the droplets at 98 °C for 10 s. After 30 cycles of PCR, DNA was held for 10 min at 72 °C to allow final extension. Then, the



voltage was switched back to 300 V, so the samples could be transported to the collection reservoirs.

#### 4.3 Experimental Procedures for Microfluidic Gibson Assembly

The experiments described in subsequent subsections were performed to achieve following objectives.

- Optimize microfluidic Gibson assembly of 12 oligos.
- Optimize dilution of assembly product prior to PCR.
- Determine PCR conditions that lead to a consistent amplification of assembly products.
- Develop an automation program for Gibson assembly followed by PCR.

A comprehensive list of reagents used in Gibson assembly is shown in Appendix A.

##### 4.3.1 Optimization of Gibson Assembly Reaction Time and Determination of Suitable Reagent Concentrations

The experiments described in this subsection were performed to determine suitable operation conditions for Gibson assembly on the DMF. The reaction time was investigated. Additionally, the assembly process was performed with and without T5 exonuclease. The experiments were conducted according to Table 5.

It has been shown in the literature that typical assembly time is 15-60 minutes [22]. Run 1 tested the reaction time on the microfluidic cartridge. The reaction was performed in the presence of T5 exonuclease. The final concentration of oligos in the reaction was 250 nM.

The main function of T5 exonuclease is to chew back DNA in a 5' to 3' direction and expose overhangs for annealing of two dsDNA strands. However, when oligos are

assembled, exonuclease can degrade them. In Run 2, the experiments were set up to see the influence of T5 exonuclease on the assembly of 250 nM oligos. The reactions were performed in different droplets to investigate reproducibility.

Table 5. Microfluidic DNA assembly experiments.

Run No.	Oligonucleotide concentration in assembly reaction (mole)	Assembly time (min)	Presence of T5 exonuclease in assembly master mix
1	250 nM	15 min	Present
		30 min	
		45 min	
		60 min	
2	250 nM	60 min	Not present
			Present

In each experiment, 50  $\mu$ L master mixes were made from fresh reagents. Assembly, oligo, and PCR master mixes were prepared with the double amounts of reagents. Equal size droplets were merged on the cartridge, to obtain a 1X final concentration. The oligo master mix was prepared by the dilution of a 1  $\mu$ M stock solution in DI water. The oligo mix also contained 0.01% of Tween 20. The surfactant was a necessary component to reduce a surface tension, which facilitated droplet dispensing and movement. The amount of surfactant was determined for each individual master mix. The enzymes suspended in storage buffers contain stabilizers. It was observed that the droplets with enzyme solutions were easily dispensed and manipulated on a cartridge without any additional surfactant. Thus, the assembly master mix and PCR master mix did not contain Tween 20. The final concentrations of reagents in the assembly reaction were 1X

isothermal (iso) buffer, 0.05 U/ $\mu$ L of Phusion polymerase, 4 U/ $\mu$ L DNA ligase, 0.08 U/ $\mu$ L T5 exonuclease, and 250 nM oligos.

Prior to mixing with assembly reagents, 1  $\mu$ L of exonuclease was diluted by 10-fold in 8  $\mu$ L of water and 1  $\mu$ L of Buffer 4. For the assembly experiments without exonuclease, T5 exonuclease was omitted. Gibson assembly iso buffer was prepared as 6 mL batch, and 500  $\mu$ L aliquots were stored at  $-20$  °C. The components of the buffer were 500 mM Tris-HCl (pH 7.5), 50 mM MgCl<sub>2</sub>, 1 mM of each deoxynucleotide, 50 mM of DTT, 25% of PEG-8000, and 5 mM of NAD [38]. The amplification reaction was composed of 1X HF detergent-free buffer, 0.25 mM of dNTPs, 0.4  $\mu$ M of each forward and reverse primers, 0.1 U/ $\mu$ L of Phusion polymerase, 0.625 mM PEG 8000, and 0.5 mM MgCl<sub>2</sub>.

#### 4.3.2. Optimization of Dilution Prior to Amplification and Determination of PCR Conditions

Additional experiments were performed to determine the optimum dilution of the assembly product before PCR. This step of the assembly process was very important because the dilution allowed the removal of unreacted oligos, misassembled sequences, and Gibson assembly reagents before the amplification. The experiments shown in Table 6 were performed to find the maximum possible dilution. Also, the amplification of the assembly product was optimized.

Table 6. Experimental design to study optimization of the microfluidic DNA assembly process.

Run No.	Oligo concentration	Dilution rate before PCR	PCR conditions (final concentration)
1	250 nM	2-fold	0.1 U/ $\mu$ L Phusion
		4-fold	
		8-fold	
		16-fold	
		32-fold	
		64-fold	
		128-fold	
2	50 nM	8-fold	0.02 U/ $\mu$ L Phusion
			0.1 U/ $\mu$ L Phusion
		16-fold	0.02 U/ $\mu$ L Phusion, 0.5 mM MgCl <sub>2</sub> , 0.625 mM PEG
			0.1 U/ $\mu$ L Phusion, 0.5 mM MgCl <sub>2</sub> , 0.625 mM PEG

In Run 1, the assembly products were diluted from 2-fold to 128-fold and amplified by PCR using the baseline microfluidic protocol shown in Table 2.

The results of Run 1 demonstrated that the dilution of the assembly product over 16-fold did not produce the correct assembly product. Thus, the 8-fold and 16-fold dilutions were tested in Run 2. The reactions were carried out to determine if the same dilution held for the 50 nM oligo assembly. Additionally, four different PCR conditions were tested to see which combination gave the best amplification of the assembly products. The first reaction had the same reagents as a standard benchtop PCR, and a second contained a 5-fold increase in the amount of Phusion. The third and fourth reaction were supplemented with 0.5 mM MgCl<sub>2</sub> and 0.625 mM of PEG 8000, and the amount of Phusion was 1X and 5X, respectively.

### 4.3.3 Automation Program for Microfluidic DNA Assembly

The first step of the process was setting up the device with an electrowetting voltage of 300 V and a frequency of 30 Hz. Then, the temperature in the assembly area was set to 50 °C. Next, the droplets containing oligos were dispensed. The droplets were transported to a waiting area where they were held while another dispenser generated Gibson master mix droplets. The assembly droplets were merged with the oligo droplets and brought to the assembly area where they were incubated for 15-60 min at 50 °C. To ensure adequate mixing, the droplets were shuttled up and down. When the reaction was finished, the assembly droplets were merged with the 2X PCR droplets, so the total volume of each droplet became 1.2  $\mu$ L. The polymerase chain reaction was performed as described in Section 4.2.3. After amplification, the droplets were moved to the collection reservoirs and recovered from the cartridge manually. For the experiments described in Table 6, a dilution step before PCR was added to the program. To perform dilutions, a dispenser containing DI water and 0.05% Tween 20 generated double droplets. Then, the droplets were merged with the assembly droplets, mixed, and split into two equal size droplets. This step was iterated to achieve the dilutions shown in Table 6.

When assembly time was variable, for example in Run 1 in Table 5, 2X droplets containing both the oligos and Gibson assembly reagents were held in a waiting area, and two droplets were moved to the assembly incubation zone in 15 min increments. This way, each condition was tested twice in two different experimental droplets.

#### 4.4 Procedures for development of the Automation Protocol for Gibson Assembly with Two CorrectASE™ Treatments

This section describes the steps in the development and validation of automation protocols for Gibson assembly with two rounds of error correction. The following objectives were investigated at this stage of the study.

- Determine temperature settings and droplet routing procedure for microfluidic error correction.
- Combine Gibson assembly, PCR, and enzymatic error correction in a single automation program.
- Develop experimental protocols for Gibson assembly of 12 oligos with two CorrectASE™ treatments.
- Test DNA assembly with error correction protocols on the Mondrian™ SP device.

##### 4.4.1 Determination of Temperature Settings for Error Correction Experiments

Enzymatic error correction experiments were conducted with a commercial enzyme CorrectASE™. The protocol provided by the manufacturer included four steps: denaturation, annealing, error correction reaction with the enzyme, and PCR amplification. As shown in Figure 20, to expose the errors in the DNA sequence, double strands have to be separated and reannealed. When the strands come together, they form heteroduplexes at mismatch sites that can be identified and removed by the error correction enzyme. During the denaturation step, DNA is diluted to 20-25 ng/μL in 1X CorrectASE™ buffer to a final volume of 50 μL and incubated at 98 °C for 2 min, 4 °C for 5 min, and 37 °C for 5 min. Then, 10 μL of DNA are mixed with 1 μL of CorrectASE™ and incubated at 25 °C for an hour. After error correction, DNA is PCR amplified.

In order to meet denature/annealing temperature requirements, several empty cartridge tests were conducted. A program was created in which heating and cooling of the cartridge was monitored. It was important to determine how quickly the denaturation area of the cartridge heated up to 98 °C, and how far heat extended throughout the denature/annealing zones. To perform this experiment, heater bar #1 situated under the denaturation area was set to 98 °C. To create conditions for annealing, two more heater bars, #2 and #3, were set to 37 °C and 25 °C, respectively. The heater #1 was shut down after 11 min, and the heater #2 was shut down after 20 min. Afterwards, the cooler was activated, and the temperature was monitored for 79 min. During the experiment the temperatures in four zones were checked and recorded every 60 s. The experiment showed that the heat spread rapidly and increased the temperature above the desired temperature of 37 °C and 25 °C in the annealing area. The denature/anneal cycle was modified by decreasing temperature set points, and turning on and off the heaters at different times. Two denature/anneal procedures were developed.

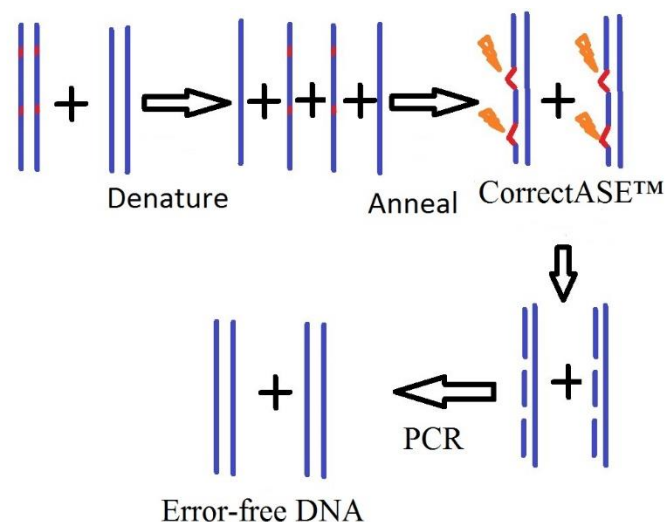


Figure 20. Error correction process with CorrectASE™ enzyme.

The first procedure was similar to the benchtop protocol. It was difficult to move the droplets at temperatures below 10 °C, so the droplets were incubated at 98 °C for 2 min, 6 min at 25 °C, and 5 min at 37 °C. In this experiment, Peltier cooler was set to 4 °C prior to the error correction pretreatment. The first heater bar was turned on for 9 min with a setting point of 111 °C to obtain 98 °C in the denature area. The next heater was turned on with 5 min delay after the first one was shut down. This heater was set to 33.9 °C to obtain 37 °C and 25 °C zones in the annealing area. The heater was kept on for 6 min. When the annealing process was done, the lanes were cooled down by the Peltier cooler for 5 min. The lanes were brought to a room temperature in 12 min. The error correction area was heated up to 25 °C by setting the heater to 24.1 °C.

In a second procedure, a modified denature/anneal cycle was developed. It was hypothesized that repeating the cycle four times should be sufficient for separation and reannealing of DNA strands. In this cycle, the droplets were incubated at 98 °C for 1



min, 25-30 °C for 1 min, and 37 °C for 1 min. To ensure that the lanes did not overheat, the cooler was set to 4 °C prior to the denature/anneal stage. The droplets were moved at a speed of 1 s/electrode. The actuation voltage was changed to 90 V when the samples were transported through the high temperature area. In the annealing area, the droplets were pulsed to provide mixing. The heater for the denaturation zone was set to 111 °C to achieve an effective temperature in the droplet of 98 °C. After the heater had switched off, the lanes were cooled down for 10 min by the cooler and for 20 min by ambient conditions. The error correction zone was set to 24.1 °C to maintain 25 °C in the incubation area.

#### 4.4.2 Automation Program for Microfluidic DNA Assembly with Error Correction

To perform gene assembly and error correction experiments, the assembly automation program described in Section 4.3.3, the PCR program shown in Section 4.2.3, and the error correction procedures from Section 4.4.1 were combined into one program. Figure 21 demonstrates the order of gene synthesis reactions and liquid handling operations that were performed on the microfluidic device. The gene synthesis process was composed of six consecutive enzymatic reactions: oligonucleotide assembly, first amplification (PCR1), first error correction (EC1), second amplification (PCR2), second error correction (EC2), third amplification (PCR3). The oligo assembly was carried in the “Assembly” block. Amplification reactions occurred in blocks “PCR1”, “PCR2”, and “PCR3”. The incubation with CorrectASE™ was performed in “EC1” and “EC2” blocks. To pretreat DNA prior to error correction, double stranded DNA was separated and reannealed in blocks “EC1 denature/anneal” and “EC2 denature/anneal”. Multiple

dilution steps were included between enzymatic reactions. The “Dilution before PCR1” block was used optionally. In the experiments where the dilution rate before PCR1 was 2-fold, no dilution was necessary. By merging assembly products with PCR droplets, assembly constructs were diluted by half. “Dilute before PCR2” and “Dilute before PCR3” blocks were made as loops, so it was convenient to change dilution rates. The “Collect droplets on lanes 1,2” block was responsible for collection of two droplets of amplified assembly products. The “Collect droplets on lanes 3,4,5” block retrieved three amplified samples after EC1, and the “Collect droplets on lanes 6,7,8” recovered three amplified EC2 droplets.

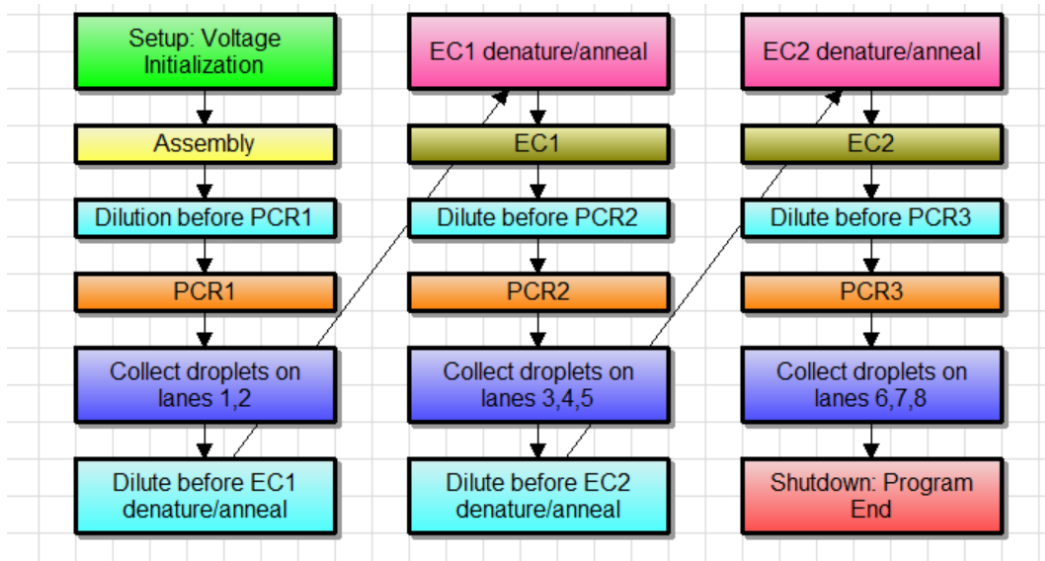


Figure 21. Automation program for microfluidic DNA assembly with two rounds of error correction.

#### 4.4.3 Experimental Protocols for Microfluidic DNA Assembly with Error Correction

Based on the experiments described in Sections 4.2 and 4.3 two DNA assembly with error correction protocols were developed. The protocols consisted of six consecutive enzymatic reactions. The process started with Gibson assembly that was carried for 60 minutes. Then, the assembly products were amplified in 30 PCR cycles. Next, DNA was treated with CorrectASE™ for 60 min. The error correction products were amplified in a second PCR and error corrected for the second time. Finally, the second error correction products were amplified in a third PCR. Table 7 compares two microfluidic and a benchtop protocols used in this study.

Table 7. Steps of DNA assembly and error correction process.

	Benchtop	Microfluidic protocol 1	Microfluidic protocol 2
Assembly reaction conditions	50 nM oligos	250 nM oligos	50 nM oligos
Dilution before PCR1	20-fold	2-fold	16-fold
		16-fold	
Dilution before EC1 denature/anneal	5-fold	32-fold	4-fold
			8-fold
			16-fold
Dilution before EC2 denature/anneal	5-fold	16-fold	4-fold
Dilution before PCR2/PCR3	25-fold	16-fold	16-fold
Denature/anneal procedure	2 min – 98 °C 5 min – 4 °C 5 min – 37 °C	2 min – 98 °C 5 min – 25 °C 5 min – 37 °C	4 cycles: 1 min – 98 °C 1 min – 25 °C 1 min – 37 °C

In the first protocol, 250 nM oligos were used for assembly. The dilutions rates before amplification and error correction pretreatments were determined by trial and

error. The second protocol was made to repeat reaction conditions and dilution rates similar to the benchtop protocol. The procedures for DNA assembly and error correction with CorrectASE™ were obtained from the J. Craig Venter Institute. In protocol 2, the concentration of oligos was 50 nM, and the dilution rates were modified from the benchtop protocol. Since merging and splitting droplets on a DMF cartridge could be performed in 2-fold increments, dilutions on the microfluidic device were rounded to 16-fold before PCR1 and 4-fold prior to error correction.

#### 4.4.4 Experimental Matrices for Validation of DNA Assembly and Error Correction Protocols on the DMF

Several experiments were performed utilizing both microfluidic protocols described in Table 7. The experimental runs are shown in Table 8. Runs 1-3 were performed using protocol 1. According to this protocol, the final concentration of oligos in the assembly reaction was 250 nM. After assembly, the product was diluted by either 2 or 16-fold. Two different denature/anneal procedures were tested. Since the PCR product after the assembly step had additional MgCl<sub>2</sub> and PEG 8000 that originated from Gibson iso buffer, two PCR master mixes were prepared. The master mix for amplification of error correction products by PCR2 and PCR3 provided 0.625 mM PEG 8000 and 0.5 mM MgCl<sub>2</sub>, whereas master mix for PCR1 did not have any additional reagents.

Table 8. Experimental matrix for microfluidic protocol 1.

Run No.	Dilution before PCR1	Denature/anneal procedure before EC1/EC2
1	2-fold	2 min – 98 °C, 6 min – 25 °C, 5 min – 37 °C
2	2-fold	4 cycles:1 min – 98 °C,1 min – 25 °C, 1 min – 37 °C
3	16-fold	4 cycles:1 min – 98 °C,1 min – 25 °C, 1 min – 37 °C

A second protocol was utilized in Runs 1-4 in Table 9. In Run 1, the conditions similar to the benchtop protocol were tested. The amount of polymerase was increased twice to account for surface effects in the microfluidic device. In Runs 2-4, amplification reactions were performed with additional polymerase, MgCl<sub>2</sub>, and PEG 8000 to ensure consistent amplification in all droplets. Also, 4, 8, and 16-fold dilutions of the assembly product were tested.

Table 9. Experimental matrix for microfluidic protocol 2.

Run No.	PCR1 conditions (final concentration)	PCR2/PCR3 conditions (final concentration)	Dilution before EC1 denature/anneal
1	0.02 U/μL Phusion	0.02 U/μL of Phusion 0.5 mM of MgCl <sub>2</sub> 0.625 mM of PEG	4-fold
2	0.1 U/μL of Phusion 0.5 mM of MgCl <sub>2</sub> 0.625 mM of PEG	0.1 U/μL of Phusion 0.5 mM of MgCl <sub>2</sub> 0.625 mM of PEG	4-fold
3	0.1 U/μL of Phusion 0.5 mM of MgCl <sub>2</sub> 0.625 mM of PEG	0.1 U/μL of Phusion 0.5 mM of MgCl <sub>2</sub> 0.625 mM of PEG	8-fold
4	0.1 U/μL of Phusion 0.5 mM of MgCl <sub>2</sub> 0.625 mM of PEG	0.1 U/μL of Phusion 0.5 mM of MgCl <sub>2</sub> 0.625 mM of PEG	16-fold

To perform experiments described in Tables 8 and 9, 10 different master mixes were prepared, which are shown in Appendix B. The master mixes contained double amounts of reagents to obtain 1X concentration after the equal size droplets were merged. The

reagents were loaded on a DMF cartridge into dedicated dispensers prescribed by the automation program. All master mixes except CorrectASE™ were loaded on the cartridge at the beginning of the process. To ensure that the enzyme stayed active and fresh, CorrectASE™ was loaded in a dispenser three minutes before it was to be used by the program. At the end of the process all droplets were collected in 20 µL of 0.05% Tween 20 solutions and retrieved from the device manually. The samples were analyzed on a 2% agarose gel and prepared for cloning into a vector, transformation into *E. coli*, and DNA sequencing.

## 4.5 Data Analysis

### 4.5.1 Preparation of Samples for Sanger Sequencing

A comprehensive list of materials used for sample preparation is shown in Appendix C. Samples recovered from Lanes 1 and 2, 3-5, and 6-8, which corresponded to assembly, EC1, and EC2 treatments, respectively, were pooled and analyzed by DNA gel electrophoresis. The samples were mixed with 6X orange DNA loading dye (Thermo Fisher Scientific), loaded on a 2% agarose gel, and run against a 1 Kb plus DNA ladder (Invitrogen). The indication of a successful experimental run was the presence of a 339 bp band. Next, DNA was prepared for Sanger sequencing. The samples were purified using Agencourt AMPure XP SPRI magnetic beads (Beckman Coulter). The ratio of magnetic beads to DNA was 0.9X. One volume of DNA was diluted into 0.9 volume of the beads.

Cleaned up DNA was cloned into pUC19 vector. In order to prepare pUC19 for cloning, it was amplified with pUC-049 cloning-R and pUC-049 cloning-F primers (IDT

DNA). Thermocycler settings as well as reagents are listed in Appendix D. To remove template plasmid, the PCR product was digested with DpnI restriction enzyme at 37 °C for 24 hours. The amplified and digested vector was cleaned with 0.9X SPRI beads.

Cloning of DNA fragments into pUC19 was done using Gibson assembly method. The concentration of vector and inserts were measured on the Nanodrop instrument and converted to fmol/μL. The number of moles of insert had to be equal to or 2-3-fold greater than the moles of a vector. The appropriate amounts of the vector and insert were mixed with 2X Gibson master mix and incubated at 50 °C for 30 min [38]. Procedures for plasmid assembly are shown in Appendix D.

The recombinant plasmids were used to transform *E. coli*. Transformations were done by the electroporation method on the Gene Pulser II Porator electroporation system (Bio-Rad). According to this method, 1 μL of plasmid and 20 μL of TransformMax EPI300 electrocompetent *E. coli* cells (Epicentre) were added in a 0.1 cm electroporation cuvette (Bio-Rad) and subjected to 1.8 kV. The cells were recovered in 1 mL of LB broth and incubated in 37 °C incubator for 60 min. After the recovery, 15 μL of cells were plated on LB agar plates with Carbenicillin selection. The transformed cells were left to form colonies overnight in a 37 °C incubator.

Resulting colonies were screened for the presence of the correct cloned insert. Screening was done by the colony PCR method with pUC5-'F and pUC3-'R primers. According to this method, 14 to 25 single colonies were selected from each plate and used as a template in the PCR reaction. The details of the colony PCR reactions are shown in Appendix E. The colony PCR products were analyzed on a 2% agarose gel.

The colonies that yielded a 419 bp band were selected to grow overnight cultures. For each sample, at least 10 colonies were grown overnight in 5 mL of LB broth (Teknova) with Ampicillin (100 µg/mL, Sigma). Overnight cultures were used to extract plasmids. Plasmid extraction was done using QIAprep Spin miniprep kit (Qiagen). Extracted plasmids were sent to Genewiz for Sanger sequencing with the M13F(-47) primer.

#### 4.5.2 Sequencing Data Analysis

Sequencing data was analyzed using Benchling software available at [www.benchling.com](http://www.benchling.com). The output files were uploaded to the Benchling website and aligned with the original template sequence, shown in Appendix A, using Benchling's sequence alignment tool. Each sequence alignment was inspected for errors in the newly assembled sequence. The errors were categorized in three groups: deletions, insertions, and substitutions. The sequences that had misincorporated oligos were treated as "misassemblies". The error frequency per 1 kb (f) was calculated using Equation 2 [35].

$$f = \frac{\sum_i^n x_i \times 1000}{n \times l_i} \quad \text{Equation 2}$$

where  $x_i$  is the number of errors in a single clone,  $n$  is the number of sequenced clones not including clones with misassemblies, and  $l_i$  is the length of a sequence in bases.

Equation 3 was used to calculate the average percent of deletions ( $P_{del}$ ), substitutions ( $P_{sub}$ ), and insertions ( $P_{in}$ ).

$$P_{del/sub/in} = \frac{\sum_j^n x_{del/sub/in}}{\sum_j^n x} \times 100\% \quad \text{Equation 3}$$

where  $x_{del/sub/in}$  is the sum of deletions, substitutions, and insertions found in sequenced clones,  $\sum_j^n x$  is the sum of all errors.



Standard deviation (SD) was calculated to demonstrate reproducibility of developed microfluidic protocols.

$$SD = \sqrt{\frac{\sum(X-\bar{X})^2}{m-1}} \times 100\% \quad \text{Equation 4}$$

where X is the value of dependent variable,  $\bar{X}$  is the mean value, and m is the number of runs.

## CHAPTER FIVE

### RESULTS

#### 5.1 Results of Microfluidic PCR Experiments

The main goal of microfluidic PCR experiments was to develop an automation protocol, which leads to reproducible DNA amplification on all lanes of the microfluidic cartridge. Multiple experiments were done with the same reagents as with conventional benchtop PCR and a 5-fold increased amount of a polymerase enzyme. No microfluidic PCR amplification was achieved using a synthetic DNA template that mimicked the Gibson assembly product. However, it was shown that sufficient amplification was achieved if PCR was performed immediately after an actual Gibson assembly reaction. The hypothesis was that some of the components of the Gibson iso buffer were responsible for PCR improvement. The results of the experimental runs described in Table 3 of Section 4.2.1 are shown in Figures 22 and 23.

Figure 22 demonstrates that the additives drastically improved amplification efficiency. Control samples, which contained 0.1 U/ $\mu$ L of Phusion polymerase, did not show any bands on the agarose gel. On the other hand, PCR supplemented with the iso buffer resulted in the desired 339 bp bands. The reactions that were only supplemented with polymerase had variable band intensities. Sample to sample variation for reactions supplemented only with Phusion polymerase suggested that the iso buffer was responsible for the PCR boost, which agrees with the hypothesis.

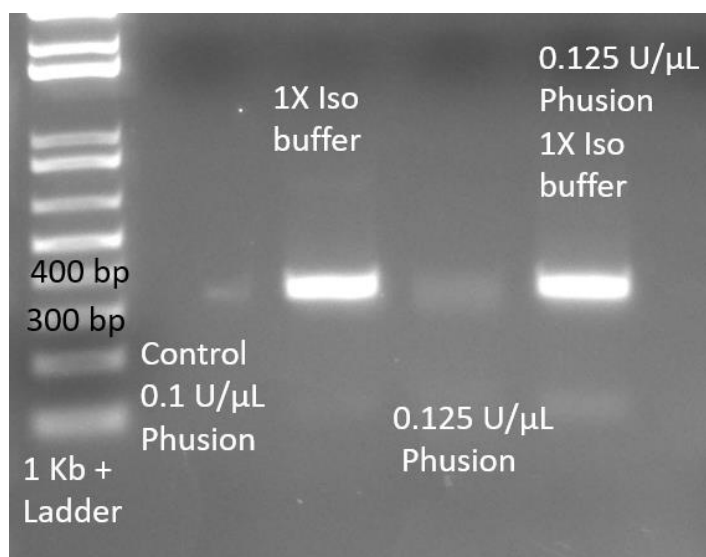


Figure 22. Polymerase chain reaction with the iso buffer and Phusion additives.

Furthermore, amplification was carried out with individual components of the iso buffer. Only the samples with the PEG 8000 additive were amplified (data not shown). This experiment demonstrated that the addition of PEG 8000 increased amplification, but the reaction was not as efficient as with the complete iso buffer.

Figure 23 shows that the combination of 1.25 mM PEG 8000 and 1 mM  $MgCl_2$  showed comparable band intensity as the iso buffer. This result demonstrated that microfluidic PCR carried with the excess Phusion must be supplemented with additional  $MgCl_2$  and PEG 8000 for successful amplification of DNA on the microfluidic device.

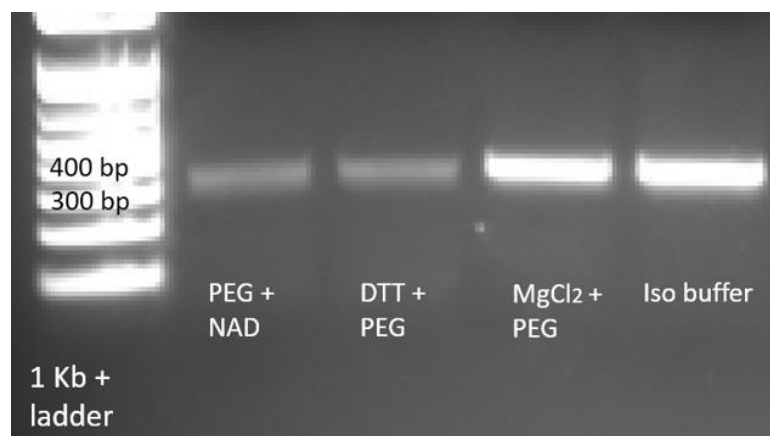


Figure 23. Polymerase chain reaction with two components of the iso buffer.

## 5.2 Reduction of Adsorption of Phusion Polymerase on the Microfluidic Surface

Even though it was shown that amplification was successful, the issue of polymerase adsorption was not solved. The main consequences of adsorption were droplet movement failure and inability to recover all samples from the microfluidic device. To minimize protein adsorption on the microfluidic surface, different methods discussed in the literature review were tested. The following results are based on the experiments shown in Table 4.

The addition of BSA to the PCR reaction mixture resulted in complete failure of a droplet movement. The droplets did not spread on the activated electrodes. The hypothesis for this experiment was that BSA would bind to the surface instead of Phusion. It has been shown that the BSA gives the same effect as a 5-fold increase of polymerase [29]. However, BSA has a high surface activity and make the droplets stick to the surface [40]. In addition, the negatively charged protein molecule interacts with the positively charged surface when a voltage is applied [27]. Thus, for the Mondrian™

SP microfluidic device, BSA had a negative effect on droplets' movement. A protein pre-coating might be effective for continuous flow microfluidic channels, but it does not work for electrowetting based digital microfluidics.

As seen in Figure 24, by increasing polymerase concentration, the intensity of the bands on the agarose gel becomes brighter. The results demonstrated that the adsorption of polymerase did not change with the addition of 0.02% w/v Pluronic F68. The highest amplification yield was achieved with 0.14 U/ $\mu$ L of Phusion, which is a 7-fold increase of the enzyme over standard benchtop PCR conditions. Since the sample that had the highest concentration of Phusion did not show the brightest band, and the sample with the lowest concentration showed a very faint band, there is a possibility that the Pluronic slightly reduced the adsorption. A subsequent experiment with four different concentrations of Pluronic and 0.02 U/ $\mu$ L of Phusion resulted in the loss of droplets from all lanes. This result suggested that the enzyme was adsorbed on the surface, and pluronic F68 is not effective in the reduction of biofouling for DMF devices.

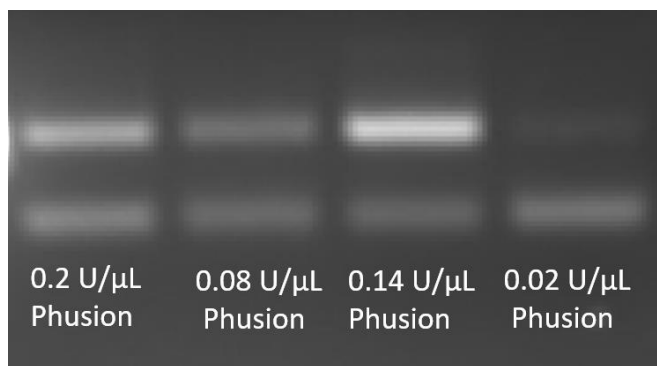


Figure 24. Microfluidic PCR with 0.02% w/v Pluronic F68 and variable Phusion concentration.

Another approach to the reduction of surface interactions was pre-coating the microfluidic surface with 10% w/v PEG 6000, PEG 4000, and PEG 3350 solutions prior to the PCR. The results of this experiment demonstrated no improvement in PCR yield, and no DNA bands appeared on the agarose gel (data not shown). Figure 25 shows that pre-coating of the surface with PEG 8000 improved PCR yield. Amplification was achieved with the benchtop concentration of Phusion (0.02 U/ $\mu$ L) and a 4-fold increase of the enzyme (0.08 U/ $\mu$ L). However, the intensity of the bands varied in samples with the same reaction conditions. One of the possible reasons was that some parts of the microfluidic surface were not forming interactions with the polymer, and the enzyme was released from the aqueous droplet. Alternatively, the absence of a band for the 0.2 U/ $\mu$ L Phusion sample could suggest that the reaction had an excess of the enzyme, which resulted in amplification failure. The Phusion polymerase user manual says that the amount of enzyme should not exceed 0.04 U/ $\mu$ L. Thus, if a 10-fold amount of the enzyme (0.2 U/ $\mu$ L) was used in a benchtop experiment, DNA would not be amplified. Even though pre-coating with PEG 8000 reduced polymerase adsorption, it was still difficult to move samples through the “hot” denaturation zone. The droplets were releasing microbubbles and were not spreading entirely on the activated electrodes. Some samples were lost during the experiment. Thus, pre-passivation was not effective in improving droplet transport.



Figure 25. Microfluidic PCR with 10% w/v PEG 8000 pre-coat.

Successful amplification was achieved on all eight lanes when the actuation voltage in the PCR cycle was reduced from 300 V to 90 V. During the experiment the droplets were moving from the denaturation to the annealing/extension area without any complications. The droplets were completely wetting energized electrodes, and no destruction of the oil/water interface was observed.

### 5.3 Results of Microfluidic DNA Assembly

The first group of experiments was conducted to identify the optimum time of reaction. Figure 26 shows the image of agarose gel. The bands for all tested times have similar brightness. This means that the oligos were assembled in 15-60 min time period, and it is an acceptable range for the microfluidic DNA assembly.

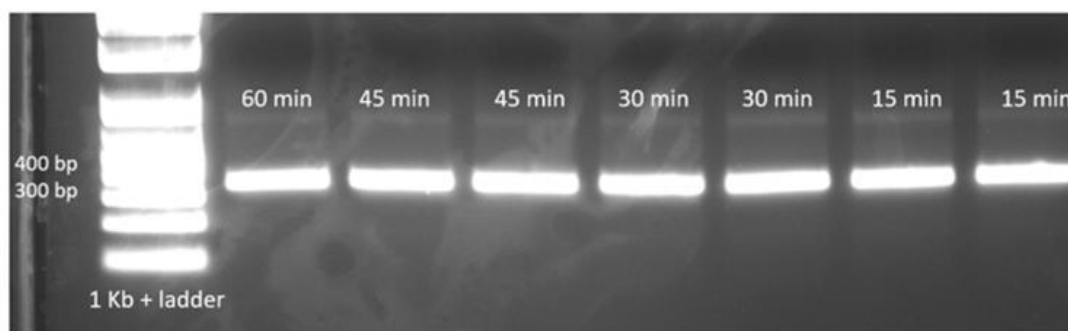


Figure 26. Microfluidic assembly at different times.

As seen in Figure 27, T5 exonuclease is an essential reagent when 250 nM oligos are assembled. Without the enzyme, the oligos did not form a double-stranded piece. Figure 27 (a) shows a smear instead of a single band. On the other hand, the assembly products that were obtained in the presence of T5 exonuclease demonstrated the bands that were the right 339 bp size. As shown in Figure 27 (b), the intensity of the bands did not vary from sample to sample, so it was concluded that for the 250 nM oligo assembly T5 exonuclease is essential.



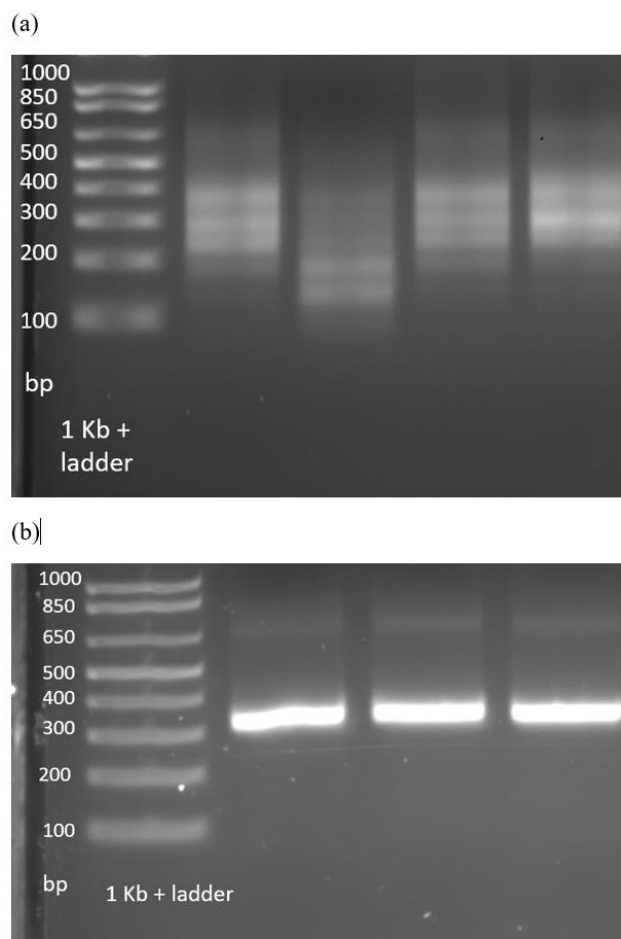


Figure 27. Microfluidic assembly of 250 nM oligos for 60 min. (a) Assembly without T5 exonuclease. (b) Assembly with T5 exonuclease.

Dilution of the assembly product prior to the amplification is an additional step that should be included in a microfluidic Gibson assembly protocol. Since the goal was to assemble the product that had the minimum number of errors, it was important to remove unreacted oligos, oligo fragments, and misassemblies that were present at a low level before amplification. As shown in Figure 28, dilution of the assembly constructs from 2-fold to 16-fold resulted in comparable amounts of the PCR product. However, 16-fold

was the maximum dilution rate that could be achieved before the PCR template was too diluted to amplify. A dilution rate greater than 32-fold did not result in amplification of the assembly product. Based on these results, it is better to keep the dilution of the assembly product no greater than 16-fold.

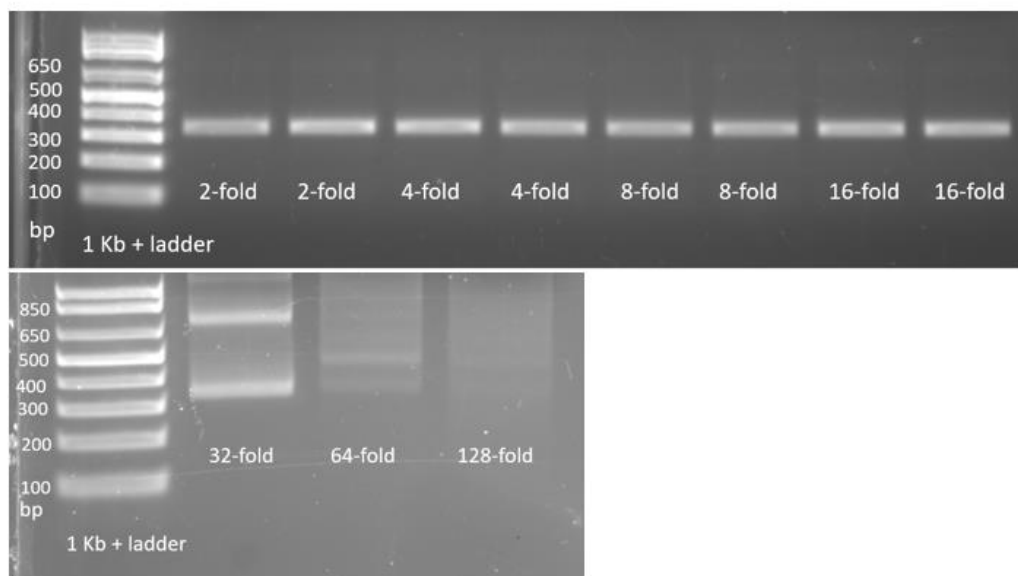


Figure 28. Dilution of the 50 nM oligo assembly product prior to PCR.

Figure 29 illustrates the results of the Gibson assembly of 50 nM oligos that were diluted by either 8 or 16-fold and amplified at four different PCR conditions. It could be concluded that both dilutions resulted in a similar amplification efficiency. However, different PCR treatments led to different results. The samples that had 0.02 U/ $\mu$ L of Phusion along with  $MgCl_2$  and PEG were not amplified. On the other hand, PCR with 0.1 U/ $\mu$ L of Phusion,  $MgCl_2$  and PEG demonstrated the largest amplification yield. The

samples amplified with 0.1 U/ $\mu$ L of Phusion had brighter bands than samples amplified with 0.02 U/ $\mu$ L of the enzyme. Also, the intensity of bands was not consistent for 0.02 U/ $\mu$ L Phusion.

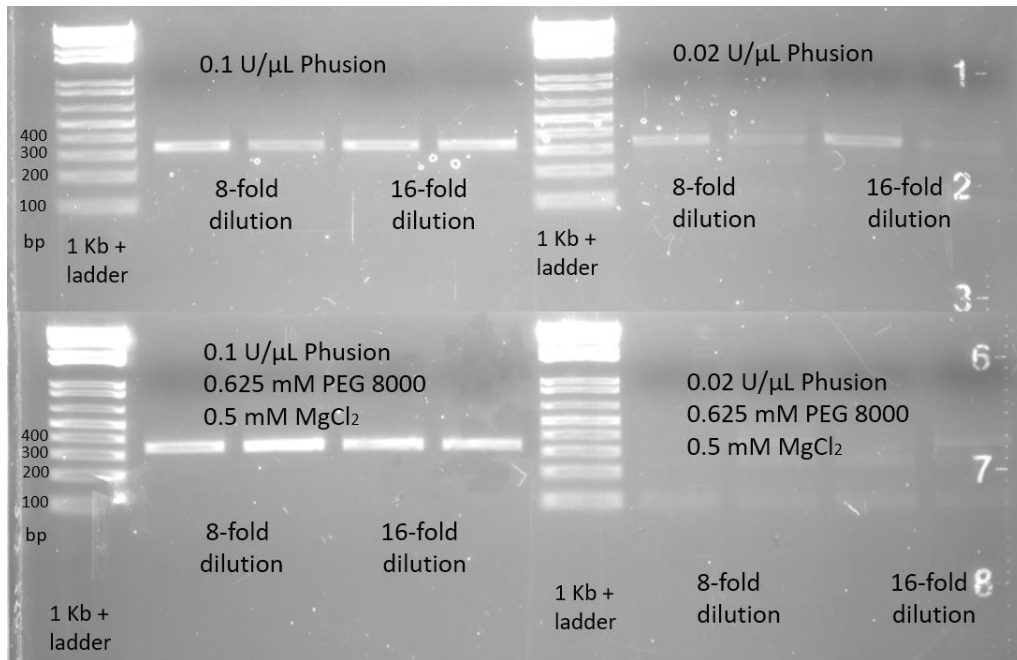


Figure 29. Dilution of assembly product by 8-fold and 16-fold followed by amplification at four different conditions: 0.1 U/ $\mu$ L Phusion; 0.02 U/ $\mu$ L Phusion; 0.1 U/ $\mu$ L Phusion, 0.625 mM PEG, and 0.5 mM MgCl<sub>2</sub>; 0.02 U/ $\mu$ L Phusion, 0.625 mM PEG, and 0.5 mM MgCl<sub>2</sub>.

#### 5.4 Temperature Settings for Error Correction Experiments

Figure 30 compares temperature variation in the denaturation, annealing, and EC incubation zones when all heaters were turned on simultaneously. The temperatures were set to maintain 95-98 °C, 37 °C, and 25 °C in the denature, annealing, and EC zones, respectively. As seen in Figure 30 (a), it took about 6 min to achieve temperatures suitable for separation of dsDNA. When the heater was on, the temperature in the denaturation zone was fluctuating between 92 °C and 96 °C. The temperature in the annealing area, which was supposed to be at 37 °C, increased to 43-51 °C.

The annealing 25 °C area drifted to 37-40 °C. As seen in Figure 30 (b), the cartridge cooled down in 25 min, and the temperature settled to 28 °C. Thus, the results of this test demonstrated that the heat in the cartridge spreads rapidly, and it takes about 25 min to cool down. To reduce overheating of annealing and EC zones, the denaturation zone heater should be shut down when it is not needed. Additionally, the temperature in those areas should be regulated by reducing temperature set points and cooled down by the adjacent Peltier cooler.

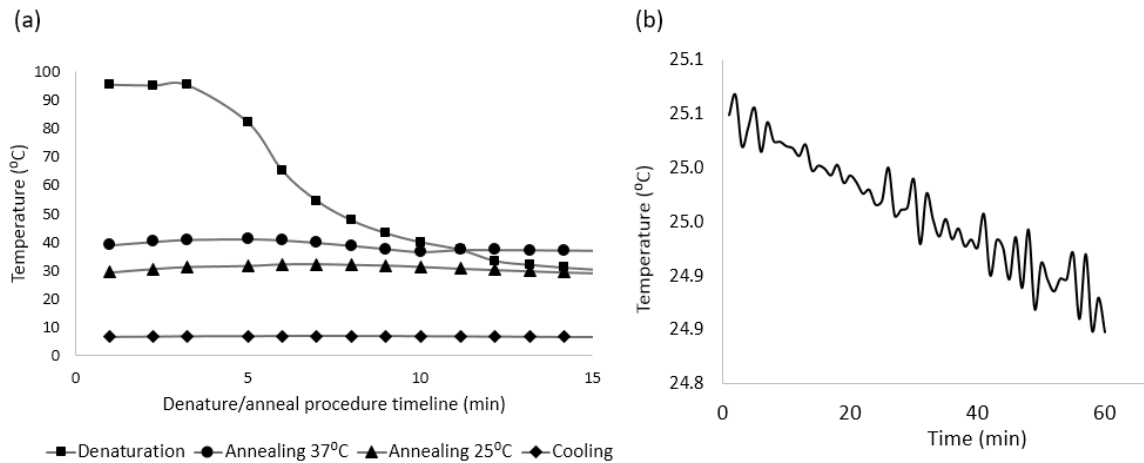


Figure 30. Variation of temperatures on the DMF cartridge. (a) During EC denature/anneal pretreatment. (b) Error correction incubation.

Figure 31 shows temperature variations in the denaturation, annealing, and cooling zones for two denature/anneal procedures. In the first procedure shown in Figure 31 (a), DNA samples were kept at 95-98 °C for 2 min before they were moved to the area between 25 °C zone and the cooling zone and incubated for 6 min. Next, the samples were transported to 37 °C where they were annealing for 5 min. By setting the denaturation zone to a higher temperature, 98 °C was achieved. By setting the 37 °C zone heater to a lower set point just before the annealing step, the cartridge could maintain this zone at the prescribed temperature. Even though the heater under 25 °C zone was not activated, this area of the cartridge was overheated by the heat transferred from the adjacent zones. To solve this issue, the droplets were moved next to the cooling area. It was not possible to determine the temperature in the area between these two zones. However, the purpose of the annealing step is a gradual reduction of temperature,

so single strands can form double strands. Since the temperature in cooling zone was about 7 °C, the temperature gradient for annealing was established.

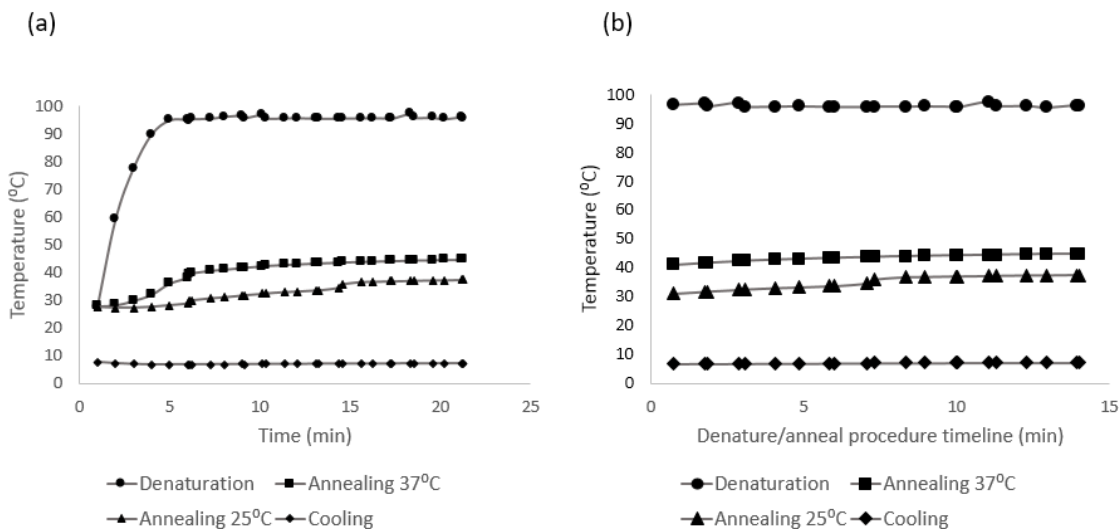


Figure 31. Average variation of temperatures during EC denature/anneal treatments. (a) 2 min at 98 °C, 6 min at 37 °C, and 5 min at 25 °C. (b) 4 cycles: 1 min at 98 °C, 1 min at 37 °C, and 1 min at 25 °C.

Figure 31 (b) shows the temperature distribution for a modified denature/anneal procedure. In this procedure, the denature and annealing steps were repeated four times. The droplets were incubated at 98 °C, 25 °C, and 37 °C for a minute. To establish the temperature gradient on a cartridge, only the 98 °C heater and Peltier cooler were activated. Like in the first procedure, the 25 °C zone was set next to the cooling area. To keep the samples at 37 °C during the first two cycles, the droplets were incubated between the 25 °C and 37 °C areas. Because the heat from the denaturation zone was spreading and raising the temperature of the DMF cartridge, in the last two cycles, the samples were transported to the 25 °C zone.

Figure 32 shows temperature variation of the EC zone during CorrectASE™ incubation. Prior to the denaturation, the cartridge was cooled down by Peltier element for 5 min. Since the temperatures lower than 10 °C affect a surface tension of aqueous solutions as well as the properties of surfactants, the cartridge was allowed to equilibrate to the ambient temperature. The denaturation area was set to 24.1 °C to maintain the optimum reaction conditions. As seen in Figure 32, the temperature was rapidly raised to 25 °C and maintained at this setting point for 60 min

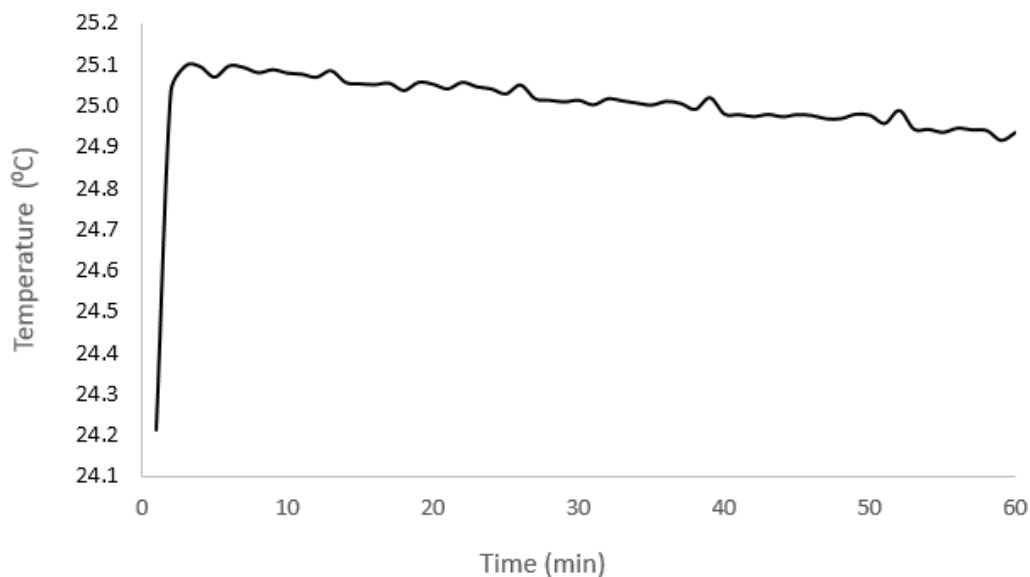


Figure 32. Average temperature variation during CorrectASE™ incubation.

## 5.5 Sanger Sequencing Results of Assembly Samples

To investigate if the concentration of oligos in the assembly reaction could influence the fidelity of assembly constructs, two sets of samples obtained by the assembly of 50 nM or 250 nM oligos were sequenced. The details about individual runs can be found in Appendix F. Figure 33 demonstrates the average error rate from five separate runs for each oligo concentration. It was determined that the average error rate for 250 nM and 50 nM oligos was 3.15 errors/kb and 2.94 errors/kb, respectively. The runs with 250 nM oligos had a standard deviation of 0.36 errors/kb and 50 nM oligos of 1.05 errors/kb.

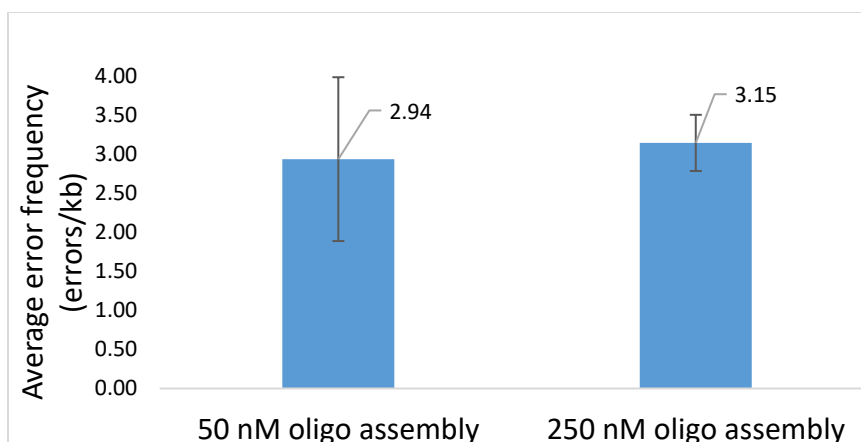


Figure 33. Average error frequency for sequences assembled from 250 nM and 50 nM oligos.

According to Table 10, single-base deletions comprised the bulk of errors. There was no preference for errors to occur between A/T or C/G bases. Both sets of samples had comparable percentages of deletions and the same amount of multiple-base deletions. The assembly of 50 nM oligos resulted in 13.1% insertions and 4.3% substitutions, whereas 250 nM assembly had 14.3% substitutions and 6.1% of insertions.



Table 10. Error analysis of assembly constructs based on Sanger sequencing.

	250 nM oligos assembly	50 nM oligos assembly
Error type		
Deletion (total)	39	38
G/C	18	15
A/T	20	21
Multiple-base deletion	2	2
Insertion (total)	3	6
G/C	2	3
A/T	1	1
Multiple-base insertion	0	2
Substitution (total)	7	2
A/T to G/C	1	0
G/C to A/T	2	0
G/C to C/G	2	0
G/C to to T/A	0	1
AT/ to C/G	1	0
A/T to T/A	1	1
Total errors	49	46
Number of sequenced bases	15594	15594
Average Error frequency (errors/kb)	3.15	2.94
Standard deviation (errors/kb)	0.36	1.05
Total clones without misassemblies	46	46
Number of clones with misassemblies	2	3
Percent of deletions	79.6%	82.6%
Percent of insertions	6.1%	13.1%
Percent of substitutions	14.3%	4.3%

## 5.6 Sanger Sequencing Results for Gibson Assembly with Error Correction for Protocol 1

The results of experiments discussed in this section were obtained using the automation protocol 1 shown in Table 7 in Section 4.4.4. Figure 34 represents the results of experimental runs described in Table 8. In these experiments, the concentration of oligos in all runs was 250 nM. Runs 1 and 2, shown in Figure 34 (a) and 34 (b), respectively, were performed to compare two denature/anneal procedures. The experiment also determined the influence of dilution of the assembly product prior to PCR1 on the error reduction. The results of a 2-fold dilution are shown in Figures 34 (a) and 34 (b), and the results of a 16-fold dilution are shown in Figure 34 (c).

As seen in Figure 34 (b), only Run 3 demonstrated an error decrease with each CorrectASE™ treatment. In this experiment, the assembly products were diluted by 2-fold before PCR1, and the modified 4-cycle denature/anneal procedure was used in the automation program. The error frequency was reduced from 3.28 errors/kb to 1.31 errors/kb after two rounds of error correction. The insertions were eliminated after the first error correction. The error frequency of substitutions decreased after the first error correction and increased after the second error correction. According to Figures 34 (a) and 34 (c), the error frequency increased after the first error correction and decreased after the second treatment. However, the overall error frequency relative to an untreated assembly sample was not observed in Run 1.

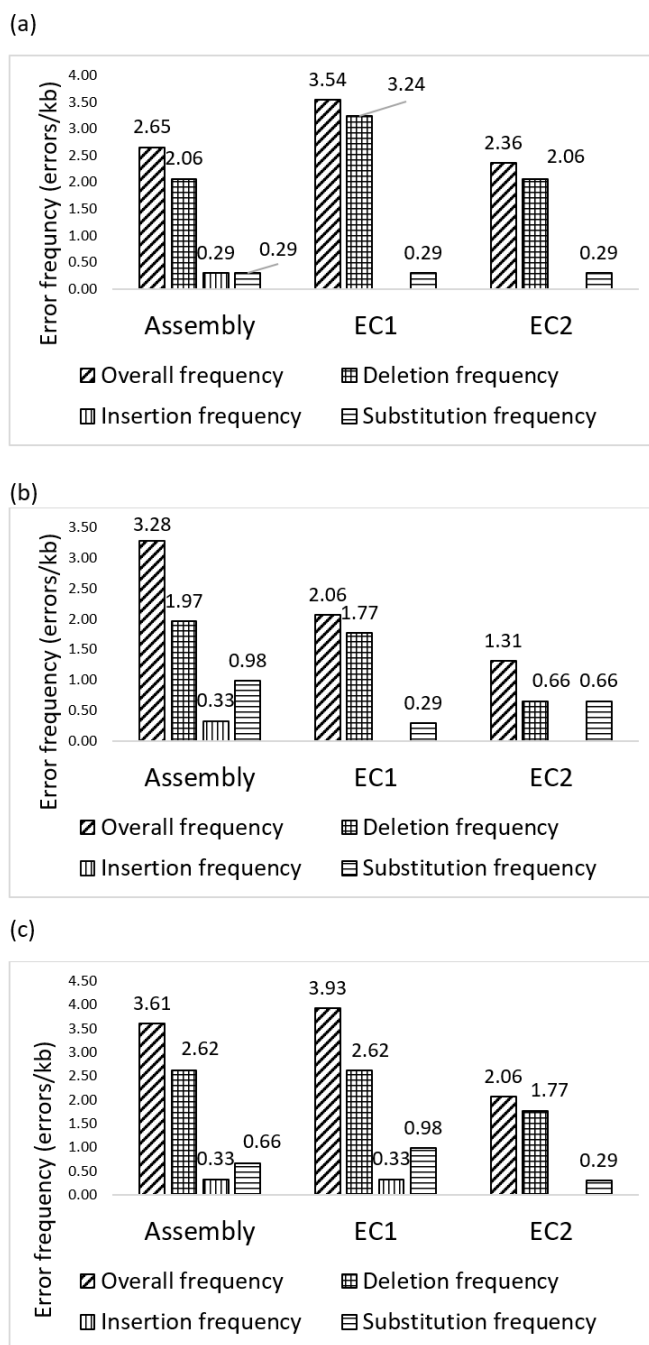


Figure 34. Error frequency of assembly samples followed by two rounds of error correction obtained using automation protocol 1. (a) 2-fold dilution before PCR1, denature/anneal procedure: 2 min – 98 °C, 5 min – 25 °C, 5 min – 37 °C. (b) 2-fold dilution before PCR1, denature/anneal procedure 4 cycles: 1 min – 98°C, 1 min – 25 °C, 1 min – 37 °C. (c). 16-fold dilution before PCR1, denature/anneal procedure 4 cycles: 1 min – 98 °C, 1 min – 25 °C, 1 min – 37 °C.

The error analysis based on sequencing data of 88 clones shown in Table 11. The number of error-free clones did not change for Run 1. Thus, the error correction failed in this experiment. In Run 2, seven clones out of nine were found to be error-free after the second error correction. In contrast, three out of nine clones were correct in the untreated sample set. This result indicates that the second error correction reaction was effective, but the first did not work. In Run 3, the number of error-free clones increased, in this case from three to five. Also, overall reduction of all types of errors was shown after the second CorrectASE™ treatment.

Assembly constructs were diluted by 2-fold in Runs 1 and 3, and by 16-fold in Run 2. The dilution of the first error correction product was kept constant. In Run 3, both error correction reactions were successful, and in Run 2, only the second error correction reaction was effective. Thus, it was concluded that the dilution of assembly product does not affect the outcome of error correction reactions.

Furthermore, Runs 2 and 3, had the modified denature/anneal cycle in which DNA molecules were denatured and reannealed four times instead of just one, as suggested by the CorrectASE™ manufacturer. Since the enzyme could only recognize and remove the mismatch if the heteroduplexes were formed, it is possible that the modified procedure created better conditions for formation of heteroduplexes, and more errors were removed by CorrectASE™.

Based on the results described above, the dilution of assembly product is not a critical factor that affects microfluidic error correction. On the other hand, four cycles of denature/anneal were recognized to improve the error removal on the DMF cartridge.

Table 11. Error analysis of assembly and error correction experiments using Protocol 1.

	Run 1 (regular denature/anneal procedure, 2-fold dilution before PCR1)			Run 2 (4-cycle denature/anneal procedure, 2-fold dilution before PCR1)			Run 3 (4-cycle denature/anneal procedure, 16-fold dilution before PCR1)		
	No EC	EC1	EC2	No EC	EC1	EC2	No EC	EC1	EC2
Error type	Number of errors								
Deletion (total)	7	11	7	6	2	2	8	8	6
Single-base deletion									
G/C	3	5	4	3	1	1	2	5	3
A/T	3	5	2	3	5	1	6	2	3
Multiple-base deletion	1	1	1	0	0	0	0	1	0
Insertion (total)	1	0	0	1	0	0	1	1	0
Single-base insertion									
G/C	1	0	0	0	0	0	1	0	0
A/T	0	0	0	1	0	0	0	1	0
Substitution (total)	1	1	1	3	1	2	2	3	1
A/T to G/C	0	0	0	1	0	2	0	0	0
G/C to A/T	0	1	0	1	0	0	1	2	0
G/C to C/G	1	0	0	0	0	0	0	0	0
G/C to T/A	0	0	1	0	0	0	0	0	1
AT/ to C/G	0	0	0	0	0	0	1	1	0
A/T to T/A	0	0	0	1	1	0	0	0	0
Total errors	9	12	8	10	7	4	11	12	7
Sequenced bases	3390	3390	3390	3051	3390	3051	3051	3051	3390
Total clones without misassemblies	10	10	10	9	10	9	9	9	10
Total clones sequenced	10	10	10	10	10	9	10	9	10
Total of clones with correct sequences	3	3	3	3	3	7	3	2	5

## 5.7 Sanger Sequencing Results for Gibson Assembly with Error Correction for Protocol 2

Figures 35 and 36 demonstrate the results of the assembly and error correction experiments that were obtained using the Protocol 2 described in Section 4.4.4 and Table 9. According to this protocol, 50 nM oligos were used in the assembly reaction. The assembly product was diluted by 16-fold before amplification to remove unreacted oligos and misassemblies. The denature/anneal procedure was done in four cycles.

A comprehensive analysis of error types found in 57 sequenced clones is shown in Table 12. Figures 35 (a) and 35 (b) illustrate the results of a microfluidic experiment that was designed with conditions similar to a benchtop protocol. Both microfluidic experiments were conducted on different days using the same reagents and automation program. As seen in Figure 35 (a), the overall error frequency was reduced from 1.31 errors/kb to 0.29 errors/kb, which is about a 4-fold decrease. In this experiment, all substitutions and insertions were eliminated. Conversely, a repeat of the same run, shown in Figure 35 (b), did not demonstrate the same level of error correction. There was some reduction of the overall error frequency from 3.32 to 2.62 errors/kb. The insertion errors were removed completely, but some substitutions appeared. Figure 35 (c) shows the error frequency of samples obtained on a conventional thermocycler using a benchtop protocol shown in Table 7. The error frequency was reduced from 2.16 to 0.29 errors/kb, which was a 10-fold error reduction.

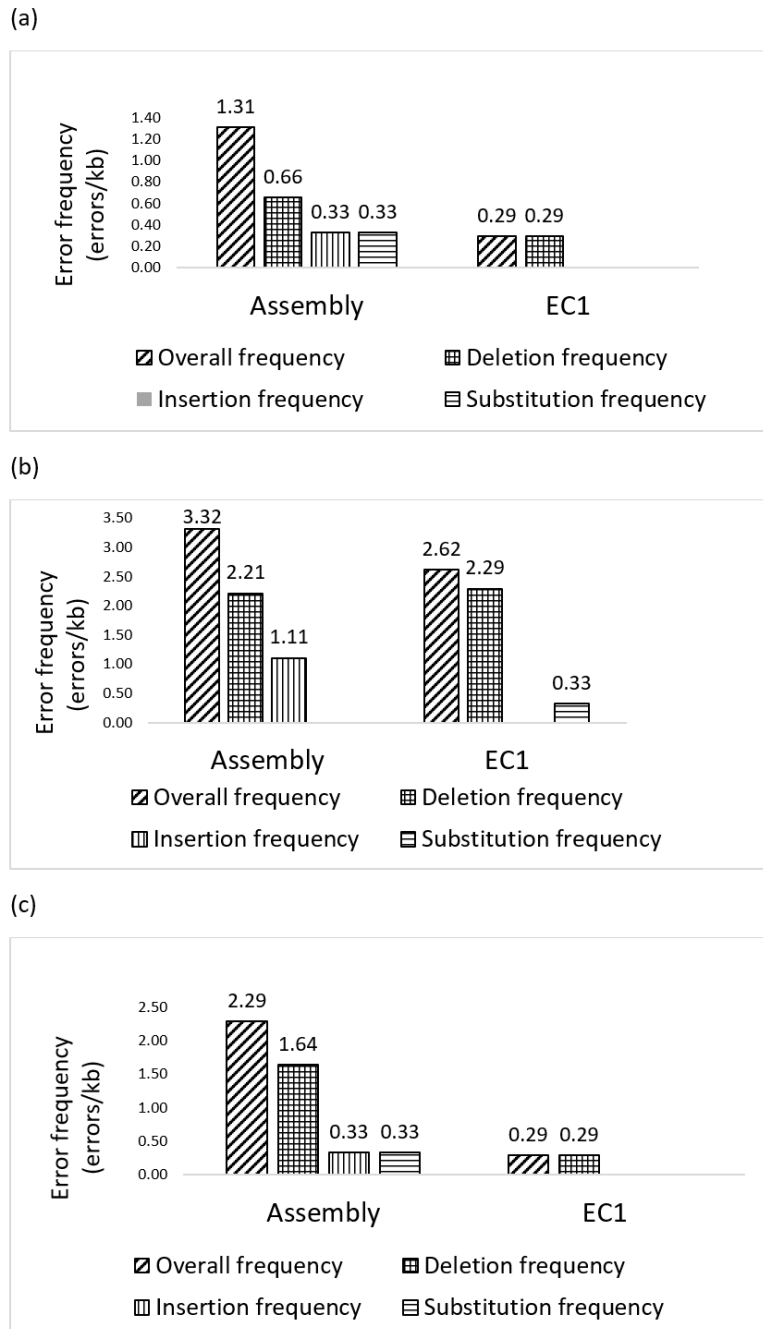


Figure 35. Error frequency of untreated and treated with CorrectASE™ samples on a benchtop and on the DMF following protocol 2. (a) PCR1 conditions –0.02 U/μL Phusion, PCR2/PCR3 conditions – 0.02 U/μL of Phusion, 0.5 mM of MgCl<sub>2</sub>, 0.625 mM of PEG. (b) PCR 1 conditions – 0.02 U/μL of Phusion, 0.5 mM of MgCl<sub>2</sub>, 0.625 mM of PEG. (c) a benchtop experiment.

Table 12. Error analysis of benchtop and microfluidic assembly and error correction samples obtained using Protocol 2.

	Run 1		Run 1 repeat		Benchtop	
	No EC	EC1	No EC	EC1	No EC	EC1
Error type	Number of errors					
Deletion (total)	2	1	6	7	5	1
Single-base deletion						
G/C	1	0	3	3	2	1
A/T	1	1	3	4	2	0
Multiple base deletion	0	0	0	0	1	0
Insertion (total)	1	0	3	0	1	0
Single-base insertion						
G/C	1	0	1	0	1	0
Multiple-base insertion	0	0	2	0	0	0
Substitution (total)	1	0	0	1	1	0
Transition						
A/T to G/C	0	0	0	0	1	0
Transversion						
G/C to C/G	0	0	0	1	0	0
A/T to T/A	1	0	0	0	0	0
Total errors	4	1	9	8	7	1
Sequenced bases	3051	3390	2712	3051	2712	3390
Total clones without misassemblies	9	10	8	9	9	10
Total clones sequenced	10	10	9	9	9	10
Total of clones with correct sequences	5	9	2	2	3	9

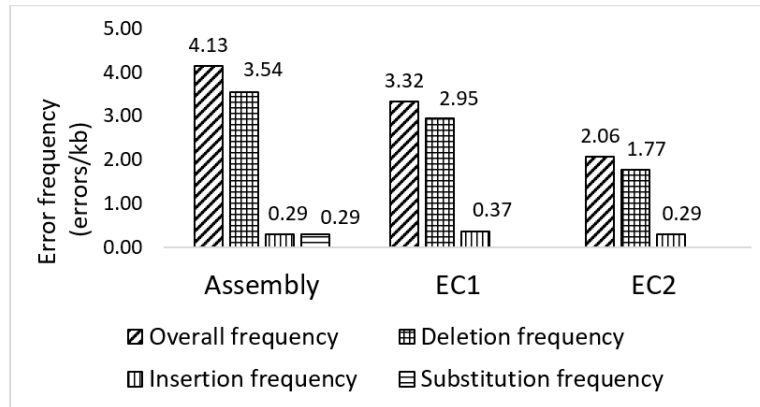
The results of these experiments demonstrated that the microfluidic error correction reaction was inconsistent. It is possible that the reaction worked on some lanes and did not work on the others. Since droplets were pooled before cloning and sequencing, this variability might have resulted in higher overall error rates. Also, the first PCR amplification with only a 2-fold increase of Phusion polymerase might not have been effective in every droplet, which led to a lower amount of the PCR product. If the



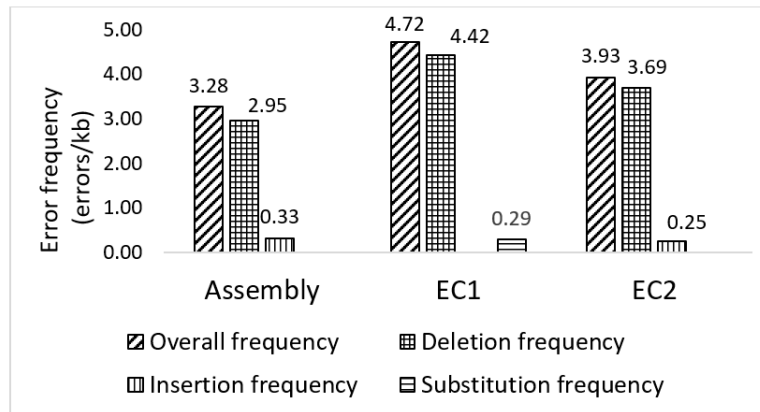
concentration of DNA was low in the error correction reaction, then the error removal process may not have been effective. The CorrectASE™ manufacturer recommends using 25-50 nM DNA for efficient error reduction. According to the protocol 2, the assembly product is diluted by 16-fold before PCR1. It is likely that there was not enough Mg<sup>2+</sup> and PEG 8000 from the assembly reaction to improve the PCR reaction efficiency. Thus, it is important to perform PCR1 with a 5-fold increased Phusion polymerase along with PEG and Mg<sup>2+</sup>.

To determine if dilution of the amplified assembly product could improve the effectiveness of the first error correction, three different dilutions were tested before the EC1 denature/anneal cycle. The following results are based on the experimental runs shown in Table 9 in Section 4.4.4. In these runs the assembly products were diluted by 4-fold, 8-fold, and 16-fold. The dilution before the second error correction was kept constant in all three experiments. As seen in Figure 36 (a), a 4-fold dilution of the assembly product resulted in a gradual reduction of errors with each error correction reaction. The error frequency was reduced by a 2-fold at the end of the process, substitutions were eliminated, but insertions were not removed. As shown in Table 13, the number of error-free clones increased after the second CorrectASE™ treatment from 0/10 to 5/11

(a)



(b)



(c)

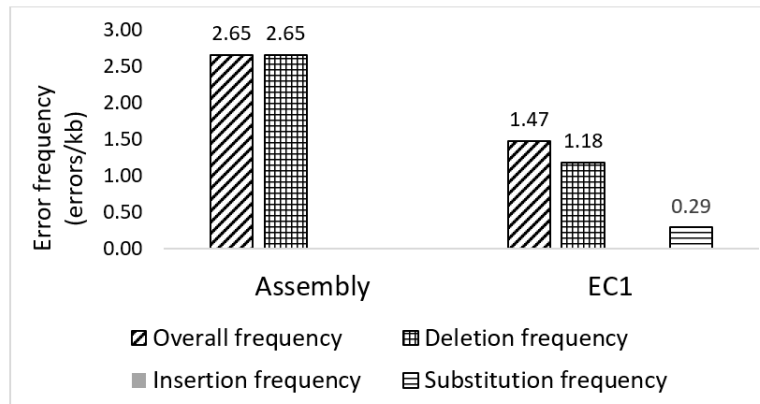


Figure 36. Error frequency of assembly samples followed by two rounds of error correction obtained using the automation protocol 2. a) 4-fold dilution before EC1; b) 8-fold dilution before EC1; c) 16-fold dilution before EC1.

Table 13. Error analysis assembly and error correction experiments using protocol 2.

	Run 2			Run 3			Run 4		
	No EC	EC1	EC2	No EC	EC1	EC2	No EC	EC1	
Error type	Number of errors								
Deletion (total)	12	8	8	9	15	15	9	4	
Single-base deletion									
G/C	5	1	3	2	2	4	4	0	
A/T	7	5	3	5	12	10	5	2	
Multiple base deletion	0	2	0	2	1	1	0	2	
Insertion (total)	1	1	1	1	0	1	0	0	
Single-base insertion									
G/C	1	1	0	0	0	1	0	0	
A/T	0	0	1	1	0	0	0	0	
Substitution (total)	1	0	0	0	1	0	0	1	
Transition									
G/C to A/T	0	0	0	0	1	0	0	0	
Transversion									
G/C to T/A	1	0	0	0	0	0	0	1	
Total errors	14	9	7	10	16	16	9	5	
Sequenced bases	3600	2880	3600	3240	3600	4230	3600	3600	
Total clones without misassemblies	10	8	10	9	10	12	10	10	
Total clones sequenced	10	8	11	10	10	13	10	14	
Total of clones with correct sequences	0	0	5	0	0	0	0	5	

The results of 8-fold dilution of the amplified assembly product are illustrated in Figure 36 (b). In this run, no overall error correction after the second CorrectASE™ treatment was observed. The error frequency of single base deletions was propagated after the first error correction. Then, the error frequency was reduced after the second error correction relative to the first error correction step. For each treatment, all sequenced clones had at least one error.

Figure 36 (c) demonstrates the results of a 16-fold dilution before EC1 denature/anneal. For this experiment, only the assembly and EC1 samples were sequenced. For this run, EC2 samples resulted in mostly misassembled products after cloning and colony PCR. Only two out of 31 screened colonies had the right size product. Based on the colony PCR, it was concluded that the EC2 step failed to yield the correct product. On the contrary, EC1 demonstrated a 1.8-fold reduction of overall error frequency. The number of single-base deletions was reduced, but multiple-base deletions and transversion of G/C to T/A appeared in some sequences. In Runs 3 and 4, five clones had completely correct sequences after the second error correction.

The results shown in Figure 36 and Table 13 demonstrated that dilution of the assembly product before the EC/denature step is important. However, it is not the only factor that leads to a successful error correction. Both a 4-fold and 16-fold dilution runs were successful in error reduction and both had misassembled sequences after the error correction reactions. Both samples demonstrated error reduction, but had an increased number of different size sequences in colony PCR screening that were considered as misassemblies (data not shown). In these misassemblies, CorrectASE™ converted single-base error into large lesions. It is evident that the enzyme cut the mismatch, but perhaps the larger lesions could be explained by hypothesizing that the problematic nucleotides were not removed by Phusion during subsequent amplification. Those incorrect partially digested sequences of various sizes were subsequently PCR amplified, and the lesion sizes may have been increased as a result of errors during amplification.

Two out of four microfluidic error correction experiments using protocol 2 were successful in error reduction. The lowest error frequency of 0.3 errors/kb was achieved, which was a 4-fold error reduction. This result was in 3-10-fold range accepted for CorrectASE™ enzyme. However, this result was not reproducible. The degree of error reduction was varied from run to run. It was concluded that error correction on the DMF was not reliable.

## CHAPTER SIX

### DISCUSSION

#### 6.1 Microfluidic PCR with Phusion Polymerase

The results of the microfluidic PCR experiments demonstrated that due to the high surface-to-volume ratio, reactions carried on the microfluidic device show a strong dependence on surface interactions. Protein molecules can adsorb at the oil/water interface, which reduces the surface tension over time [27, 40]. Additionally, adsorption of a protein at the droplet interface could facilitate exposure of hydrophobic groups that may lead to change of a conformation and inactivation. At high temperatures, the exposed hydrophobic groups of the protein could lead to protein denaturation.

Adsorption and denaturation reduces the amount of available enzyme. Therefore, the amplification reaction is inefficient due to the lack of the catalyst. It has been shown in the literature that to achieve amplification efficiency similar to a benchtop PCR, the amount of polymerase must be increased up to a 10-fold [24, 25]. The results of PCR experiments presented here demonstrated that sufficient and repeatable PCR amplification could be achieved with a 5-fold increase of Phusion polymerase.

The efficiency and specificity of PCR is affected by the  $Mg^{2+}$  concentration. Magnesium ions help the polymerase to fold in the active conformation. Also,  $Mg^{2+}$  stabilizes dsDNA and increases the melting temperature ( $T_m$ ) of primers. Thus, it is crucial to have the correct amount of free magnesium. If magnesium is scarce, the reaction will not proceed as efficiently. It has been observed that the concentration of free magnesium is reduced because of precipitation on microfluidic surfaces, capture by

chelating agents present in reagents and storage buffers, and by binding to dNTPs [25]. According to the Phusion manufacturer, the optimum concentration of  $\text{MgCl}_2$  is between 0.5-1 mM. The experimental results demonstrated that the addition of 0.5-1 mM of magnesium to 1.5 mM  $\text{MgCl}_2$ , presented in Phusion HF buffer, improved polymerase activity, but this effect was inconsistent from lane to lane. However, it was shown that the synergistic effect of magnesium and PEG 8000 created favorable conditions for PCR amplification.

Polyethylene glycol (PEG) is recognized as a molecular crowding agent and frequently used as a PCR enhancer and an enzyme immobilization agent. Molecular crowding creates the conditions similar to a natural cell environment in which the enzyme was evolved. It was reported that macromolecular crowding affects the enzyme reaction kinetics by increasing the viscosity of a medium that in turn influences diffusion of reagents. Also, the polymers preserve native protein conformation and facilitate binding to a substrate. It has been shown that PEG 8000 stabilized polymerase at high temperatures [41, 42]. Since Phusion is a type of polymerase, it is possible that PEG 8000 formed weak bonds with the enzyme and reduced hydrophobic interactions with the Teflon coating. Additionally, PEG could have prevented hydrophobic groups from adsorbing to the oil/water interface of the DMF cartridge. As a result, the activity of the enzyme was increased and amplification yield was improved [30]. Consequently, microfluidic PCR is affected by adsorption as well as the by interactions of reaction components with interfaces. In order to achieve amplification on the DMF, the reaction must be carried out with the final concentration of 0.1 U/ $\mu\text{L}$  of Phusion (a 5-fold increase

relative to standard benchtop conditions), 0.5-1 mM of MgCl<sub>2</sub>, and 0.625-1.25 mM of PEG 8000.

Multiple methods that have been reported in the literature to reduce biofouling in microfluidics were tested in this research. The only method that improved PCR yield and transport of droplets was the reduction of the electrowetting voltage from 300 V to 90 V during PCR [20]. This result showed that at the lower voltage, the oil film between the aqueous droplet and the Teflon coated surface stayed intact and eliminated hydrophobic interactions between the polymerase and the surface. According to Kleinert *et al.*, the actuation voltage has a significant influence on the oil film [33]. At high actuation voltage when the droplet moves, the film becomes unstable, breaks down, and tiny oil droplets get trapped under the aqueous phase. In addition, the excess of surfactant destabilizes the oil film. Mohajeri and colleagues demonstrated that the critical micellar concentration of nonionic surfactants such as Tween 20 decreases with raising temperatures [34]. Thus, in the denaturation zone, less surfactant is necessary to reduce the surface tension. If there is an excessive amount of surfactant, the oil film becomes unstable, and the adsorption of the protein occurs, which is further enhanced at high temperatures. It is important to use lower voltage and minimize the amount of Tween 20 to avoid loss of Phusion polymerase and subsequent droplet transport failure.



## 6.2 Microfluidic Gibson Assembly

Microfluidic DNA assembly protocols developed in this work produce results similar to the results published in the literature. It was reported by Gibson's group and other researchers that DNA assembly reaction proceeds in 15-60 min [6, 23, 38]. The microfluidic DNA assembly protocol generated double-stranded DNA fragments from oligonucleotides in a similar 15-60 min time frame.

The results of this study show that T5 exonuclease plays essential role in the assembly of 250 nM oligos. The enzyme is known for its ability to chew back DNA overlaps from the 5'- end, but it also possesses endonuclease activity towards ssDNA. It can degrade oligos into smaller fragments such as trimers, tetramers, and pentamers [43]. Assembly of high concentration oligos should not be done without the exonuclease. One of the advantages of assembly with exonuclease is that the enzyme could remove the overlaps, which were created by incorrect oligo alignment to prevent the appearance of misassemblies. The results demonstrated that microfluidic assembly protocols work well in 50-250 oligo nM concentration range.

To ensure that the excess of oligos and misassemblies are removed, the DMF assembly protocol has a dilution step after assembly and before PCR. It was shown that the dilution by 16-fold was sufficient to keep enough template for further amplification. If the dilution step before PCR is employed, the amplification mix must contain 0.1 U/ $\mu$ L of Phusion, 0.625 mM PEG 8000, and 0.5 mM MgCl<sub>2</sub>. The results of the experiments demonstrated that the 5-fold increase in Phusion concentration on its own did not provide the same yield of the assembly product in all experimental droplets. On the other hand,

2-fold Phusion with  $Mg^{2+}$  and PEG leads to production of different sized constructs. As discussed in Section 6.1, the excess magnesium could lead to incorrect binding of primers, which may create errors in DNA sequence and amplification of misassemblies. Consequently, it is important to keep  $Mg^{2+}$  at optimum concentration, if the assembly product is diluted before amplification.

Error analysis of sequences assembled with 50 nM and 250 nM oligos demonstrated similar error rates. This suggests that the concentration of oligos during assembly does not affect the fidelity of the resulting sequence. Both DNA assembly methods demonstrated an error frequency in the 1-10 errors/kb range, which was similar to the values reported in the literature [7]. For instance, Saem *et al.* reported 1.9 errors/kb, Sequeira *et al.* reported 3.45 errors/kb, Kosuri *et al.* reported 4 errors/kb, and Yehezkel *et al.* reported 2.2 errors/kb [20, 36, 37, 39]. The analysis of error types demonstrated that the majority of errors belonged to single-base deletions with a small percentage of insertions and substitutions. These results are comparable to 75.6% deletions, 2.2% insertions, and 22.2% substitutions, obtained by Sequeira *et al.* [39]. However, several clones in both data sets had misincorporated oligos. The occurrence of misassemblies could have arisen from oligo misplacement and improper alignment as a consequence. This issue could be solved by improving the design of oligo sequences. Since the 50 nM oligo data set had 1.5 times more clones with misassemblies, degradation of some oligos by T5 exonuclease could be the cause of misincorporation. The results demonstrated that the Gibson assembly method performed on the DMF is efficient. The error frequencies

for microfluidic synthesized sequences are in line with those found for benchtop DNA synthesis in the published literature.

### 6.3 Microfluidic Error Correction with CorrectASE™

The results of the current work show that error correction with CorrectASE™ on the DMF is not yet reliable. Since all experiments were run on different days using identical automation programs, there might be some issues with variability of equipment or microfluidic cartridges. Additionally, the repeatability could be related to the size of the droplets that may be consistently generated. Considering that reaction is carried in 1.2  $\mu\text{L}$  reactors that are incubated with CorrectASE™ for 60 min, volume differences and resulting concentration differences from merging droplets of slightly different volume could be a possible reason for error correction failure.

Since the enzymes show the best activity at optimum reagent concentrations, evaporation of water will increase the concentration of salts making the enzyme less active. Another possible reason is the adsorption of protein molecules on the oil/water interface. According to Baldursdottir *et al.*, protein molecules tend to aggregate on the oil/water interface in a multilayer. The adsorption rate is affected by the molecular weight and a saturation concentration. Large protein molecules tend to adsorb faster than small ones due to the large surface available for contact with the interface. Also, hydrophobic proteins tend to adsorb more due to the hydrophobic interactions with hydrophobic substances [44]. If some of the protein molecules adsorb on the interface, hydrophobic and hydrophilic groups will rearrange, and it will cause the protein to change the conformation. For proteins molecules, shape determines its function, so the

adsorption can lead to the loss of activity. As a consequence, the concentration of enzyme is not going to be optimum, and the reaction will not proceed with the maximum yield.

According to a patent describing the method of error removal using a mix of Surveyor nuclease and Exonuclease III enzymes, the Surveyor nuclease cuts the product near the site of a mismatch. Then, the endonuclease digests the mismatched nucleotide in both 3' to 5' and 5' to 3' directions [38]. Then, the sequence is repaired by Phusion polymerase during subsequent PCR reactions. Since CorrectASE™ is a proprietary blend, we do not know which enzymes it contains. However, the mechanism of error removal by CorrectASE™ is very similar to Surveyor and Exonuclease III. According to Invitrogen, the enzyme nicks both DNA strands at the 3' site. Then, endonuclease removes the mismatch in a 3' to 5' direction. In the experiments that demonstrated some amount of error correction, the number of sequences containing large insertions, which were categorized as misassemblies, increased with each CorrectASE™ treatment. This suggests that the 3' to 5' exonuclease activity was not present or was not as effective on the DMF device. It is likely that the activity of the enzyme is affected by either the adsorption of some protein molecules at the oil/water interface, microfluidic surface or by the interaction with the components carried through previous gene assembly steps.

It was demonstrated in Section 5.2 that the presence of a molecular crowding agent such as PEG significantly increased the activity of Phusion polymerase. According to Sasaki *et al.* the activity of DNase I to degrade supercoiled DNA and linear DNA was improved in the presence of 20% w/v PEG. A kinetic analysis demonstrated that the rate

of the DNA cleavage reaction increased with the increasing of concentration of PEG. However, molecular crowding did not improve the activity of Exonuclease III and inhibited the activity of Exonuclease I [45]. Consequently, macromolecular crowding could be the reason why the CorrectASE™ activity is inconsistent on the microfluidic device, and future experiments will be needed to determine whether the addition of PEG will improve the performance of this step. As we observed in the amplification of the assembly product with excess of magnesium relative to Phusion, the PCR product was amplified incorrectly. Thus, the loss of polymerase specificity could also have contributed to a failure of error removal in the error correction experiments.

## CHAPTER SEVEN

### CONCLUSIONS

Automated DNA assembly and error correction protocols for the Mondrian™ SP digital microfluidic device by Illumina Inc. were developed in this thesis. The process involved automation of the polymerase chain reaction, Gibson assembly of 12 oligonucleotides, and enzymatic error correction reaction with CorrectASE™. The final protocol consisted of the assembly of oligonucleotides, three PCRs, and two error correction reactions.

The development of the microfluidic PCR protocol consisted of two major tasks. The first task was to determine the optimum reagent concentrations for a consistent and repeatable DNA amplification. It was shown that in order to achieve reliable amplification, the PCR reaction mix must contain an additional 0.5-1 mM MgCl<sub>2</sub> over that required for bench top protocols, and 1.25 mM PEG 8000. Magnesium is responsible for activation of the Phusion polymerase, and PEG 8000 preserves the enzyme's structure and brings reagents into close proximity.

The second task was minimization of adsorption of Phusion polymerase on the microfluidic surface. The adsorption of Phusion was eliminated by a reduction of actuation voltage from 300 V to 90 V during thermocycling. The lower voltage keeps stable the oil film under the droplet, which prevents adsorption at the liquid/solid interface. The adsorption of the enzyme on the oil/water interface was also minimized by increasing the enzyme concentration by 5-fold.

The automation protocol for microfluidic DNA assembly consisted of the Gibson assembly reaction, dilution of the assembly product, and subsequent amplification of DNA constructs by PCR. It was shown that the assembly times of 15-60 min gave the right size assembly product. Additionally, a 16-fold dilution of the assembly products before PCR gave enough template for amplification and removed unreacted oligos and misassembled sequences. It was determined that the concentration of oligonucleotides for successful assembly should be in 50-250 nM range. The protocol was validated for 50 nM and 250 nM oligo assembly by Sanger sequencing. The sequencing results demonstrated that both oligo concentrations produce sequences with error frequencies about 3 error/kb, which falls in the 1-10 error/kb range reported in the literature. The errors were categorized into deletions, substitutions, and insertions. The majority of errors were single-base deletions.

The Gibson assembly, PCR, and error correction reactions were combined in a single protocol. To be able to monitor the changes after each step in the process, the amplified assembly, EC1, and EC2 products were Sanger sequenced. The results of sequencing showed that the 4 cycles denature/anneal procedure for the DMF was shown to be better at forming heteroduplexes in a place of mismatches. Dilution of the unamplified and amplified assembly products did not demonstrate a significant effect on the outcome of the error correction reaction. Some samples from the experiments that showed a gradual error frequency reduction after each treatment were found to have large lesions at the beginning or the end of the sequence. The occurrence of lesions could be due to 3' to 5' inactivity of CorrectASE™ related to surface chemistry of protein molecules under a

high surface-to-volume conditions or interactions with the reagents carried from previous gene synthesis steps. It was concluded that microfluidic error correction with CorrectASE™ did not give repeatable results, and the inhibition of enzyme should be investigated in future studies.



## CHAPTER EIGHT

### FUTURE STUDIES

Automation of routine molecular biology reactions brings many benefits for scientists. It reduces the cost of reagents and labor, eliminates human errors, and saves time-consuming steps such as pipetting, mixing reagents, and tube labeling. In this study, a gene assembly protocol for digital microfluidics was developed. It was shown that the protocol gives results comparable to conventional benchtop protocols. However, the reduction of errors in synthetic genes on the DMF was inconsistent. In future studies, the adsorption of CorrectASE™ on the oil/water interface should be investigated. Additionally, the effects of macromolecular crowding on CorrectASE™ activity should be tested by the addition of various polymer molecules. The carryover of magnesium from error correction reaction to subsequent PCR should be investigated. Error correction with CorrectASE™ should be compared to other enzymes such as Surveyor nuclease, Exonuclease III, and T7 Endonuclease I.

## REFERENCES

1. C.A. Hutchison 3rd, R.Y. Chuang, V.N. Noskov, N. Assad-Garcia, T.J. Deerinck, M.H. Ellisman, J. Gill, K. Kannan, B.J. Karas, L. Ma, J.F. Pelletier, Z.Q. Qi, R.A. Richter, E.A. Strychalski, L. Sun, Y. Suzuki, B. Tsvetanova, K.S. Wise, H.O. Smith, J.I. Glass, C. Merryman, D.G. Gibson and J.C. Venter, "*Design and synthesis of a minimal bacterial genome*," *Science*, **351**, 1414-1415 (2016).
2. J.W. CHIN, M.A. ANDERSON, J. CUI and M. SPIEKER, "*Production of 1, 3-propanediol in cyanobacteria*," *Metabolic Engineering*, **34**, 97-103 (2016).
3. Michael L. Shuler and F Kargi, *Bioprocess Engineering Basic Concepts*, 2nd ed. (Prentice Hall Inc, New Jersey, USA, 2002), pp. 40-46.
4. B. Karas, J. Jablanovic, L. Sun, J. Stam, L. Ma, A. Ramon, J. Venter, P. Weyman, D. Gibson, Glass, JI Hutchison C., H. Smith and Y. Suzuki, "*Direct transfer of whole genomes from bacteria to yeast*," *Nat Meth*, **10**, 410-412 (2013).
5. S. Ma, N. Tang and J. Tian, "*DNA synthesis, assembly and applications in synthetic biology*," *Current Opinion in Chemical Biology*, **16**, 260-267 (2012).
6. D.G. Gibson, H.O. Smith, C.A. Hutchison III, J.C. Venter and C. Merryman, "*Chemical synthesis of the mouse mitochondrial genome*," *Nature Methods*, **7**, 901-903 (2010).
7. S. Ma, I. Saaem and J. Tian, "*Error correction in gene synthesis technology*," *Trends in Biotechnology*, **30**, 147-154 (2011).
8. J. Lee, H. Moon, J. Fowler, T. Schoellhammer and C. Kim, "*Electrowetting and electrowetting-on-dielectric for microscale liquid handling*," *Sensors and Actuators A: Physical*, **95**, 259-268 (2002).
9. F. Mugele and J. Baret, "*Electrowetting: From basics to applications*," *Journal of Physics: Condensed Matter*, **17**, 706-770 (2005).
10. S. Teh, R. Lin, L. Hung and A.P. Lee, "*Droplet microfluidics*," *Lab on a Chip*, **8**, 198-220 (2008).
11. C.N. Baroud, F. Gallaire and R. Dangla, "*Dynamics of microfluidic droplets*," *Lab on a Chip*, **10**, 2032-2045 (2010).
12. M.J. Czar, J.C. Anderson, J.S. Bader and J. Peccoud, "*Gene synthesis demystified*," *Trends in Biotechnology*, **27**, 63-72 (2009).

13. D.S. Kong, P.A. Carr, L. Chen, S. Zhang and J.M. Jacobson, "*Parallel gene synthesis in a microfluidic device*," *Nucleic Acids Research*, **35**, 61-70 (2007).
14. M.C. Huang, H. Ye, Y.K. Kuan, M. Li and J.Y. Ying, "*Integrated two-step gene synthesis in a microfluidic device*," *Lab on a Chip*, **9**, 276-285 (2009).
15. J. Quan, I. Saaem, N. Tang, S. Ma, N. Negre, H. Gong, K.P. White and J. Tian, "*Parallel on-chip gene synthesis and application to optimization of protein expression*," *Nature Biotechnology*, **29**, 449-452 (2011).
16. J. Tian, H. Gong, N. Sheng, X. Zhou, E. Gulari, X. Gao and G. Church, "*Accurate multiplex gene synthesis from programmable DNA microchips*," *Nature*, **432**, 1050-1054 (2004).
17. G. Linshiz, E. Jensen, N. Stawski, C. Bi, N. Elsbree, H. Jiao, J. Kim, R. Mathies, J.D. Keasling and N.J. Hillson, "*End-to-end automated microfluidic platform for synthetic biology: From design to functional analysis*," *Journal of Biological Engineering*, **10**, 1 (2016).
18. S.C. Shih, G. Goyal, P.W. Kim, N. Koutsoubelis, J.D. Keasling, P.D. Adams, N.J. Hillson and A.K. Singh, "*A versatile microfluidic device for automating synthetic biology*," *ACS Synthetic Biology*, **4**, 1151-1164 (2015).
19. U. Tangen, G.A.S. Minero, A. Sharma, P.F. Wagler, R. Cohen, O. Raz, T. Marx, T. Ben-Yehezkel and J.S. McCaskill, "*DNA-library assembly programmed by on-demand nano-liter droplets from a custom microfluidic chip*," *Biomicrofluidics*, **9**, 044103 (2015).
20. T. Ben Yehezkel, A. Rival, O. Raz, R. Cohen, Z. Marx, M. Camara, J.F. Dubern, B. Koch, S. Heeb, N. Krasnogor, C. Delattre and E. Shapiro, "*Synthesis and cell-free cloning of DNA libraries using programmable microfluidics*," *Nucleic Acids Research*, **44**, e35. doi: 10.1093/nar/gkv1087 (2016).
21. W.P.C. Stemmer, A. Cramer, K.D. Ha, T.M. Brennan and H.L. Heyneker, "*Single-step assembly of a gene and entire plasmid from large numbers of oligodeoxyribonucleotides*," *Gene*, **164**, 49-53 (1995).
22. D.G. Gibson, L. Young, R. Chuang, J.C. Venter, C.A. Hutchison and H.O. Smith, "*Enzymatic assembly of DNA molecules up to several hundred kilobases*," *Nature Methods*, **6**, 343-345 (2009).
23. E.H. Akama-Garren, N.S. Joshi, T. Tammela, G.P. Chang, B.L. Wagner, D.Y. Lee, W.M. Rideout Iii, T. Papagiannakopoulos, W. Xue and T. Jacks, "*A modular*

- assembly platform for rapid generation of DNA constructs*," Scientific Reports, **6**, 16836 (2016).
24. M. Krishnan, D.T. Burke and M.A. Burns, "*Polymerase chain reaction in high surface-to-volume ratio SiO<sub>2</sub> microstructures*," Analytical Chemistry, **76**, 6588-6593 (2004).
  25. F. Wang and M.A. Burns, "*Performance of nanoliter-sized droplet-based microfluidic PCR*," Biomedical Microdevices, **11**, 1071-1080 (2009).
  26. Z. Hua, J.L. Rouse, A.E. Eckhardt, V. Srinivasan, V.K. Pamula, W.A. Schell, J.L. Benton, T.G. Mitchell and M.G. Pollack, "*Multiplexed real-time polymerase chain reaction on a digital microfluidic platform*," Analytical Chemistry, **82**, 2310-2316 (2010).
  27. J. Yoon and R.L. Garrell, "*Preventing biomolecular adsorption in electrowetting-based biofluidic chips*," Analytical Chemistry, **75**, 5097-5102 (2003).
  28. A.R. Prakash, M. Amrein and K.V. Kaler, "*Characteristics and impact of taq enzyme adsorption on surfaces in microfluidic devices*," Microfluidics and Nanofluidics, **4**, 295-305 (2008).
  29. I. Erill, S. Campoy, N. Erill, J. Barbé and J. Aguiló, "*Biochemical analysis and optimization of inhibition and adsorption phenomena in glass-silicon PCR-chips*," Sensors and Actuators B: Chemical, **96**, 685-692 (2003).
  30. Y. Xia, Z. Hua, E. Gular, O. Srivannavit and A.B. Ozel, "*Minimizing the surface effect of PDMS - glass microchip on polymerase chain reaction by dynamic polymer passivation*," Journal of Chemical Technology and Biotechnology, **82**, 33-38 (2007).
  31. V.N. Luk, G.C. Mo and A.R. Wheeler, "*Pluronic additives: A solution to sticky problems in digital microfluidics*," Langmuir, **24**, 6382-6389 (2008).
  32. S.H. Au, P. Kumar and A.R. Wheeler, "*A new angle on Pluronic additives: advancing droplets and understanding in digital microfluidics*," Langmuir, **27**, 8586-8594 (2011).
  33. J. Kleinert, V. Srinivasan, A. Rival, C. Delattre, O.D. Velev and V.K. Pamula, "*The dynamics and stability of lubricating oil films during droplet transport by electrowetting in microfluidic devices*," Biomicrofluidics, **9(3)**, 034104. doi: <http://dx.doi.org/10.1063/1.4921489> (2015).
  34. E. Mohajeri and G.D. Noudeh, "*Effect of Temperature on the Critical Micelle Concentration and Micellization Thermodynamic of Nonionic Surfactants:*

- Polyoxyethylene Sorbitan Fatty Acid Esters*, "E-Journal of Chemistry, **4**, 2268-2274 (2012).
35. M. Fuhrmann, W. Oertel, P. Berthold and P. Hegemann, "*Removal of mismatched bases from synthetic genes by enzymatic mismatch cleavage*," *Nucleic Acids Research*, **33**, e58. doi:10.1093/nar/gni058 (2005).
  36. S. Kosuri, N. Eroshenko, E.M. LeProust, M. Super, J. Way, J.B. Li and G.M. Church, "*Scalable gene synthesis by selective amplification of DNA pools from high-fidelity microchips*," *Nature Biotechnology*, **28**, 1295-1299 (2010).
  37. I. Saaem, S. Ma, J. Quan and J. Tian, "*Error correction of microchip synthesized genes using surveyor nuclease*," *Nucleic Acids Research*, **40**, e23. doi:10.1093/nar/gkr887 (2012).
  38. D.G. Gibson, N. Caiazza and T.H. Richardson, Materials and methods for the synthesis of error-minimized nucleic acid molecules. US Patent 20130225451, Aug 29 2013.
  39. A.F. Sequeira, C.I. Guerreiro, R. Vincentelli and C.M. Fontes, "*T7 endonuclease I mediates error correction in artificial gene synthesis*," *Molecular Biotechnology*, **58**, 573-584 (2016).
  40. C.J. Beverung, C.J. Radke and H.W. Blanch, "*Protein adsorption at the oil/water interface: Characterization of adsorption kinetics by dynamic interfacial tension measurements*," *Biophysical Chemistry*, **81**, 59-80 (1999).
  41. R.K. Saiki, S. Scharf, F. Faloona, K.B. Mullis, G.T. Horn, H.A. Erlich and N. Arnheim, "*Enzymatic amplification of beta-globin genomic sequences and restriction site analysis for diagnosis of sickle cell anemia*," *Science (New York, N.Y.)*, **230**, 1350-1354 (1985).
  42. S.B. Zimmerman and B. Harrison, "*Macromolecular crowding increases binding of DNA polymerase to DNA: An adaptive effect*," *Proceedings of the National Academy of Sciences of the United States of America*, **84**, 1871-1875 (1987).
  43. T.A. Ceska and J.R. Sayers, "*Structure-specific DNA cleavage by 5' nucleases*," *Trends in Biochemical Sciences*, **23**, 331-336 (1998).
  44. S.G. Baldursdottir, M.S. Fullerton, S.H. Nielsen and L. Jorgensen, "*Adsorption of proteins at the oil/water interface--observation of protein adsorption by interfacial shear stress measurements*," *Colloids and Surfaces.B, Biointerfaces*, **79**, 41-46 (2010).

45. Y. Sasaki, D. Miyoshi and N. Sugimoto, "*Effect of molecular crowding on DNA polymerase activity*," *Biotechnology Journal*, **1**, 440-446 (2006).

## Appendix A: Materials

- HA 049 sequence cloned in a plasmid DNA (prepared by the J. Craig Venter Institute)

GAATTCGAGCTCGGTACCCGGCGGCCGCTTTGAGTCAGCCATCTCATGTT  
CCTGTAGAATGAATCTGAACATGATTTGCTTGTTCAGTGTAAGTCACATTCC  
AGATTGTGTCTGGGAATATTTGGATTCTTTGGTAGGAACTAGAGGAACTAAA  
GAGTGTTCTGAGTTCCTCTAAGTTTCCACATCCAGGGTAAACACGTTCCAT  
TTACAGCTGATGGTCTTTCAACGATGTAGGACCATCTCTTCCCCCAACAAC  
AGATCACAAGAAGGGTTACCATAGACAAGTCCTTCAATAGTGCATGTGTGCGC  
GGCCGCGATCCTCTAGAGTCGACCTG

- Oligonucleotides 1  $\mu$ M each (Integrated DNA Technologies). Sequences are shown in Table 14
- Tween 20 (Sigma Aldrich)
- DNase, RNase-free UltraPure™ DI water (Invitrogen)
- Phusion High-Fidelity (HF) DNA polymerase 2 U/ $\mu$ L (Thermo Fisher Scientific)
- 5X Phusion HF detergent-free buffer (Thermo Fisher Scientific)
- Forward PCR primer: 100  $\mu$ M Oligo HA 049-1 (IDT DNA):  
5'CAGGTCGACTCTAGAGGATCGCGGCCGCGACACATGCACTATTGA  
AGGACTT
- Reverse primer: 100  $\mu$ M Oligo HA 049-12 (IDT DNA):  
5'GAATTCGAGCTCGGTACCCGGCGGCCGCTTTGAGTCAGCCATCTCATGT  
TCCT
- 100 mM deoxynucleotide kit (Thermo Fisher Scientific)
- PEG 8000 (Sigma)
- PEG 6000 (Sigma)
- PEG 4000 (Sigma)
- PEG 3350 (Sigma)

Table 14. A list of oligonucleotide sequences.

Oligo name	Sequence	Length (bases)
HA 049-1	CAGGTCGACTCTAGAGGATCGCGGCCGCGACACATG CACTATTGAAGGACTT	52
HA 049-2	AGATCACAAGAAGGGTTACCATAGACAAGTCCTTCA ATAGTGCATGTGTCGC	52
HA 049-3	GTCTATGGTAACCCTTCTTGTGATCTGTTGTTGGGGG GAAGAGAATGGTCCT	52
HA 049-4	TACAGCTGATGGTCTTTCAACGATGTAGGACCATTCT CTTCCCCCAACAAC	52
HA 049-5	ACATCGTTGAAAGACCATCAGCTGTA AATGGAACGT GTTACCCTGGGAATGT	52
HA 049-6	GTGTTCTGAGTTCCTCTAAGTTTTCCACATTCCCAGG GTAACACGTTCCATT	52
HA 049-7	GGAAACTTAGAGGAACTCAGAACACTCTTTAGTTC CTCTAGTTCCTACCAA	52
HA 049-8	ATTGTGTCTGGGAATATTTGGATTCTTTGGTAGGAAC TAGAGGAACTAAAGA	52
HA 049-9	AGAATCCAAATATTTCCAGACACAATCTGGAATGTG ACTTACACTGGAACAA	52
HA 049-10	GTAGAATGAATCTGAACATGATTTGCTTGTTCAGT GTAAGTCACATTCCAG	52
HA 049-11	GCAAATCATGTTTCAGATTCATTCTACAGGAACATGA GATGGCTGACTCAAAG	52
HA 049-12	GAATTCGAGCTCGGTACCCGGCGGCCGCTTTGAGTC AGCCATCTCATGTTCTT	53

- 10% Pluronic F68 (Sigma)
- 10 mg/mL BSA (NEB)
- 5X Gibson isothermal buffer [38]
- 10 mM MgCl<sub>2</sub> solution (Thermo Fisher Scientific)
- 12.5 mM PEG 8000 (Amersham)
- 2 mM NAD (Sigma)



- 20 mM DTT (Sigma)
- T5 exonuclease 10,000 U/mL (NEB)
- 10X buffer 4 (NEB)
- Taq DNA ligase 40,000 U/mL (NEB)
- CorrectASE™ (Invitrogen)
- 10X CorrectASE™ Buffer (Invitrogen)
- Elution buffer (Qiagen)

## Appendix B: Master Mixes for Microfluidic Assembly and Error Correction Experiments

The master mixes for assembly and error correction experiments were prepared to contain double amounts of reagents. When the equal size droplets were merged on the DMF, the 1X final concentration of reagents was obtained.

Table 15. Oligo master mixes.

Reagent	Concentration	
Oligonucleotides 1 $\mu$ M (Integrated DNA Technologies)	500 nM	100 nM
Tween 20 (Sigma Aldrich)	0.01%	
Ultra Pure™ DI water (Invitrogen)	Add to a final volume	

Table 16. Gibson assembly master mix.

Reagent	Concentration
T5 Exonuclease 10,000 U/mL (NEB)	0.08 U/ $\mu$ L
Taq DNA ligase 40,000 U/mL (NEB)	4 U/ $\mu$ L
Phusion polymerase 2U/ $\mu$ L (Thermo Fisher Scientific)	0.1 U/ $\mu$ L
Gibson isothermal buffer	2.5X
Tween 20 (Sigma Aldrich)	0.001%
Ultra Pure™ DI water (Invitrogen)	Add to a final volume

Table 17. PCR master mixes.

Reagent	Concentration			
5X-HF Phusion detergent-free buffer (Thermo Fisher Scientific)	2.5X	2.5X	2.5X	2.5X
25 mM of dATP, dGTP, dTTP, dCTP (Thermo Fisher Scientific)	0.5 mM	0.5 mM	0.5 mM	0.5 mM
Forward and reverse PCR primers 10 $\mu$ M each (IDT DNA)	0.8 $\mu$ M	0.8 mM	0.8 mM	0.8 mM
Phusion polymerase 2 U/ $\mu$ L (Thermo Fisher Scientific)	0.2 U/ $\mu$ L	0.04 U/ $\mu$ L	0.2 U/ $\mu$ L	0.04 U/ $\mu$ L
50 mM MgCl <sub>2</sub> (Thermo Fisher Scientific)	1 mM	1 mM	0	0
12.5 mM PEG 8000 (Sigma)	1.25 mM	1.25	0	0
Ultra Pure™ DI water (Invitrogen)	Add to a final volume			

Table 18. Dilution master mix.

Reagents	Concentration
Tween 20 (Sigma Aldrich)	0.01%
EB buffer (Qiagen)	Add to a final volume

Table 19. Denature/anneal master mix.

Reagents	Concentration
10X CorrectASE™ buffer (Invitrogen)	5X
Ultra Pure™ DI water (Invitrogen)	Add to a final volume

Table 20. CorrectASE™ master mix.

Reagent	Concentration
CorrectASE™ (Invitrogen)	2X
10X CorrectASE™ buffer (Invitrogen)	5X
Ultra Pure™ DI water (Invitrogen)	Add to a final volume

## Appendix C: List of Materials Used to Prepare Samples for Sanger Sequencing

- Agencourt AMPure XP SPRI magnetic beads (Beckman Coulter)
- 1 Kb Plus DNA ladder (Invitrogen)
- 6X Orange DNA loading dye (Thermo Fisher Scientific)
- pUC-049 cloning-R reverse primer (IDT DNA)  
5'- CCGGGTACCGAGCTCGAATTCAGT
- pUC-049 cloning-F primers forward primer (ITD DNA)  
5'- GATCCTCTAGAGTCGACCTGCAGGC
- 100 pg/ $\mu$ L pUC19 vector (Epicentre)
- DpnI restriction enzyme 20,000 U/mL (NEB)
- Phusion polymerase 2 U/ $\mu$ L (Thermo Fisher Scientific)
- 5X-HF Phusion buffer (Thermo Fisher Scientific)
- Taq DNA ligase 40,000 U/mL (NEB)
- T5 exonuclease 10,000 U/mL (NEB)
- 5X Isothermal Gibson buffer [38]
- 100 mM dNTPs kit (Thermo Fisher Scientific)
- Ampicillin (J. Craig Venter Institute)
- LB agar plates with 100  $\mu$ g/mL Carbenicillin (Stanford Genome Technology Center)
- LB broth (Teknova)
- TransforMax EPI300 electrocompetent *E. coli* cells (Epicentre)
- pUC19 -5'F 100  $\mu$ M forward primer (prepared at J. Craig Venter Institute)  
5'- TCCCAGTCACGAC GTTGTAAAACGAC
- pUC19 -3'R 100  $\mu$ M reverse primer (prepared at J. Craig Venter Institute)

5'-ACACAGGAAACAGCTATGACCATGATTACG

- QIAprep spin miniprep kit (Qiagen)
- Taq DNA polymerase 5 U/ $\mu$ L (Thermo Fisher Scientific)
- 25 mM MgCl<sub>2</sub> (Thermo Fisher Scientific)
- 10X Taq buffer with KCl (Thermo Fisher Scientific)

## Appendix D: Procedures for Cloning of DNA Samples to pUC19 Vector

Table 21. Master mix for amplification of pUC19 plasmid DNA.

Reagent	Final concentration
pUC19 -5'F + pUC19 -3'R primers (10 $\mu$ M each)	0.4 $\mu$ M
5X-HF Phusion buffer (Thermo Fisher Scientific)	1X
dNTPs 25 mM each (Thermo Fisher Scientific)	0.5 mM
100 pg/ $\mu$ L pUC19 vector (Epicentre)	0.1 ng/ $\mu$ L
Phusion polymerase 2 U/ $\mu$ L (Thermo Fisher Scientific)	0.04 U/ $\mu$ L
Ultra Pure™ DI water (Invitrogen)	Up to a final volume

### Thermocycler settings

Initial denaturation 98 °C – 30 s

30 cycles:

Denaturation 98 °C – 10 s

Annealing/extension 60 °C – 15 s

Final extension 72 °C – 2 min

Final extension 72 °C – 5 min

### Assembly of Puc19 and DNA samples

To perform cloning three reactions were set up: 2.5  $\mu$ L of the assembly sample were combined with 2.5  $\mu$ L of the vector and 5  $\mu$ L of 2X CBA; 2.5  $\mu$ L of the EC1 sample were combined with 2.5  $\mu$ L of the vector and 5  $\mu$ L of 2X CBA; 2.5  $\mu$ L of the EC2 sample were combined with 2.5  $\mu$ L of the vector and 5  $\mu$ L of 2X CBA.

Table 22. Example of Gibson assembly DNA fragments into pUC19 vector.

DNA name	Concentration	Size	Concentration
Assembly	7.2 ng/ $\mu$ L	339 bp	32.2 fmol/ $\mu$ L
EC1	4.7 ng/ $\mu$ L	339 bp	21.0 fmol/ $\mu$ L
EC2	5 ng/ $\mu$ L	339 bp	22.4 fmol/ $\mu$ L
pUC19	29.9 ng/ $\mu$ L	2700 bp	17.0 fmol/ $\mu$ L

Table 23. Master mix 2X CBA for cloning.

Reagent	Concentration
5X isothermal buffer [38]	2.5X
Phusion polymerase 2 U/ $\mu$ L (Thermo Fisher Scientific)	0.05 U/ $\mu$ L
Taq DNA ligase 40,000 U/mL (NEB)	4 U/ $\mu$ L
T5 exonuclease 10,000 U/mL (NEB)	0.08 U/ $\mu$ L
Ultra Pure™ DI water (Invitrogen)	Add to a final volume

## Appendix E: Procedures for Colony PCR

A sterile pipette tip was used to touch a single colony. Then, the tip was inserted in PCR tube containing amplification reagents. The same pipette tip was used to plate the colonies on a new LB agar plate with antibiotic selection. *E. coli* cells were serving as template. During PCR, the cells were heated to 95 °C to lyse cell walls and released to the reaction media. Thermocycler settings and reagent concentrations are shown in table below.

### Thermocycler settings

Initial denaturation 95 °C – 5 min

30 cycles:

Denaturation 95 °C – 15 s

Annealing 60 °C – 30 s

Extension 72 °C – 30 s

Final extension 72 °C – 5 min

Table 24. Colony PCR Master Mix.

Reagent	Final concentration
Taq DNA Polymerase 5 U/μL (Thermo Fisher Scientific)	0.625 U/μL
25 mM MgCl <sub>2</sub> (Thermo Fisher Scientific)	1.56 mM
10X Taq Buffer with KCl (Thermo Fisher Scientific)	1X
dNTPs 25 mM each (Thermo Fisher Scientific)	0.625 mM
Ultra Pure™ DI water (Invitrogen)	Add to a final volume



## Appendix F: Microfluidic Assembly Sanger Sequencing Results

Table 25. Sequencing results of 50 nM oligos assembly samples.

	Run 1 (11/10/16)	Run 2 (12/6/17)	Run 3 (1/4/17)	Run 4 (1/18/17)	Run 5 (1/20/17)
Deletion (total)	2	6	12	9	9
Single-base deletion					
G/C	1	3	5	2	4
A/T	1	3	7	5	5
Multiple base deletion	0	0	0	2	0
Insertion (total)	1	3	1	1	0
Single-base insertion		0			
G/C	1	1	1	0	0
A/T	0	0	0	1	0
Double-base insertion	0	2	0	0	0
Substitution (total)	1	0	1	0	0
Transition					
A/T to G/C	0	0	0	0	0
G/C to A/T	0	0	0	0	0
Transversion					
G/C to C/G	0	0	0	0	0
G/C to to T/A	0	0	1	0	0
A/T to C/G	0	0	0	0	0
A/T to T/A	1	0	0	0	0
Number of clones with misassemblies	1	1	0	1	0
Total errors	4	9	14	10	9
Number of sequenced bases	3051	2712	3390	3051	3390
Total without misassemblies	9	8	10	9	10
Total clones sequenced	10	9	10	10	10
Overall frequency (errors/kb)	1.31	3.32	4.13	3.28	2.65
Deletion frequency (errors/kb)	0.66	2.21	3.54	2.95	2.65
Insertion frequency (errors/kb)	0.33	1.11	0.29	0.33	0
Substitution frequency (errors/kb)	0.33	0	0.29	0	0

Table 26. Sequencing results of 250 nM oligos assembly samples.

	Run 1 (12/17/15)	Run 2 (10/5/16)	Run3 (10/24/16)	Run4 (11/5/16)	Run 5 (11/9/16)
Deletion (total)	8	7	10	8	6
Single-base deletion					
G/C	4	3	6	2	3
A/T	4	3	4	6	3
Double-base deletion	1	1	0	0	0
Insertion (total)	0	1	0	1	1
Single-base insertion					
G/C	0	1	0	1	0
A/T	0	0	0	0	1
Double-base insertion	0	0	0	0	0
Substitution (total)	0	1	1	2	3
Transition					
A/T to G/C	0	0	0	0	1
G/C to A/T	0	0	0	1	1
Transversion					
G/C to C/G	0	1	1	0	0
AT/ to C/G	0	0	0	1	0
A/T to T/A	0	0	0	0	1
Total errors	8	9	11	11	10
Number of sequenced bases	2712	3390	3390	3051	3051
Error frequency (errors/kb)	2.95	2.65	3.24	3.61	3.3
Total clones without misassemblies	8	10	10	9	9
Number of clones with misassemblies	0	0	0	1	1
Total clones sequenced	8	10	10	10	10
Deletion frequency (errors/kb)	2.95	2.06	2.95	2.62	1.97
Insertion frequency (errors/kb)	0.00	0.29	0.00	0.33	0.33
Substitution frequency (errors/kb)	0.00	0.29	0.29	0.66	0.98